IMPACT OF PROBENECID, A PANX1 CHANNEL INHIBITOR, ON THE SYNAPTIC AND SPATIAL MEMORY DEFECTS IN A MOUSE MODEL OF ALZHEIMER'S DISEASE

Tesis entregada a

LA UNIVERSIDAD DE VALPARAÍSO

En el Cumplimiento Parcial de los requisitos para optar al grado de

Doctor en Ciencias con Mención en Neurociencia

Facultad de Ciencias

Por

Paula Fernanda Mujica Covarrubias

Enero, 2023

Dirigida por: Dr. Álvaro Ardiles Araya

Co-Dirigida por: Dra. Arlek González Jamett

FACULTAD DE CIENCIAS

UNIVERSIDAD DE VALPARAÍSO

INFORME DE APROBACIÓN

TESIS DE DOCTORADO

Se informa a la Facultad de Ciencias que la Tesis de Doctorado presentada por:

PAULA FERNANDA MUJICA COVARRUBIAS

Ha sido aprobada por la comisión de Evaluación de la tesis como requisito para optar al grado de Doctor en Ciencias con mención en Neurociencia, en el examen de Defensa de Tesis rendido el día 17 del Mes de Agosto de 2023

Director de Tesis:

Dr. Álvaro Ardiles Araya ……

Co-Directora de Tesis:

Dra. Arlek González Jamett ……

Comisión de Evaluación de la Tesis

Dr. Andrés Chávez ……

Dr. Juan Carlos Sáez ……

Dra. Claudia Duran Aniotz ……

Dedication

I dedicate the result of this work to my entire family. Mainly, to my parents who supported me and contained the bad moments and the less bad ones. Thank you for teaching me to face difficulties without ever losing my mind or dying trying.

They have taught me to be the person I am today, my principles, my values, my perseverance, and my commitment. All this with a huge dose of love and without asking for anything in return.

I also want to dedicate this work to my boyfriend Ronald. For your patience, for your understanding, for your commitment, for your strength, for your love, because I love it. I must apologize because you have suffered the direct impact of the consequences of the work you have done. He really helped me achieve the balance that allows me to give my full potential. I will never stop being grateful for this.

Also, I want to dedicate this work to my daughter Consuelo. Her birth, whether by chance or causality, has coincided with the completion of this thesis. Without a doubt, she is the best thing that has happened to me, and she has arrived at the right time to give me the last push that I needed to finish the project.

Acknowledgement

First, I want to thank my advisors Alvaro Ardiles and Arlek Gonzalez, for their patience and all advice, and kind critics in the numerous meetings over all these years. I'm sure that this thesis would not be the same without you. Second, I want to thank Claudia Duran for her kind advice and for letting me use the equipment in her laboratory, and for all the corrections that aid me to improve this project.

This work was supported by ANID 21170120 doctorate scholarship to PFMC, FONDECYT Grant 1201342 to AOA , and Millenium Institute CINV ICN09-022.

Index

Table List

Figure List

Annexes Figures and Tables List

Symbol List, abbreviations, or nomenclature

AD	Alzheimer's disease
Aβ	Amyloid-beta
AChR	Acetylcholine receptor
APP	Amyloid precursor protein
APOE	Apolipoprotein E
Cx	Connexin
EDTA	Ethylenediaminetetraacetic acid
IL	Interleukin
KO	Knock-out
LTP	Long-Term potentiation
LTD	Long-Term depression
mGluR5	Metabotropic glutamate receptor 5
m.o	Months old
MWM	Morris water maze
NMDAR	N-methyl-D-aspartate receptor
NOR	Novel object recognition
OAT	Organic Anion Transporter
Panx1	Pannexin 1

PPF	Paired-pulse facilitation
PSEN	Presenilins
PSD	Post synaptic density
TBS	Theta burst stimulation
TNF	Tumor necrosis factor

Abstract

Alzheimer's disease (AD) is a chronic, progressive, and irreversible neurodegenerative disorder with clinical features including memory loss, dementia, and cognitive impairment. It has been shown that one of the earliest events in AD is the synaptic loss induced by soluble oligomeric forms of the amyloid β peptide (sAβos) which is thought to be the major cause of cognitive deficits in AD. Pannexin 1 (Panx1), a membrane protein implicated in cell communication and intracellular signaling, modulates the induction of excitatory synaptic plasticity under physiological contexts and contributes to neuronal death under inflammatory conditions. Probenecid (PBN) is an FDA-approved drug used for gout treatment that has been shown to block the Panx1 channel activity and that has been suggested as a neuroprotective agent, although the related mechanisms have never been described. Previously, we reported that the *ex vivo* treatment with 100μM PBN improves synaptic plasticity, toxic biochemical pathways and cell viability in the brain of 6 months old (m.o) APP/PS1 mice, a transgenic mouse model of AD. To further explore the therapeutic potential of PBN in the AD context we evaluated the impact of 1-month treatment with PBN in 3, 12, and 18 m.o APP/PS1 mice and their wildtype (WT) littermates. After treatment, we assessed a battery of behavioral tasks to analyze spatial and recognition memory using the Morris Water Maze (MWM) and the Novel Object Recognition (NOR) tests, respectively. *Ex vivo* electrophysiological-field recordings were done to analyze synaptic transmission and plasticity in hippocampal

slices. Additionally, immunolabeling of histopathological AD markers and staining of the neuronal morphology, dendritic arborization, and spine density were also performed. Our data show that the treatment with PBN prevented the defects in recognition and spatial memory observed in both male and female 12 m.o APP/PS1 mice. The treatment with PBN also increased dendritic arborization and spine density in both WT and APP/PS1 mice, we observed an early loss of spines in the 3 m.o TG females, in contrast to males, where the loss of spines was observed in older TG animals. We also observed that PBN prevented synaptic plasticity defects in APP/PS1 mice where we observed a similar correlation with respect to the structure of the synapse, that is, a deterioration in plasticity in young TG females and old TG males. As the PBN treatment reduced the Panx1-activity, estimated by the uptake of a fluorescent dye in the *ex vivo* hippocampal slices, all these results strongly suggest that a “neuroprotective” effect of PBN could rely on the blockade of Panx1 channels.

Resumen

La enfermedad de Alzheimer (EA) es una enfermedad neurodegenerativa crónica, progresiva e irreversible con características clínicas de pérdida de memoria, demencia y deterioro cognitivo. Se ha demostrado que uno de los eventos más tempranos en la EA es la pérdida sináptica funcional, inducida por formas oligoméricas solubles del péptido **β** amiloide (sA**β**os), que se cree que es la causa principal de los déficits cognitivos en la EA. Panexina 1 (Panx1), una proteína de membrana implicada en la comunicación celular y la señalización intracelular, modula la inducción de la plasticidad sináptica excitatoria en contextos fisiológicos y contribuye a la muerte neuronal en condiciones inflamatorias. El probenecid (PBN) es un medicamento aprobado por la FDA que se usa para el tratamiento de la gota que ha demostrado bloquear la actividad del canal de Panx1 y que se ha sugerido como un agente neuroprotector, aunque nunca se han descrito los mecanismos relacionados.

Anteriormente, reportamos que el tratamiento ex vivo con 100 μM PBN mejora la plasticidad sináptica y reduce algunas vías de señalización tóxica y la viabilidad celular en el cerebro de ratones APP/PS1 de 6 meses de edad (m.e), un ratón transgénico modelo de EA. Para explorar más a fondo el potencial terapéutico del PBN en el contexto de la EA, evaluamos el impacto del tratamiento de 1 mes con PBN en ratones APP/PS1 de 3, 12 y 18 m.e y de sus hermanos de camada de tipo salvaje (WT). Transcurrido el tratamiento, aplicamos una batería de tareas conductuales para analizar la memoria

espacial y de reconocimiento utilizando las pruebas de Morris Water Maze (MWM) y Novel Object Recognition (NOR), respectivamente. Se realizaron registros electrofisiológicos de campo en rebanadas hipocampales ex vivo para analizar la transmisión y plasticidad sináptica; además, se realizó el inmunomarcaje de marcadores histopatológicos de la EA y tinción de Golgi para evaluar la morfología neuronal, la arborización dendrítica y la densidad de espinas dendríticas. Nuestros datos mostraron que el tratamiento de 1 mes con 100 mg/kg PBN previno los defectos en la memoria de reconocimiento y memoria espacial observados en ratones APP/PS1 de 12 m.e, además de aumentar la arborización dendrítica y la densidad de espinas tanto en ratones WT como APP/PS1. También observamos que PBN previno los defectos de plasticidad sináptica en ratones APP/PS1. Como el tratamiento con PBN también redujo la actividad de Panx1, estimada por la captación de trazadores fluorescentes en las rebanadas hipocampales, estos resultados sugieren que los efectos de PBN podrían depender del bloqueo de los canales de Panx1.

Introduction

AD and the amyloid hypothesis

AD is a progressive neurological disorder that causes brain atrophy and neuronal death; it is the most prevalent neurocognitive disorder in the elderly, that lead to the progressive decline in cognitive and social skills, affecting the person's ability to live independently (Goedert & Spillantini, 2006). According to the World Health Organization (WHO), fifty million people worldwide live with dementia since 2018. It is estimated that these numbers will increase more than threefold, reaching 152 million people affected by 2050 (Patterson, 2018). In Chile, there is no epidemiological data regarding AD, however, an approximation can be made according to other tools. Based on the National Dependency Study and the National Health Survey, it can be estimated that the prevalence of AD in people over 60 years old is 3% and this is greater than 40% over 80 years (MINSAL, 2010). Currently, in our country, about 200.000 people suffer from AD. The number would rise as the population ages (MINSAL, 2015).

Mutations in the amyloid precursor protein (APP), presenilin 1 (PSEN1), and presenilin 2 (PSEN2) genes are related to early-onset familial forms of AD, instead, polymorphisms in the Epsilon 4 allele of the apolipoprotein E (APOE) gene are an important risk factor for late-onset AD (Bertram, et al. 2010; Goedert & Spillantini, 2006). Nonetheless, most of the cases of AD are sporadic forms of the disease, with aging being the major risk factor (Goedert & Spillantini, 2006).

AD is characterized by the appearance of two lesions in cells and cerebral microvessels that correspond to the abnormal accumulation of protein-aggregates forming amyloid plaques and neurofibrillary tangles (Figure 1) (Haas & Selkoe, 2007). The amyloid plaques correspond to extracellular deposits of the amyloid-β peptide (aβ), which is produced from the altered enzymatic processing of the APP by α-, β- and γ-secretases (Goedert & Spillantini, 2006). The neurofibrillary tangles correspond to intracellular aggregates constituted by hyperphosphorylated forms of Tau, a microtubule-associated protein (Haas & Selkoe, 2007).

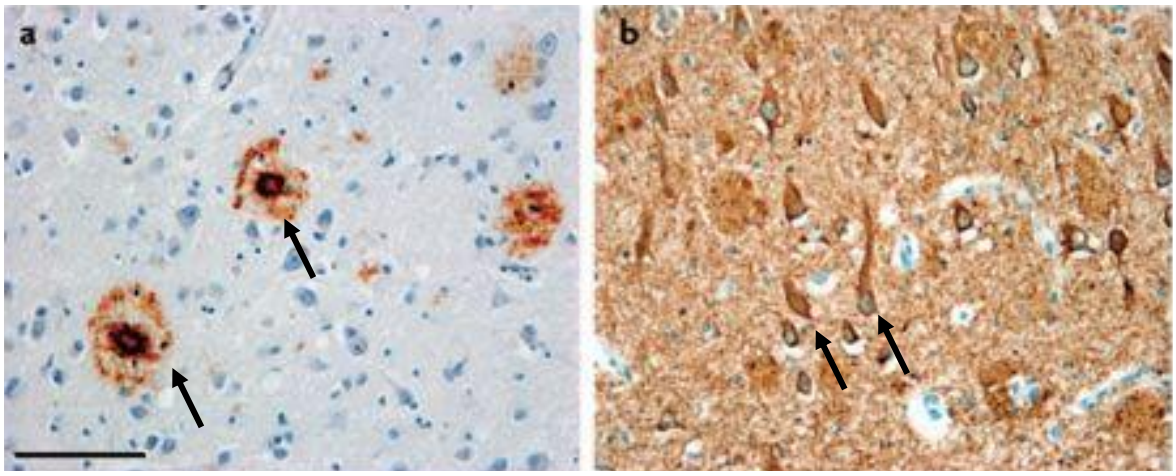

Figure 1 Histopathological hallmarks of Alzheimer's disease. A. *Aβ-positive senile plaques.* ***B.*** *tau-positive neurofibrillary tangles, neutrophil threads, and dystrophic neurites. Arrows indicate both markers- Modified from (Haas & Selkoe, 2007)*

Both lesions are used for *postmortem* confirmation of AD, and there is growing evidence indicating that the amyloid aggregation precedes the abnormal hyperphosphorylation of Tau protein (Haas & Selkoe, 2007), suggesting that accumulation and aggregation of Aβ is an early relevant factor in the AD pathophysiology. Although it has been proposed that both pathological changes trigger a series of modifications that eventually lead to neurodegeneration and dementia, the lack of

correlation between these markers and the onset of the cognitive decline suggests that the synaptic loss could be the major factor contributing to the early cognitive defects in AD (Masliah, et al., 2001; Hatanpää, et al., 1999; Terry, et al., 1991). Indeed, a number of evidence point that the accumulation of soluble oligomeric forms of Aβ, identified in AD patients (Fukumoto, et al., 2010; Gong, et al., 2003) and in AD animal models (Price, et al., 2014; Mucke, et al., 2000), precede the fibrillar amyloid deposition and tau pathology. Soluble oligomeric forms of Aβ have been implicated in the synaptopathy observed before the appearance of neurodegeneration (Sheng, et al., 2012), supporting a pathogenic role for these structures in the development of AD (Haas & Selkoe, 2007; Li, et al., 2009).

Aβ is a peptide comprising 40 to 42 amino acids, that is generated by the proteolytic cleavage of APP. It is normally produced at low concentrations (Abramov, et al., 2009), however when its production increases, particularly the Aβ 42 isoform (Goedert & Spillantini, 2006), it forms soluble aggregates that easily diffuse and adopt an insoluble fibrillar configuration. Depending on the enzyme cutting the APP, Aβ can be generated or not (Figure 2). Whether it is cut by α-secretase, sAPPα will be released which, unlike Aβ, plays a positive role in brain plasticity and in protection against excitotoxicity (Chow, et al., 2010). On the other hand, if it is cut by the enzyme β-secretase and then by the γ-secretase, Aβ is formed (Goedert & Spillantini, 2006; Haas & Selkoe, 2007). Within the main components of the atypical aspartyl protease -secretase, PSEN constitute the catalytic subunit required for the cleavage of APP (Goedert & Spillantini, 2006).

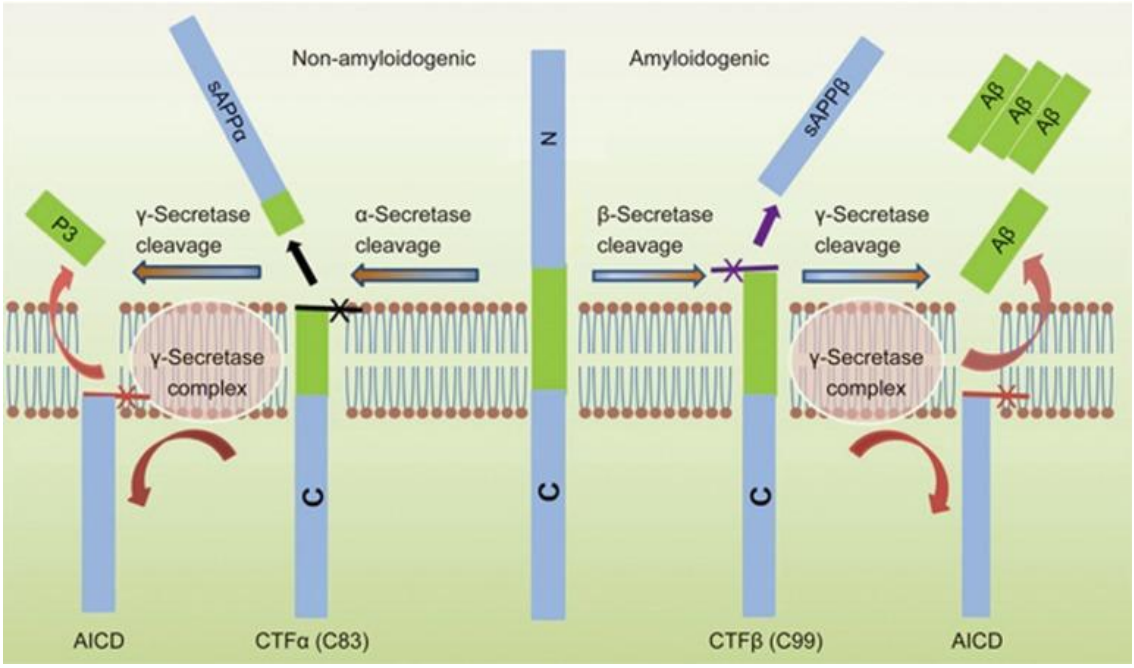

Figure 2 Generation of Aβ from APP. *Cleavage by β-secretase generates the N terminus and intramembranous cleavage by γ-secretase gives rise to the C terminus of Aβ. Cleavage by α-secretase precludes Aβ formation (Chen, et al., 2017)*

The more prominent hypothesis for AD pathogenesis is the amyloid hypothesis. It states that the gradual accumulation and aggregation of these peptides initiates a slow and toxic cascade that leads to synaptic alterations, microglial and astrocytic activation, modification of the normally soluble tau protein into oligomers and then into insoluble paired helical filaments, and progressive neuronal loss associated with multiple neurotransmitter deficiencies and cognitive failures (Haas & Selkoe, 2007). Thereby, soluble Aβ oligomers can induce synaptic dysfunction by selectively affecting postsynaptic components, some of which act as a receptor for these toxic species (Brody & Strittmatter, 2018). In particular, these oligomers tend to accumulate in the excitatory synapses, where they interact with several neurotransmitter receptors, such as nicotinic acetylcholine receptors (AChR), glutamate receptors (NMDA/AMPA/mGluR5)

(Venkitaramani, et al., 2007), and other membrane proteins such as the prion protein (Laurén, et al., 2009) impacting on their functionality and leading to defects in the synaptic transmission. In this way, a great deal of evidence suggests that soluble Aβ oligomer accumulation induces Ca^{2+} deregulations in the dendritic spines, in a way dependent on the over-activation of NMDA and mGluR5 glutamate receptors (Decker, et al., 2010; Renner, et al., 2010; Um, et al., 2013). This latter appears to produce an imbalance in the Ca^{2+}-signaling responsible for the induction of synaptic plasticity and has been proposed to be the cause of the synapse loss and cognitive defects in AD (Alberdi , et al., 2010; De Felice, et al., 2007; Demuro, et al., 2005; Kelly & Ferreira, 2006; Paula-Lima, et al., 2011).

Impaired excitatory synaptic transmission and plasticity in AD

Synaptic plasticity is defined as a series of structural and functional modifications that manifest as changes in the efficacy of the synaptic transmission, which have been proposed to be the cellular mechanisms of memory and learning (Citri & Malenka, 2008). Two common forms of synaptic plasticity are long term potentiation (LTP) and long term depression (LTD) of the excitatory synapses, which correspond to an increase and a decrease in the synaptic efficacy respectively (Bear & Malenka, 1994). These changes in the efficacy of the synaptic response correlate with changes in the density, shape, and size of dendritic spines, highly dynamic structures present in dendrites that contain the synaptic machinery for most of the excitatory synaptic contacts (Lisman & Harris, 1993). This is how, LTP is expressed by an increase in the postsynaptic density (PSD) size, spines enlargement, and maturation, whereas LTD manifests with PSD-reduction and shrinkage of spines (Okamoto, et al., 2009).

In the AD pathological context, it has been described that Aβ oligomers impair synaptic plasticity by reducing the size and number of dendritic spines (Hsieh, et al., 2006; Lacor, et al., 2007), preventing LTP (Walsh, et al., 2002; Wang, et al., 2002) and promoting synaptic mechanisms that lead to LTD (Chen, et al., 2013; Hu, et al., 2014; Kim, et al., 2001; Li, et al., 2009). This latter is ultimately reflected as cognitive dysfunctions and impaired spatial memory (Cleary, et al., 2005; Lesne, et al., 2006; Reed, et al., 2011).

The potential contribution of Panx1 channels to synaptic plasticity

Previous works have demonstrated that Pannexin 1 (Panx1) (figure 3), a non-selective membrane channel implicated in cell communication and intracellular signaling (Bao, et al., 2004) participates in the modulation of excitatory synaptic plasticity (Prochnow, et al., 2012). This is how the acute blockade of Panx1 channels, as well as the knock-out (KO) of their expression, modify the threshold for the induction of excitatory synaptic plasticity and the excitation/inhibition (E/I) balance facilitating LTP (Ardiles, et al., 2014; Gajardo, et al., 2018; García-Rojas, et al., 2023). Furthermore, it was demonstrated that the constitutive knock-out of Panx1 promotes dendritic spine morphogenesis enhancing connectivity in cortical neurons (Sanchez-Arias, et al., 2019). The latter suggests that Panx1 acts as a “break” for structural synaptic plasticity and that

its absence facilitates the structural changes that correlate with modifications in synaptic efficacy.

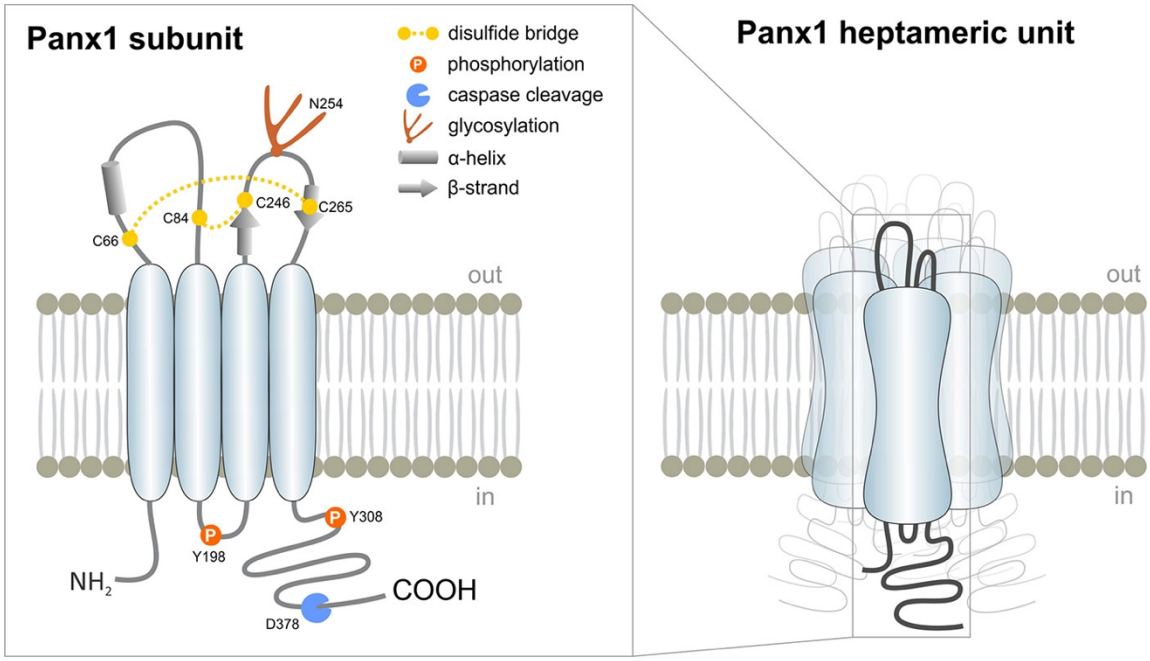

Figure 3: Structure of Panx1 glycoprotein and heptameric channel indicating sites of posttranslational modifications and secondary structures of extracellular loops *(Navis, et al., 2020)*.

In fact, hippocampal neurons from Panx1-KO mice show increased size and maturation in compared to the WT condition (Flores-Muñoz, et al., 2022) in accordance with the reported facilitation in the potentiation of the synaptic strength in absence of Panx1 (Ardiles, et al., 2014; Gajardo, et al., 2018). The latter suggests that the suppression of Panx1 activity goes in the opposite direction to that observed in the AD context (Flores-Muñoz, et al., 2020), making these channels potential players in the structural and functional synaptic defects that lead to the LTP/LTD imbalance in AD.

How Panx1 channel activity could modulate synaptic impairments? Panx1 is a heptameric protein (Qu, et al., 2020; Michalski, et al., 2020; Mou, et al., 2020; Deng, et al., 2020) that forms non-selective membrane channels in which adenosine triphosphate (ATP) and other molecules can cross the cell membrane (Bao, et al., 2004; Iglesias & Spray, 2012). In fact, diverse metabolites and signaling molecules including endocannabinoids (Bialechi, et al., 2020; García-Rojas et al., 2023), and Ca^{2+} (Abeele, et al., 2006; Thompson, et al., 2008; Weilinger, et al., 2016; Patil, et al., 2022) have also been proposed to pass directly through these channels while the release of inflammatory mediators such as interleukin -1(IL-1) (Brough, et al., 2009; Pelegrint & Supernant, 2006), IL-6 and IL-8 (Wei, et al., 2016) has been shown to depend on Panx1 activity, In the brain, Panx1 is expressed in different cell types (Vogt, et al., 2005; Bruzzone, et al., 2003; Ray, et al., 2005) and is preferentially located at the post-synaptic membrane of cortical and hippocampal neurons (Zoidl, et al., 2007). It has been demonstrated that Panx1 channels associate with aberrant glutamatergic transmission in different neuropathological contexts (Sanchez-Arias et al., 2021). Such association promotes Panx1 channel opening and induces de-regulations in the Ca^{2+} signal and neuronal injury. For instance, under ischemic conditions, Panx1 channels are opened by the over-activation of NMDAR (Thompson, et al., 2006; Weilinger, et al., 2012; Weilinger, et al., 2016) triggering an epileptic activity that can be inhibited by the pharmacological blockade of Panx1 channels (Thompson, et al., 2008). Likewise, it was confirmed in a mice model of epilepsy (Aquilino, et al., 2020) and in cortical slices from epilepsy drug-resistance patients (Dossi, et al., 2018). On the other hand, the production of persistent bursts of hippocampal neuronal activity triggered by the activation of mGluR5 can be prevented by the inhibition of Panx1 channels, suggesting a role of Panx1 channels in the mGluR5-induced pathological epileptic activity (Lopatar, et al., 2015).

Regarding AD, an exacerbated trafficking of Panx1 towards the plasma membrane and increased Panx1 channel activity have been correlated with the Aβ-induced neuronal death in hippocampal slices (Orellana, et al., 2011). Furthermore, Panx1 channels seem to be required for the Aβ-triggered degranulation of mast cells as seen in the brain of APP/PS1 mice, an animal model of AD, promoting early inflammatory processes (Harcha, et al., 2015). Both Panx1 channels and connexin (Cx) hemichannels exhibit exacerbated activity in microglia and astrocytes derived from APP/PS1 mice (Yi, et al., 2016). In turn, an increased hemichannel activity triggers a massive release of gliotransmitters such as ATP and glutamate, exacerbating the neurotoxicity in the AD context (Abudara, et al., 2015). Remarkably, it has been observed a greater contribution of the Panx1 activity in reactive astrocytes surrounding amyloid plaques in APP/PS1 brains (Yi, et al., 2016) which decreases in the presence of inflammation inhibitors (Yi, et al., 2016) suggesting that Panx1 channels are over-active as a consequence of inflammation. In this sense, the treatment with boldine, and alkaloid with reported anti-inflammatory actions (Backhouse, et al., 1994) was able to reduce the levels of pro-inflammatory cytokines tumor necrosis factor α (TNF-α) and IL-1β while reduced hemichannel activity in brain slices of APP/PS1 mice (Yi, et al., 2017). Furthermore, Panx1 channel inhibition with the ^{10}Panx1 mimetic peptide also reduced neuronal activity (Yi, et al., 2017), suggesting the over-activation of Panx1 in AD-neurons. In agreement with this idea, we previously demonstrated that Panx1 is overexpressed in synaptosomes and PSDs isolated from hippocampal tissue of APP/PS1 mice (Flores-Muñoz, et al., 2020), suggesting that Panx1 channel could be a novel therapeutic target to intervene the neuropathology of AD.

Moreover, the acute inhibition of Panx1 activity with PBN mitigates the defects in excitatory synaptic plasticity observed in hippocampal slices from APP/PS1 mice, namely LTP reduction and LTD augmentation (Flores-Muñoz, et al., 2020). Remarkably, the treatment with PBN has been correlated with a lower risk to develop dementia in humans (Engel, et al., 2018; Khan, et al., 2016; Lu, et al., 2016), reduced neuroinflammation (García-Rodriguez et al., 2023) and neuroprotection (Colin-Gonzalez & Santamaria, 2013), suggesting that Panx1 channel inhibition could be a feasible strategy to soften the cognitive defects associated to AD.

Probenecid: a neuroprotective Panx1 inhibitor?

Probenecid (PBN, Figure 4) is a drug that belongs to the uricosurics compounds. It is primarily used to treat gout and other conditions associated with high levels of uric acid in the blood by increasing the renal excretion of uric acid (Talbott, 1951; Talbott, et al., 1951). PBN works by blocking the reabsorption of uric acid in the kidneys, which results in more uric acid being excreted in the urine (Talbott, 1951; Talbott, et al., 1951). This helps to reduce the levels of uric acid in the blood, preventing the formation of uric acid crystals in the joints that can cause inflammation and pain. PBN may also have other uses, such as in the treatment of certain infections and as a neuroprotective agent (Colin-Gonzalez & Santamaria, 2013).

PBN acts by blocking the action of organic anion transporters (OAT) in the proximal tubules of the kidneys, which is responsible for the reabsorption of uric acid (Donovan, et al., 2015; Hagos, et al., 2017). In addition to its effects on uric acid metabolism, PBN has been shown to have other pharmacological effects, including the activation of transient receptor potential cation channel subfamily V2 (TRPV2) (Bang, et al., 2007) and the inhibition of purinergic channels, such as P2X7R (Bhaskaracharya, et

al., 2014), organic cation transporters (OCTs) (Gisclon, et al., 1989; Inotsume, et al., 1990; McKinney, et al., 1981) and Panx1 channels (Silverman, et al., 2008; Ma, et al., 2009), which has been implicated in various cellular processes, including inflammation and cell death (Jian, et al., 2016; García-Rodriguez et al., 2023).

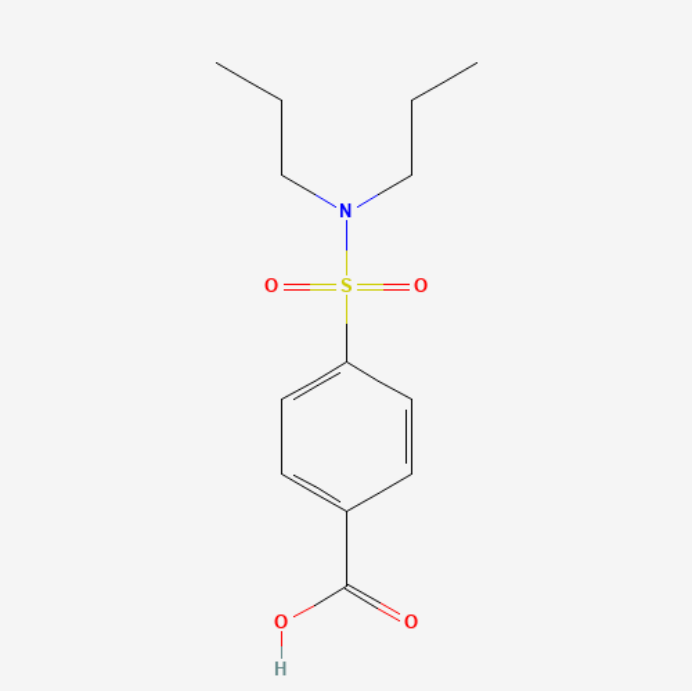

Figure 4 Probenecid chemical structure. *PBN is a sulfonamide in which the nitrogen of 4-sulfamoylbenzoicacid is substituted with two propyl groups. [4-(dipropyl sulfamoyl) benzoic acid] (https://pubchem.ncbi.nlm.nih.gov/compound/Probenecid).*

Probenecid is well-absorbed after oral administration and has a bioavailability of approximately 90% (Selen, et al., 1982)). It reaches its peak in plasma concentration within 2 to 4 hours after oral administration. The elimination half-life of PBN is approximately 4 to 8 hours, and it's primarily excreted in the urine through glomerular filtration and active tubular secretion. This drug is extensively metabolized in the liver, with approximately 50% of the dose excreted in the urine as metabolites (Cunningham, et al., 1981).

PBN has been investigated for its potential neuroprotective activity in various preclinical studies and experimental models (Garcia-Rodriguez, et al., 2023). While the exact mechanisms underlying its neuroprotective effects are not fully understood, several mechanisms have been proposed:

1**.- Inhibition of Panx1 channels:** PBN has been shown to inhibit Panx1 channels (Silverman, et al., 2008), which are involved in cell-to-cell communication and have been implicated in neuroinflammation and neuronal death (Seo, et al., 2021; Silverman, et al., 2009). By blocking Panx1 channels, PBN may help to reduce neuronal overactivity and inflammation and prevent cell damage in the brain.

2.- Anti-inflammatory effects: PBN has been reported to exert anti-inflammatory effects by inhibiting the production of pro-inflammatory cytokines and reducing the activation of inflammatory pathways (Silverman, et al., 2009; Jian, et al., 2016; Zheng, et al., 2022). These anti-inflammatory properties may contribute to its neuroprotective activity in various neurodegenerative conditions.

3.- Glutamate modulation: PBN has been found to modulate glutamate release and uptake in the brain (Urenjak, et al., 1997; Taylor, et al., 1997; Orellana, et al., 2015). Excessive glutamate release can lead to excitotoxicity, a process that contributes to neuronal damage in various neurological disorders (Lewerenz & Maher, 2015). By modulating glutamate levels, probenecid may help to protect neurons from neurotoxicity.

4.- Antioxidant activity: Oxidative stress plays a significant role in neurodegenerative diseases (Kim, et al., 2015; Zheng, et al., 2022). Some studies suggests that probenecid may have antioxidant properties and can scavenge free radicals, reducing oxidative stress and protecting neurons from damage (Du, et al., 2016).

It is important to note that while preclinical studies have shown promising neuroprotective effects of PBN (for more details see Table 2 (Garcia-Rodriguez, et al.,

2023)), further research is needed to validate these findings and to determine its clinical efficacy in humans. Clinical trials evaluating the neuroprotective potential of PBN are limited at present (https://beta.clinicaltrials.gov/study/NCT04746989), and its use as a neuroprotective agent in clinical settings remains to be elucidated.

Research Question

Does the PBN treatment preventing the loss of synaptic structure and cognitive function in a murine model of AD?

Hypothesis

“The PBN treatment inhibits the activity of Panx 1 channels, preventing the loss of synaptic structures and cognitive function in a murine model of AD”

General aim

To evaluate the impact of the treatment with PBN on the Panx1 channel activity, synaptic structure and cognitive function in a murine model of AD.

Specific aims

1. To determine the impact of the treatment with PBN on the spatial and recognition memory impairments in APP/PS1 mice, a murine model of AD.
2. To demonstrate that the treatment with PBN inhibits the Panx1 activity in hippocampal slices of APP/PS1 mice.
3. To analyze the impact of the treatment with PBN on the excitatory synaptic transmission and plasticity in hippocampal slices of APP/PS1 mice.
    a. To analyze the effect of the treatment with PBN on the basal strength of the synaptic transmission in acute hippocampal slices of APP/PS1 mice.
    b. To analyze the effect of the treatment with PBN on the induction of NMDA-dependent LTP in acute hippocampal slices of APP/PS1 mice.
4. To determine the effect of the treatment with PBN on the spine loss in hippocampal neurons of APP/PS1 mice
    a. To determine the effect of the treatment with PBN on the density and size of dendritic spines in hippocampal neurons of APP/PS1 mice.

Complementary aims

1. To analyze the effects of the PBN treatment on neurodegeneration in hippocampal slices of APP/PS1 mice

Materials and Methods

Animals

All experiments were carried out in 3, 12, and 18 m.o C57BL/6 wild type (WT) or APPswe/PSEN1ΔE9 transgenic mice (TG), which express the APP_{SWE} (K595N/M596L) double mutation and PSEN1 deletion of the exon 9 (stock 004462). The original colony of these mice was purchased from Jackson Laboratory (Bar Harbor, ME, USA). Male and females were used in the study.

Mice were housed in groups of up to five in individually ventilated cages under standard conditions (22°C, 55% humidity, 12 h light-dark cycle) receiving food and water *ad libitum*. All animal manipulations were carried out in accordance with standards regulations and approved by the Ethics and Animal Care Committee of Universidad de Valparaíso (BEA064-2015).

Experimental Design

All mice were randomly assigned into four groups according to their age: wild-type (WT) or transgenic (TG); vehicle (control) or probenecid (PBN) (Table 1). The treatment consisted of one serving of MediGel sucralose (MediGel Sucralose, Clear H2O, Portland, ME) supplemented with vehicle or 100 mg/kg PBN (P8761, Sigma, USA) that started at 3, 12, or 18 m.o and finished after day 45 (Figure 5). All the behavioral tests were performed on day 31 of the treatment.

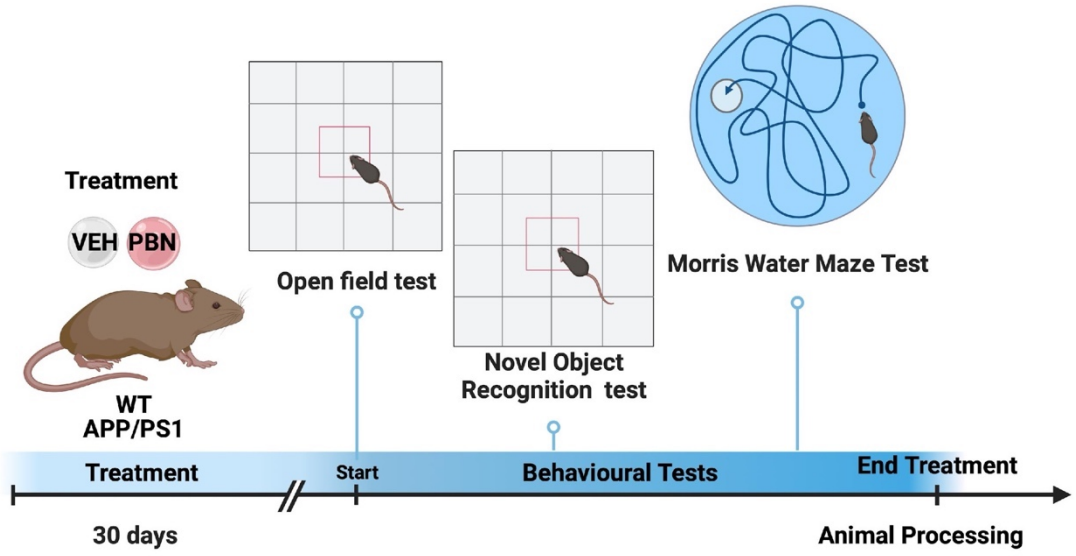

Figure 5 Schematic organization of the pharmacological treatment and behavioral tests for APP/PS1 mice and their WT littermates. *The vehicle (VEH) corresponded to NaOH 1M; Probenecid (PBN) was administered at a dose of 100 mg/kg/day for 30 days. Created with BioRender.*

Probenecid administration

Mice were weighed every morning approximately 1 hour after the lights were on, during all the study and until animals were sacrificed. Four weeks before and during the behavioral characterization, mice were individually housed in ventilated cages and administered with an aqueous gel (MediGel Sucralose, Clear H2O, Portland, ME) as previously reported with modifications (Christy et al., 2014). After that, a group of animals was fed with gel supplemented with PBN (100mg/kg), whereas the rest of the animals remained with gel plus vehicle (NaOH). If any of the animals experienced a sudden fall in their weight (more than a 50% decrease in their body weight) the treatment with the aqueous gel was suspended and the animal was not included in the experiments.

Behavioral studies

Locomotor activity and cognitive function was evaluated by Open field (OF), Novel Object recognition (NOR), and Morris Water Maze (MWM) tests, respectively.

1. **Open Field (OF):**

Mice were placed in a plexiglass open field maze (40cm long x 40cm wide). Each 40cm x 40cm unit was digitally divided into 9 quadrants of equal size using ANY-maze video tracking software. The four central quadrants were collectively referred to as the center zone, and the 4 peripheral quadrants were collectively referred to as the corner zone as previously described (Liu et al 2013). Data were collected continually for 10 minutes, and the distance traveled (m), and the time spent in the central zone versus the peripheral zone were recorded and scored automatically.

2. **Novel Object Recognition test**

The NOR test used the same square white acrylic box of the OF in which mice explored freely for 5 min throughout three phases: (i) sample (10 min), where mice explored a pair of identical objects; (ii) retention (1 hour), where mice were removed for cleaning and changing objects; and (iii) choice (5 min), where mice explored a pair of different objects: a familiar object (F) and a new object (N). Each session was repeated for 3 days. The time that mice spent exploring F or N was quantified, 20 seconds (N+F) was considered as a minimum exploration time to be considered in data analysis. A discrimination index (DI) was calculated as [(N – F / total time of exploration) * 100], and the percentage of time they explored the novel object.

3. Morris Water Maze test

MWM test was applied as previously described with minor modifications (Gajardo, et al., 2018). In this assessment, animals are taught to swim to a hidden platform under the water. All experimental mice were placed in the pool and allowed to explore it for 1 min (Habituation phase). The testing room was equipped with spatial cues for orientation. This acquisition procedure was performed six times a day for four consecutive days per animal. On the fifth day, the platform was removed from the pool to measure the time that the animals spend in the target quadrant until one minute lapse. Additionally, during the acquisition phase, the time spent finding the platform was also measured per each animal.

Behavioral data were analyzed with AnyMaze software.

Ethidium bromide uptake assay

Hippocampal slices were stabilized in a chamber with oxygenated (95% O_2 and 5% CO_2) artificial cerebrospinal fluid (ACSF), pH 7.4 for 1 hour and then incubated with 20 μM of Ethidium bromide for 5 min. Then, they were washed five times for 2 min with ACSF, fixed at room temperature with 4% paraformaldehyde and 15% sucrose for 30 min, and maintained in PBS buffer. After that, slices were cut into 25 μm sections using a cryostat (Leica CM1900). Sections were stained with primary mouse anti NEUN (MAB328, Abcam; 1:500) or rabbit anti GFAP (Dako 1:100) followed by secondary Alexa fluor 488-conjugated goat anti-mouse or anti-rabbit antibodies (Invitrogen, Carlsbad, CA, USA; 1:500). Mounted sections were examined in an Olympus IX81 Custom microscope coupled to an Olympus F-View Monochromatic CCD camera. Images were acquired with a 20-objective using Xcellence Pro software and processed with a custom-made

algorithm based on Fiji (Image J software). The dye uptake ratio was calculated as the mean fluorescence intensity of the population of positive NeuN cells and normalized to the WT group. At least three fields were selected in every slice.

Electrophysiology analysis

Hippocampal slices were prepared as we previously reported (Ardiles, et al., 2014; Ardiles, et al., 2017). Mice were deeply anesthetized with isoflurane, and their brains were quickly removed. Slices (350 μm) were dissected in ice-cold dissection buffer using a vibratome (Leica VT1200S, Leica Microsystems, Nussloch, Germany). Hippocampal slices were incubated at 30℃ for 30 min and then maintained at 28℃ for at least 1 h before the experiment as described previously (Ardiles, et al., 2014). After recovery, the slices were placed in a recording chamber at 25℃ and perfused with oxygenated artificial cerebrospinal fluid (ACSF) containing 124 mM NaCl, 2.5 mM KCl, 1 mM NaH_2PO_4, 25 mM $NaHCO_3$, 10 mM glucose, 2 mM $CaCl_2$, and 2 mM $MgSO_4$ at a rate of 1 ml/min. Synaptic responses were evoked by stimulating the CA3-Schaffer collaterals with 0.2 ms. pulses delivered through concentric bipolar stimulating electrodes and recorded extracellularly in the stratum radiatum of the CA1 subfield.

1. **Basal excitatory synaptic transmission**

Basal synaptic transmission was assayed by determining input-output relationships from field excitatory post-synaptic potentials generated by gradually increasing the stimulus intensity; the input was measured as the peak amplitude of the fiber volley (FV), and the output was the initial slope of field excitatory post-synaptic potentials.

2. Paired pulse facilitation

PPF was obtained by stimulating at different intervals in a range between 25-300 ms and recording excitatory fEPSP. A PPF index was calculated by dividing the amplitude of the second response over the first one (R2/R1).

3. NMDA-dependent synaptic plasticity

Long-term potentiation (LTP) was induced by a standard theta burst stimulation protocol (10 trains of four pulses at 100 Hz; 5 Hz inter-burst interval) delivered at 0.1 Hz. LTP magnitude was calculated as the average (normalized to baseline) of the responses recorded 50-60 min after conditioning stimulation. For measuring LTP, the stimulation intensity was adjusted to produce a fEPSP slope that was approximately 40% of the maximum slope for that slice. All LTP experiments were recorded after obtaining a stable baseline. Field potentials were amplified, low-pass filtered (1700 Differential AC Amplifier, A-M Systems), and then digitized (NI PCI-6221; National Instruments) for measurement. Data were monitored, analyzed online, and reanalyzed offline using a homemade routine, based on the Igor program. Representative traces are an average of five consecutive responses and stimulus artifacts were blanked for clarity.

Input-output curve and paired-pulse ratio data were analyzed using repeated-measures two-way ANOVA. LTP data (average of the last 5 min of recordings) were analyzed using an unpaired two-tailed t-test. All the data are represented as mean±SEM.

Golgi Staining

Dissected mouse brains were maintained for 1 h at room temperature in ACSF, bubbled with a mixture of 5% CO_2 and 95% O_2. After 1 h stabilization in ACSF, brain

sections were processed for Golgi impregnation following the manufacturer's instructions (FD NeuroTechnologies, Columbia, MD). Coronal sections of 150 μm thickness brain slices were obtained using a semi-automatic cryostat microtome (Kedee KD-2950, Germany) at -20ºC and mounted on gelatin-coated slides, developed with solutions of the same kit, dehydrated with a growing battery of alcohols (50-100%) and mounted using Entellan media (Millipore-Sigma, Germany). Images of pyramidal hippocampal neurons were acquired by a Leica Application Suite X (LASX, Leica Microsystems, USA) under bright-field microscopy at 40X or 63X magnification using similar light conditions between experimental groups.

Dendritic length and spine density (number of spines per 1 μm of dendritic shaft) were analyzed. All morphological analyzes were performed blind to the experimental conditions.

Histological analysis

Brain serial slices of 10 μm from all animal groups were processed in parallel for histological analyses. Mouse-derived tissues were processed from lambda 0 to lambda -4mm. For thioflavin staining, sections were deparaffinized and hydrated and then incubated with Thioflavin-S (ThS) solution (0.025% in 50% ethanol) for 8 min, and coverslipped with DPX mounting medium. Samples were analyzed using an epifluorescent microscope (DMI6000B, Leica, Buffalo Grove, IL, USA) and images were analyzed using the ImageJ software. For cresyl violet staining, sections were deparaffinized and hydrated and then incubated in cresyl violet solution for 10 minutes previously heated at 57ºC and filtered, then rehydrated, cleared and coverslipped with DPX. Images were acquired in an upright microscope (Leica DM500) attached to a Leica

ICC50W camera. ThS burden was defined as the area of the brain labeled per the total area analyzed. Burden quantification was performed by an investigator blinded to the experimental groups.

Statical Analysis

All results are expressed as mean ± SEM. A normality test was applied to all data using a D'Agostino-Pearson test and then, data were analyzed using a Three-way ANOVA test with Tukey's multiple comparisons tests. Differences were considered significant at p- values <0.05.

Results

1. Probenecid treatment does not affect body weight in mice.

In order to evaluate the impact of the PBN on the cognitive and synaptic functions in a murine model of AD, we administered a daily oral dose of 100mg/kg PBN to APP/PS1 and age-matched WT mice. Male and female mice of 3,12 and 18 m.o were used in this work. Mice were weighed every day at the same hour since they were 3, 12, or 18 m.o The PBN or VEH treatment started when they reached that age and lasted 45 days in total (Annexes figure 32). As observed in Figure 6, the PBN treatment did not change the body weight gain during the experiment. However, at all ages, female APP/PS1 mice exhibited lower weights compared to male APP/PS1 (Figure 6), such differences were significant at 3 m.o (Figure 6).

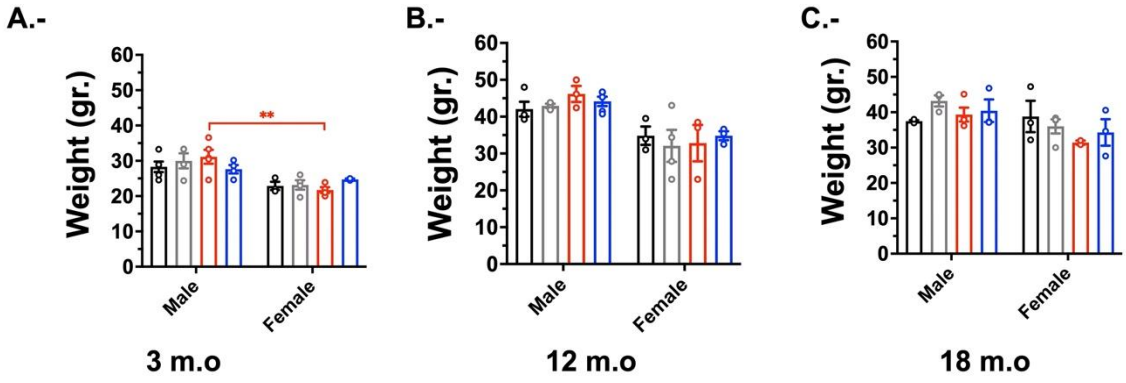

Figure 6 Average weight of APP/PS1 and WT mice along the pharmacological treatment with PBN or its vehicle. A.- *Average weight of male and female 3 m.o APP/PS1 mice (male: N=5 WT VEH (black), N=6 WT PBN (gray), N=6 TG VEH (red), N=4 TG PBN (blue); female: N=4 WT VEH (black), N=6 WT PBN (gray), N=4 TG VEH (red), N=2 TG PBN (blue)). Gender (F(1,13)=24.44, *** p=0.0003) was the primary source*

*of variation by Three-Way ANOVA, and Tukey's multiple comparison tests revealed a significant difference between male TG VEH – female TG VEH ** p=0.0040.* ***B.-*** *Average weight of male and female 12 m.o APP/PS1 mice (male: N=5 WT VEH (black), N=3 WT PBN (gray), N=4 TG VEH (red), N=7 TG PBN (blue); female: N=3 WT VEH (black), N=4 WT PBN (gray), N=3 TG VEH (red), N=3 TG PBN (blue)). Gender (F(1,12)=25.67, *** p=0.0003) was the primary source of variation by Three-Way ANOVA.* ***C.-*** *Average weight of male and female 18 m.o APP/PS1 mice (male: N=3 WT VEH (black), N=3 WT PBN (gray), N=4 TG VEH (red), N=3 TG PBN (blue); female: N=3 WT VEH (black), N=4 WT PBN (gray), N=3 TG VEH (red), N=3 TG PBN (blue)). Gender (F(1,10)=25.67, * p=0.0278) was the primary source of variation by Three-Way ANOVA. All data are represented as mean ± SEM.*

2. Probenecid treatment does not affect locomotor activity.

30 days after the PBN treatment started, mice were subjected to the behavioral paradigms to evaluate locomotion, learning, and memory capabilities. First, locomotor activity was evaluated with the open field (OF) test. As shown in figure 7A there was no difference in the total distance traveled between male experimental groups at the different ages assessed. However, in general, we observed a significant decrease in the total distance traveled with age, as was reported previously (Jardanhazi-Kurutz, et al., 2010; Chaney, et al., 2018; Webster, et al., 2014; Ferguson, et al., 2013). When we analyzed the time that mice spent in the center and in corners in the OF, we observed that the young transgenic (TG) mice remained longer in the corners compared to their controls (WT). This behavior increased significantly with age (Figure 7B). In general, younger animals (TG and WT) explored the center of the OF arena longer than the older animals, however, the TG 3 m.o mice explored the center much less compared to their respective WT controls (Figure 7C).

In female APP/PS1 mice, there was no difference between groups in the total distance traveled in the OF task (Figure 8A). As in male mice, we observed that aged female mice traveled less distance than younger ones, and that the TG-VEH mice walked a shorter distance when compared to the other conditions, as was reported previously

(Webster, et al., 2014). Contrary to male APP/PS1 mice, female mice spent more time in the corners similarly between groups, and this behavior was independent of age, genotype, and treatment (Figure 8B).

When we compared the differences between gender at 3 m.o (Annexes Figure 33), 12 m.o (Annexes Figure 34) and 18 m.o (Annexes figure 35) APP/PS1 mice, we did not find differences in the parameters considered for analysis in this behavioral test.

Table 1 Average results open field test. Data are presented as mean ± SEM.

	Total Distance Travelled		**% Time in the Corners**		**% Time in the Center**	
3 m.o	**Male**	**Female**	**Male**	**Female**	**Male**	**Female**
WT VEH	24.85 ± 2.81	21.61 ± 4.43	40.45 ± 7.67	58.62 ± 5.42	17.25 ± 5.91	9.41 ± 2.67
WT PBN	20.27 ± 3.02	23.66 ± 3.51	52.65 ± 5.30	55.39 ± 2.88	11.84 ± 1.97	10.27 ± 2.06
TG VEH	20.98 ± 5.53	25.16 ± 5.97	59.67 ± 9.34	55.89 ± 3.56	7.90 ± 2.66	5.78 ± 0.96
TG PBN	20.02 ± 3.49	16.66 ± 1.97	45.83 ± 6.30	61.57 ± 7.31	16.31 ± 4.55	9.30 ± 7.17
12 m.o	**Male**	**Female**	**Male**	**Female**	**Male**	**Female**
WT VEH	16.84 ± 4.16	20.56 ± 5.98	62.56 ± 10.07	65.57 ± 12.83	8.61 ± 3.64	6.10 ± 3.58
WT PBN	13.62 ± 5.02	17.71 ± 6.94	75.98 ± 12.27	52.94 ± 18.67	2.41 ± 1.56	23.30 ± 18.78
TG VEH	12.34 ± 2.50	11.48 ± 3.51	75.22 ± 6.83	75.25 ± 9.56	2.82 ± 1.05	5.29 ± 4.85
TG PBN	11.12 ± 2.88	19.16 ± 3.47	77.13 ± 6.66	63.12 ± 4.22	3.58 ± 1.41	6.11 ± 1.31
18 m.o	**Male**	**Female**	**Male**	**Female**	**Male**	**Female**

WT VEH	12.33 ± 3.11	12.45 ± 7.42	55.66 ± 3.53	77.52 ± 13.47	7.10 ± 2.53	3.66 ± 3.17
WT PBN	12.33 ± 3.11	16.77 ± 5.06	55.20 ± 13.58	68.96 ± 10.61	16.06 ± 7.43	5.38 ± 2.73
TG VEH	10.43 ± 5.46	4.72 ± 2.32	70.76 ± 7.68	63.93 ± 16.78	1.98 ± 1.03	4.07 ± 2.53
TG PBN	12.51 ± 3.92	12.00 ± 3.39	59.03 ± 1.56	51.10 ± 15.89	7.65 ± 2.40	21.09 ± 13.36

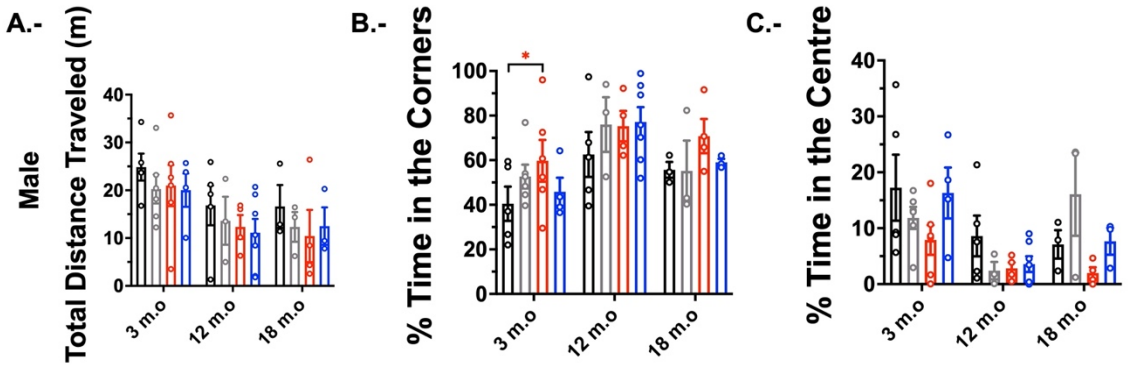

Figure 7 The treatment with probenecid does not affect *locomotor activity in male mice.* WT and APP/PS1 male mice *of 3, 12 or 18 m.o were* treated during 30 days with a dose of 100 mg/kg of PBN or its vehicle and then subjected to an Open field test. ***A.-*** *Average Total distance traveled during 10 min in the Open field maze of APP/PS1 animals (3m.o N=5 WT VEH (black); N=6 WT PBN (gray); N=6 TG VEH (red) and N=4 TG PBN (blue)12 m.o N=5 WT VEH (black); N=3 WT PBN (gray); N=4 TG VEH (red) and N=7 TG PBN (blue) 18 m.o N=3 WT VEH (black); N=3 WT PBN (gray); N=4 TG VEH (red); N=3 TG PBN (blue)). There was no significant difference between groups by Three-way ANOVA, but age was a significant source of variation F(2,25)=4.971 *p=0.0152* ***B.-*** *Percentage of the time spent in the corners in the Open field maze of APP/PS1 animals. There was no significant difference between groups by Three-way ANOVA, but age was a significant source of variation F(2,25)=6.841 **p=0.0043* ***C.-*** *Percentage of the time spent in the center of the Open field maze of APP/PS1 animals. There was no significant difference between groups by Three-way ANOVA, but age (F(2,25)=6.071 **p=0.0071) and genotype (F(1,16)=6.155 *p=0.0246) were significant sources of variation. Data are presented as mean ± SEM.*

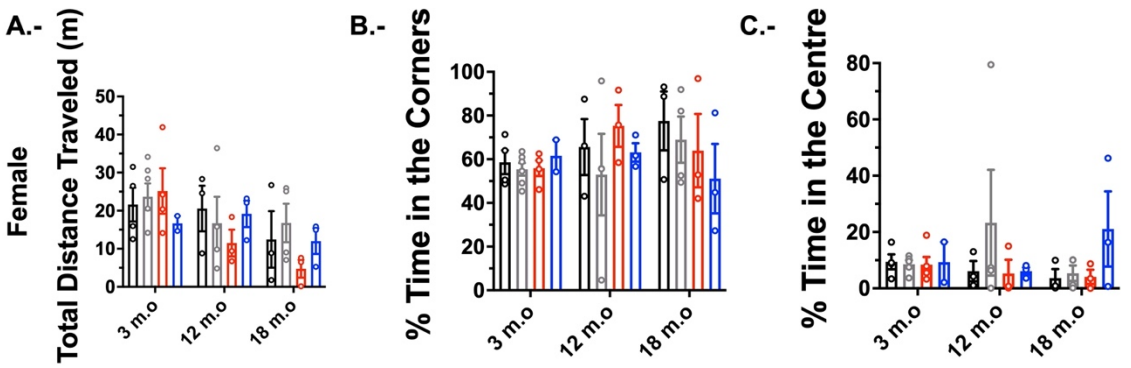

Figure 8. The treatment with probenecid does not affect* locomotor activity in female mice.** WT and APP/PS1 female mice of 3, 12 or 18 m.o were treated during 30 days with a dose of 100 mg/kg of PBN or its vehicle and then were subjected to an Open field test. ***A.- *Average Total distance traveled during 10 min in the Open field maze of APP/PS1 animals (3m.o N=4 WT VEH (black)*; N=6 *WT PBN (gray); N=4 TG VEH (red) and* N=2 *TG PBN (blue)12 m.o N=3 WT VEH (black); N=4 WT PBN (gray); N=2 TG VEH (red) and N=3 TG PBN (blue) 18 m.o N=3 WT VEH (black); N=4 WT PBN (gray); N=2 TG VEH (red); N=3 TG PBN (blue)). There was no significant difference between groups by T*hree-*way ANOVA.* ***B.-*** *Percentage of the time spent in the corners in the Open field maze of APP/PS1 animals. There was no significant difference between groups by* Three-*way ANOVA.* ***C.-*** *Percentage of the time spent in the center of the Open field maze of APP/PS1 animals. There was no significant difference between groups by T*hree-*way ANOVA. Data are presented as mean ± SEM.*

3. Probenecid Treatment prevents recognition memory defects in aged APP/PS1 mice.

After the evaluation of the locomotion activity with the OF test, we tested recognition memory by applying the NOR test. It has been previously reported that in APP/PS1 mice the performance in the NOR test is impaired at advanced ages according to the neuropathological progression (Webster, et al., 2014). As shown in Figure 9, male APP/PS1 and WT mice of all the experimental groups were exposed to the same pair of objects (object A and object B) for 3 days in an open field maze (sample phase). The Three-way ANOVA showed no significant difference in the time exploring the same pair of objects at 3 m.o, 12 m.o, and 18 m.o APP/PS1 and WT male and female mice.

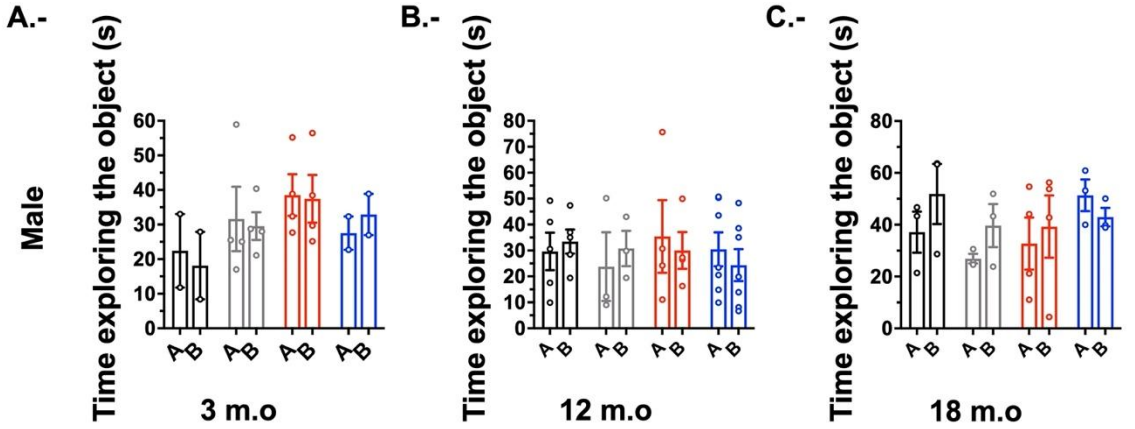

Figure 9 Probenecid treatment does not affect the time exploring the same pair of objects by male APP/PS1 mice in the sample phase of the Novel object recognition test. A.- *Average time exploring the same pair of objects of 3 m.o APP/PS1 animals (N=2 WT VEH (black); N=4 WT PBN (gray); N=4 TG VEH (red) and N=2 TG PBN (blue)). There was not a significant difference between groups by Three-way Anova.* ***B.-*** *Average time exploring the same pair of objects of 12 m.o APP/PS1 animals (N=5 WT VEH (black); N=3 WT PBN (gray); N=4 TG VEH (red) and N=7 TG PBN (blue). There was not a significant difference between groups by Three-way ANOVA.* ***C.-*** *Average time exploring the same pair of objects of 18 m.o APP/PS1 animals (N=3 WT VEH (black); N=3 WT PBN (gray); N=4 TG VEH (red); N=3 TG PBN (blue)). There was not a significant difference between groups by Three-way ANOVA. A and B correspond to the two identical objects presented to mice in the retention phase. Data are presented as mean ± SEM.*

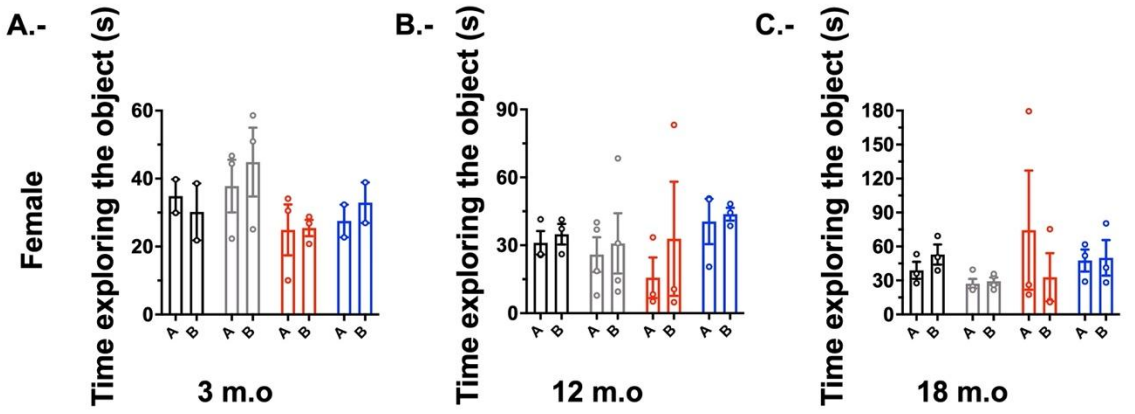

Figure 10 Probenecid treatment does not affect the time exploring the same pair of objects by female APP/PS1 mice in the sample phase of the Novel object recognition test. A.- *Average time exploring the same pair of objects of 3 m.o APP/PS1 animals (N=2 WT VEH (black); N=3 WT PBN (gray); N=3 TG VEH (red) and N=2 TG PBN (blue)). Genotype (F(1,4)=7.794 *p=0.0492) was a significant source of variation by Three-way Anova.* ***B.-*** *Average time exploring the same pair of objects of 12 m.o APP/PS1 animals (N=3 WT VEH (black); N=4 WT PBN (gray); N=3 TG VEH (red) and N=3 TG PBN (blue). There was not a significant difference between groups by Three-way ANOVA.* ***C.-*** *Average time exploring the same pair of objects of 18 m.o APP/PS1*

animals (N=3 WT VEH (black); N=4 WT PBN (gray); N=3 TG VEH (red); N=3 TG PBN (blue)). There was not a significant difference between groups by Three-way ANOVA. A and B correspond to the two identical objects presented to mice in the retention phase. Data are presented as mean ± SEM.

After a retention phase, in which mice returned to their cages for 1 h, one of the objects was replaced by a new one and the preference of the animals for the new object was estimated as the time that they spent exploring each one (Figures 11 and 12); the minimal time of exploration considered for further analysis was 20 seconds for both objects (N+F). According to what was expected, both male and female mice maintained their preference for novelty, which was reflected in a longer exploration time of the novel object over the familiar object (Tables 2 and 3). As was previously reported by other authors (Chaney, et al., 2018; Cheng, et al., 2019; Coles, et al., 2020; Faivre & Hölscher, 2013), older TG VEH mice spent less time exploring the novel object than the familiar one compared to their WT littermates, suggesting alterations in the recognition memory (Figures 11B and C and 12B and C). Interestingly, in the TG mice treated with PBN, we observed a significant increase in the time that males at 12-18 m.o explored the novel object (Figures 11B and 11C), while in female TG group treated with PBN at 18 m.o the exploration time was only significantly different compared to WT VEH.

To assess whether there was a gender effect on the exploration time of the novel object, the performance of males and females by age was compared (Annexes Figure 36), however, we observed that gender did not affect the exploration time of the novel object at the different ages.

***Table 2.* Average Time exploring the novel and the familiar objects in the test-phase of the Novel object recognition test for 3, 12, and 18 m.o male WT and APP/PS1 mice.**

Male	WT VEH		WT PBN		TG VEH		TG PBN	
	Familiar	Novel	Familiar	Novel	Familiar	Novel	Familiar	Novel
3 m.o	10.3 ± 2.5	18.6 ± 4.9	13.3 ± 1.5	22.8 ± 3.6	13.0 ± 1.7	30.6 ± 6.1 *	12.9 ± 3.0	17.4 ± 0.4
12 m.o	14.3 ± 2.8	21.9 ± 7.0	8.9 ± 4.6	12.6 ± 3.8	10.0 ± 5.4	9.6 ± 3.2	10.2 ± 2.1	17.3 ± 3.5 ⊥
18 m.o	27.4 ± 10.8	38.1 ± 11.1	10.1 ± 1.7	15.2 ± 6.0	21.9 ± 10.8	18.2 ± 1.2	19.7 ± 3.6	35.2 ± 6.9 ⊥

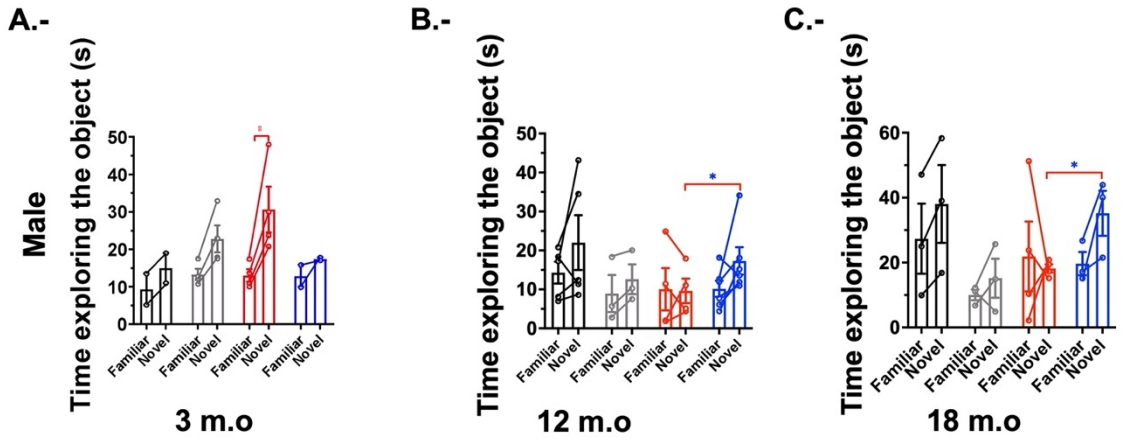

Figure 11 Probenecid treatment improved the time exploring the Novel object in the test phase of the Novel object recognition test in 12 and 18 m.o male APP/PS1 mice. A.- *Average time exploring different pairs of objects of 3 m.o male APP/PS1 animals (N=2 WT VEH (black); N=4 WT PBN (gray); N=4 TG VEH (red); N=2 TG PBN (blue)). The object (F(1,16)=10.00 **p=0.006) and genotype x treatment (F(1,16)=4.518 *p=0.0495) were significant sources of variation by Three-way Anova.* ***B.-*** *Average time exploring a different pair of objects of 12 m.o male APP/PS1 animals (N=5 WT VEH (black); N=3 WT PBN (gray); N=4 TG VEH (red) and N=6 TG PBN (blue). There was not a significant difference between groups by Three-way Anova, but multiple t-tests revealed significant differences between TG VEH and TG PBN (* p = 0.0494).* ***C.-*** *Average time exploring a different pair of objects of 18 m.o male APP/PS1 animals (N=3 WT VEH (black); N=3 WT PBN (gray); N=4 TG VEH (red); N=3 TG PBN (blue)). Genotype x treatment (F(1,18)=6.101, * p = 0.0237) was a significant source of variation by Three-way ANOVA, and multiple t-tests revealed significant differences between TG VEH and TG PBN (* p = 0.036).*

<u>Table 3</u>. Average Time exploring the novel and the familiar objects in the test-phase of the Novel object recognition test for 3, 12, and 18 m.o female WT and APP/PS1 mice.

Female	WT VEH		WT PBN		TG VEH		TG PBN	
	Familiar	Novel	Familiar	Novel	Familiar	Novel	Familiar	Novel

3 m.o	11.2 ± 4.1	22.2 ± 10.2	14.6 ± 0.9	25.3 ± 5.9	8.3 ± 2.6	11.7 ± 2.8	11.2 ± 0.3	21.8 ± 0.3
12 m.o	16.5 ± 5.8	18.5 ± 5.3	10.4 ± 1.2	16.9 ± 5.7	14.4 ± 11.7	5.9 ± 4.3 *	14.2 ± 4.1	22.3 ± 6.7
18 m.o	46.5 ± 18.5	39.8 ± 3.6	23.1 ± 7.9	30.6 ± 5.3	67.1 ± 52.1	14.4 ± 2.3	18.1 ± 2.7	47.5 ± 16.6

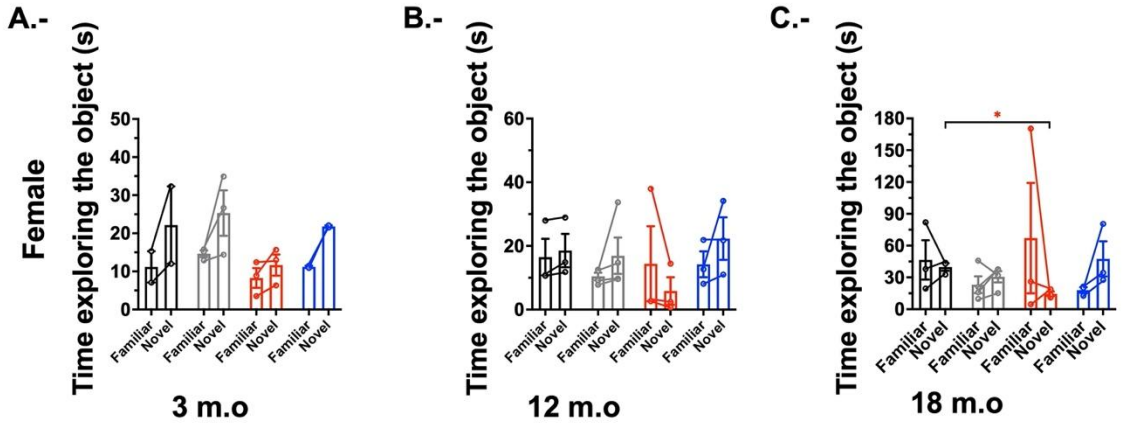

Figure 12 Probenecid treatment improved the time exploring the Novel object in the test phase of the Novel object recognition test of 12 and 18 m.o female APP/PS1 animals. A.- *Average time exploring different pairs of objects of 3 m.o female APP/PS1 animals (N=2 WT VEH (black); N=3 WT PBN (gray); N=3 TG VEH (red); N=2 TG PBN (blue)). The object (F(1,8)=7.391 *p=0.0263) was a significant source of variation by Three-way Anova.* ***B.-*** *Average time exploring a different pair of objects of 12 m.o female APP/PS1 animals (N=3 WT VEH (black); N=4 WT PBN (gray); N=3 TG VEH (red) and N=3 TG PBN (blue). There was not a significant difference between groups by Three-way Anova.* ***C.-*** *Average time exploring a different pair of objects of 18 m.o female APP/PS1 animals (N=3 WT VEH (black); N=4 WT PBN (gray); N=3 TG VEH (red); N=3 TG PBN (blue)). There was not a significant difference between groups by Three-way ANOVA, and multiple t-tests revealed significant differences between WT VEH and TG VEH (* p = 0.0214).*

Another way to assess the recognition memory with the NOR test was through the Discrimination Index (DI) and the percentage of time exploring the novel object (Figures 13 and 14). The discrimination index (DI) was calculated as [(N – F / total time of exploration) * 100] (Figures 13A and 14A). Positive values of the DI indicate a greater preference for the novel object, zero corresponds to the exploration of both objects

equally, and negative values indicate a greater exploration of the familiar object. Reflecting the above results, young male and female TG VEH mice (Figures 13A and 14A) had a greater preference for exploring the novel over the familiar object. However, both 12 m.o and 18 m.o TG VEH mice had a greater preference for exploring the familiar object than the novel object, according to what has been reported for this model at those ages (Chaney, et al., 2018; Cheng, et al., 2019; Coles, et al., 2020; Faivre & Hölscher, 2013). Surprisingly, the treatment with PBN in male and female 12 m.o, and 18 m.o APP/PS1 mice prevented this recognition memory defect, increasing their preference for the novel object over the familiar one.

To assess whether there was a gender effect on the DI, the performance of males and females was compared at different ages (Annexes Figure 37). Nevertheless, we didn´t found differences between gender. Also, we assessed the percentage of time exploring the novel object and found that both male (Figure 13B) and female (Figure 14B) young APP/PS1 mice explored the novel object to a similar extent, whilst older TG VEH animals explored the novel object to a lesser extent compared to their respective control, strongly suggesting a cognitive impairment. Remarkably, in the TG-groups, the treatment with PBN significantly increased the percentage of exploration time of the novel object compared to TG VEH, reaching similar levels as those exhibited by WT animals. Finally, comparison of the percentage of the novel object exploration time between gender at different ages revealed no differences (Annexes Figure 38).

Together, these data evidenced a deterioration in the recognition memory in the 12 m.o and 18 m.o APP/PS1 TG mice, as suggested by a worse performance than their WT littermates in both, the discrimination index and in the percentage of the exploration of the novel object. Such deterioration appeared to be prevented by the treatment with PBN.

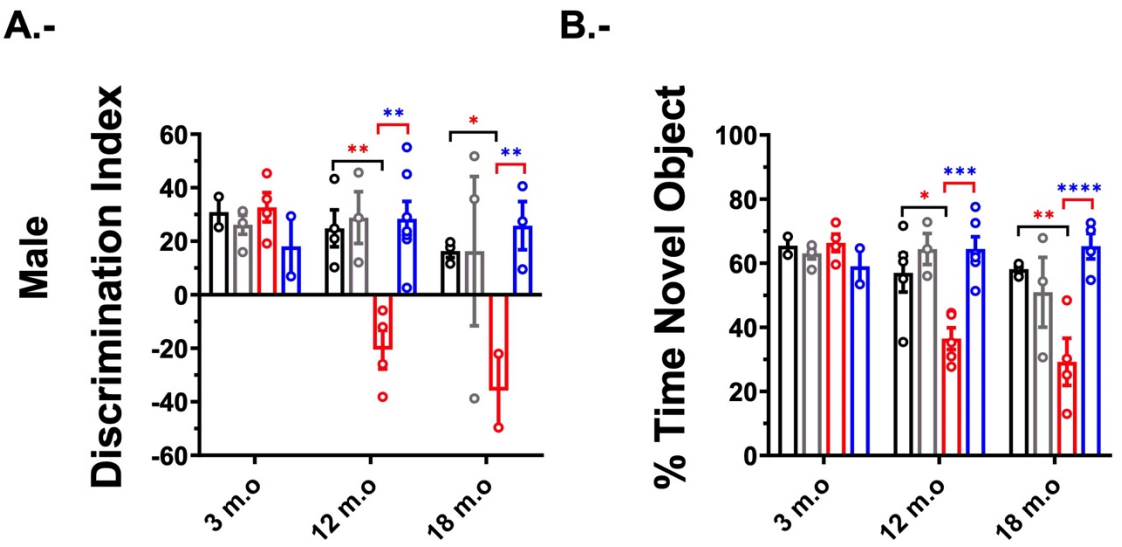

Figure 13. Probenecid treatment prevents impairments in the recognition memory in aged male APP/PS1 mice. A.- Average Discrimination Index (DI) of 3 m.o (N=2 WT VEH (black); N=4 WT PBN (gray); N=4 TG VEH (red) and N=2 TG PBN (blue)), 12 m.o (N=5 WT VEH (black); N=3 WT PBN (gray); N=4 TG VEH (red) and N=6 TG PBN (blue) and 18 m.o (N=3 WT VEH (black); N=3 WT PBN (gray); N=4 TG VEH (red); N=3 TG PBN (blue)) male APP/PS1 animals. Age ($F(2,29)=3.555$ * $p=0.0416$), genotype ($F(1,29)=6.598$ *$p=0.0156$), and treatment ($F(1,29)=6.655$ *$p=0.0152$) were significant sources of variation, and there was a significant interaction between age x treatment ($F(2,29)=4.040$ *$p=0.0283$) and genotype x treatment ($F(1,29)=6.873$ *$p=0.0138$) by Three-way ANOVA and Tukey's multiple comparison tests revealed significant differences between 12 m.o: WT VEH-TG VEH ** p=0.086; TG VEH-TG PBN ** p = 0.0012 18 m.o: WT VEH-TG VEH * p=0.0217; TG VEH-TG PBN ** p = 0.0054. **B.-** Average the percentage of time exploring the novel object of 3 m.o, 12 m.o, and 18 m.o male APP/PS1 animals. Age ($F(2,33)=4.788$ * $p=0.0149$) and treatment ($F(1,33)=8.364$ ** $p=0.0067$) were significant sources of variation and there was a significant interaction between Age x treatment ($F(2,33)=4.538$ * $p=0.0181$), genotype x treatment ($F(1,33)=9.752$ ** p = 0.0037), age x genotype x treatment ($F(2,33)=4.377$ *$p=0.0206$) by Three-way ANOVA and Tukey's multiple comparison tests revealed significant differences between 12 m.o: WT VEH-TG VEH * p=0.0135; TG VEH-TG PBN *** p = 0.0003 18 m.o: WT VEH-TG VEH ** p =0.0032;TG VEH-TG PBN **** p<0.0001. Data are presented as mean ± SEM.

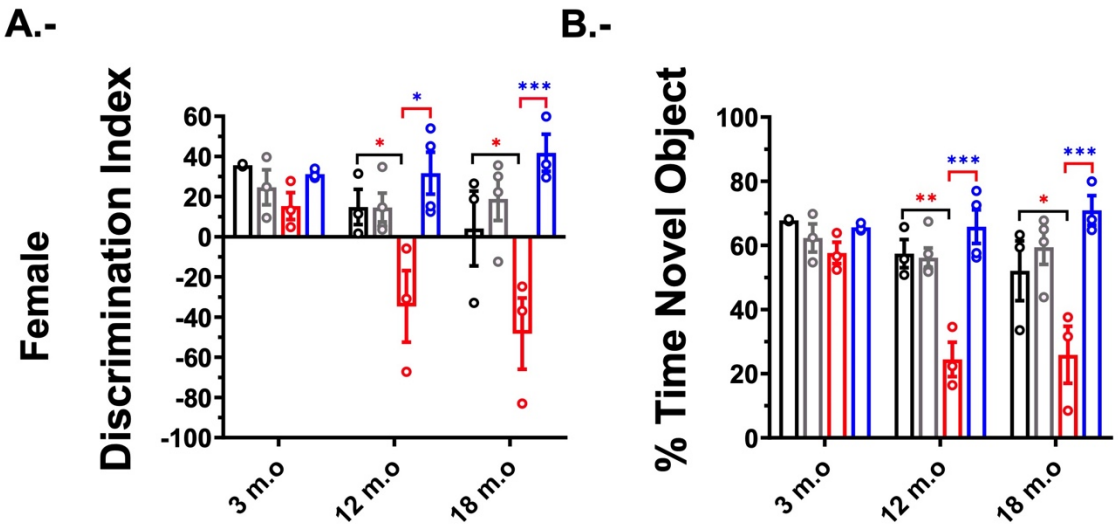

Figure 14. Probenecid treatment prevents recognition memory impairments in female aged-APP/PS1 mice. A.- *Average Discrimination Index (DI) of 3 m.o (N=2 WT VEH (black); N=3 WT PBN (gray); N=3 TG VEH (red) and N=2 TG PBN (blue)), 12 m.o (N=3 WT VEH (black); N=4 WT PBN (gray); N=3 TG VEH (red) and N=3 TG PBN (blue) and 18 m.o (N=3 WT VEH (black); N=4 WT PBN (gray); N=3 TG VEH (red); N=3 TG PBN (blue)) female APP/PS1 animals. Genotype (F(1,12)=7.714 *p=0.0167), and treatment (F(1,14)=12.52 **p=0.0033) were significant sources of variation, and there was a significant interaction between genotype x treatment (F(1,12)=41.18 ****p<0.0001) by Three-way ANOVA and Tukey's multiple comparison tests revealed significant differences between 12 m.o: WT VEH-TG VEH * p=0.0229; TG VEH-TG PBN * p = 0.0104; 18 m.o: WT VEH-TG VEH *p= 0.0152 TG VEH-TG PBN *** p = 0.0003* ***B.-*** *Average the percentage of time exploring the novel object of 3 m.o, 12 m.o, and 18 m.o female APP/PS1 animals. Age (F(2,15)=4.699 * p=0.0260) genotype (F(1,12)=9.419 ** p=0.0097) and treatment (F(1,15)=19.00 *** p=0.0006) were significant sources of variation and there was a significant interaction between Age x treatment (F(2,15)=4.350 * p=0.0324), genotype x treatment (F(1,12)=41.65 **** p<0.0001) by Three-way ANOVA and Tukey's multiple comparison tests revealed significant differences between 12 m.o: WT VEH-TG VEH ** p=0.0050; TG VEH-TG PBN *** p = 0.0003 18 m.o: WT VEH-TG VEH * p =0.0288;TG VEH-TG PBN *** p = 0.0001. Data are presented as mean ± SEM.*

4. Probenecid Treatment prevents the loss of spatial and reference memory in 12 and 18 m.o APP/PS1 mice.

To evaluate the effect of the PBN treatment in the spatial memory in mice we applied the MWM task. The animals were trained for five days (6 trials per day) to find an escape platform in a pool, following visual cues (Acquisition phase) (Figures 15 and 16).

As shown in figure 15, there were no significant differences between 3 m.o male and female WT and TG mice treated with VEH as revealed by the escape latency in the acquisition phase (Figure 15A and 16A), nor in the last day of training (Figure 17) as expected in the early stages of the disease.

When applying the MWM test to aged 12 m.o mice (Figures 15B and 16B), we found that the male and female groups of TG VEH mice presented a deteriorated performance in the acquisition phase compared to their WT littermates, as it has been described by other authors (Webster, et al., 2014; Currais, et al., 2014; Daugherty, et al., 2017; Faivre & Hölscher, 2013; Fan, et al., 2018; Fragoulis, et al., 2017; Habib, et al., 2019). Remarkably, the treatment with PBN prevented such deterioration in the performance of 12 m.o male and female TG mice which exhibited a lower escape latency (Figure 15B and 16B).

In the group of 18 m.o mice (Figures 15C and 16C), we found that the female TG VEH animals presented a deteriorated performance in the acquisition phase compared to their WT littermates, as it has been previously described by other authors (Hashimoto, et al., 2021; Heneka, et al., 2013; Savonenko, et al., 2005) and notably PBN treatment in TG PBN female group prevented the reduction in the escape latency as observed in TG VEH mice (Figure 16C).

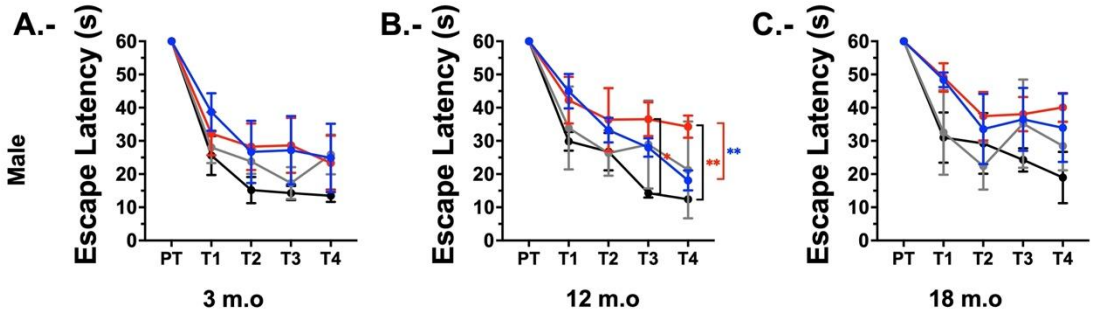

Figure 15: Probenecid treatment prevents spatial memory impairments in 12m.o male APP/PS1 mice. A.- *Young APP/PS1 animals did not show cognitive impairment in Spatial learning in the acquisition phase of the MWM task (N=6 WT VEH (black); N = 6 WT PBN (gray); N=6 TG VEH (red) and N=4 TG PBN (blue)). Time (F(4,68)=59.11, **** p<0.0001) was the main source of variation by Three-way ANOVA.* ***B.-*** *12 m.o male APP/PS1 animals presented cognitive impairment in a spatial memory task, that was prevented by the treatment with Probenecid. (N=5 WT VEH (black); N = 5 WT PBN (gray); N=5 TG VEH (red) and N=7 TG PBN (blue)). Time (F(4,56)=59.85 **** p<0.0001) was the main source of variation and there was a significant interaction of time x genotype x treatment (F(4,56)=2.609, * p=0.0451) by Three-way ANOVA. Tukey's multiple comparisons test T3 * p = 0.022 T4 WT VEH – TG VEH ** p = 0.009; TG VEH - TG PBN ** p=0.0071.* ***C.-*** *18 m.o male APP/PS1 animals presented cognitive impairment in a spatial memory task, that was not prevented by the treatment with Probenecid. (N=3 WT VEH (black); N = 3 WT PBN (gray); N=4 TG VEH (red) and N=3 TG PBN (blue)). Time (F(4,36)=21.16, **** p<0.0001) was the main sources of variation by Three-way ANOVA. Data are presented as mean ± SEM.*

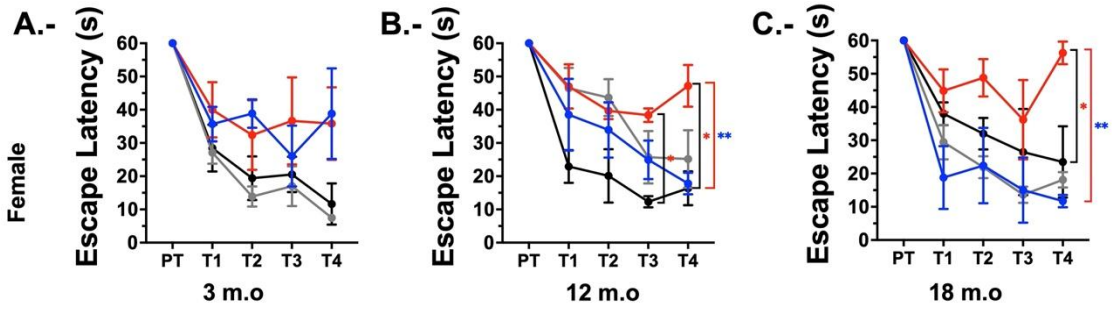

Figure 16 Probenecid treatment prevents spatial memory impairments in 12m.o and 18 m.o female APP/PS1 mice. A.- *Young female APP/PS1 animals did not show cognitive impairment in Spatial learning in the acquisition phase of the MWM task (N=4 WT VEH (black); N = 6 WT PBN (gray); N=4 TG VEH (red) and N=3 TG PBN (blue)). Time (F(4,52)=40.25, **** p<0.0001) and genotype (F(1,13)=7.901, * p=0.0147) were the main source of variation and there was a significant interaction between time x genotype (F(4,52)=4.633, ** p=0.0028 by Three-way ANOVA.* ***B.-*** *12 m.o female APP/PS1 animals presented cognitive impairment in a spatial memory task, that was prevented by the treatment with Probenecid. (N=3 WT VEH (black); N = 4 WT PBN (gray); N=3 TG VEH (red) and N=3 TG PBN (blue)). Time (F(2.055,16.44)=26.18, **** p<0.0001) was the main source of variation and there was a significant interaction of genotype x treatment (F(1,8)=9.309, * p=0.0158) by Three-way ANOVA. Tukey's multiple comparisons test T3*

** p = 0.0286 T4 WT VEH – TG VEH * p = 0.0104; TG VEH - TG PBN ** p=0.0073.* ***C.-*** *18 m.o female APP/PS1 animals presented cognitive impairment in a spatial memory task, that was prevented by the treatment with Probenecid. (N=3 WT VEH (black); N = 4 WT PBN (gray); N=3 TG VEH (red) and N=2 TG PBN (blue)). Time (F(4,32)=35.32, **** p<0.0001) and treatment (F(1,8)=11.75, ** p=0.0090) were the main sources of variation and there was a significant interaction between time x treatment (F(4,32)=3.559, * p=0.0164) by Three-way ANOVA. Data are presented as mean ± SEM.*

To further analyze the impact of the PBN treatment on spatial memory in TG mice, we compared the escape latency time for all the age-groups in both male and female APP/PS1 mice during the last day of the acquisition phase (Figure 17). Both male (Figure 17A) and female (Figure 17B) TG mice showed a progressive increase in the latency time with age. In male APP/PS1 mice, we observed a preventive effect of PBN at 12 m.o, whilst in females, we observed this preventive effect of PBN at both 12 and 18 m.o

Further comparison of males and females escape latency performances by age revealed no significant differences (Annexes Figure 39).

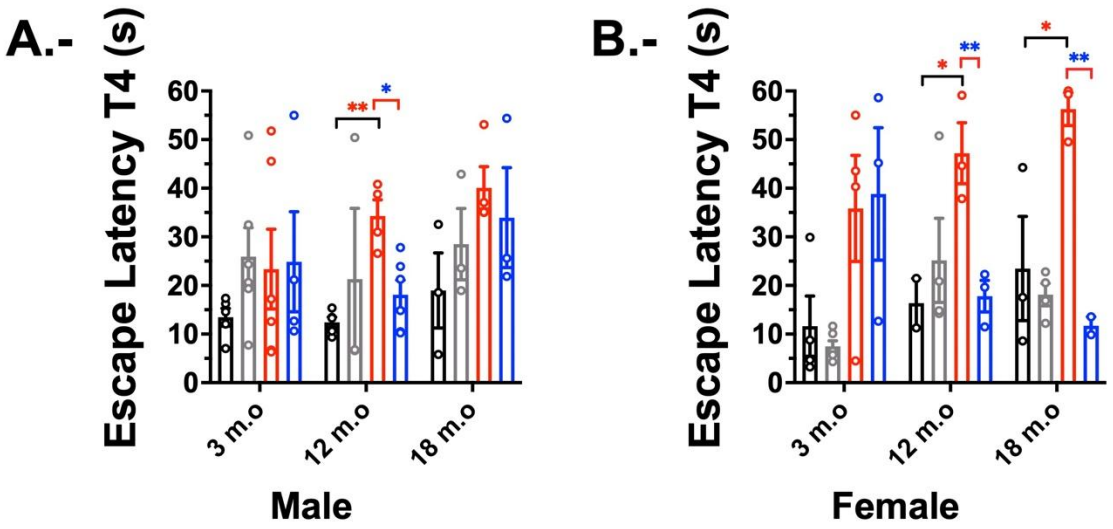

Figure 17 Probenecid treatment prevented spatial memory impairments in 12m.o male and female and 18 female APP/PS1 animals. A.- *Average escape latency on the last day of training in the acquisition phase of the Morris water maze task of 3 m.o 12 m.o*

*and 18 m.o male APP/PS1 animals (3 m.o N=5 WT VEH (black); N = 6 WT PBN (gray); N=6 TG VEH (red) and N=4 TG PBN (blue); 12 m.o N=5 WT VEH (black); N = 3 WT PBN (gray); N=3 TG VEH (red) and N=7 TG PBN (blue); 18 m.o N=3 WT VEH (black); N = 3 WT PBN (gray); N=4 TG VEH (red) and N=3 TG PBN (blue)). Genotype (F(1,16)=9.308, ** p=0.0076) was the main source of variation and there was a significant interaction between genotype x treatment (F(1,16)=8.928, ** p=0.0087 by Three-way ANOVA and Tukey's multiple comparisons tests revealed a significant difference between 12 m.o: WT VEH - TG VEH ** p=0.0090 and TG VEH – TG PBN * p=0.0338.* ***B.-*** *Average escape latency on the last day of training in the acquisition phase of the Morris water maze task of 3 m.o 12 m.o and 18 m.o female APP/PS1 animals (3 m.o N=4 WT VEH (black); N = 6 WT PBN (gray); N=4 TG VEH (red) and N=3 TG PBN (blue); 12 m.o N=3 WT VEH (black); N = 4 WT PBN (gray); N=3 TG VEH (red) and N=3 TG PBN (blue); 18 m.o N=3 WT VEH (black); N = 4 WT PBN (gray); N=3 TG VEH (red) and N=2 TG PBN (blue)). Genotype (F(1,11)=16.52, ** p=0.0019) and treatment (F(1,18)=7.542, * p=0.0133) were the main sources of variation and there was a significant interaction between genotype x treatment (F(1,11)=7.352, * p=0.0202 by Three-way ANOVA and Tukey's multiple comparisons tests revealed a significant difference between 12 m.o: WT VEH - TG VEH * p=0.0104 and TG VEH – TG PBN ** p=0.0073; 18 m.o: WT VEH - TG VEH * p=0.0253 and TG VEH – TG PBN ** p=0.0051.*

In a second test-phase of the MWM task, the escape platform was hidden keeping the visual cues, and we evaluated the time that animals spent in the quadrant where the platform was previously visible (Figures 18 and 19). In this "test phase", in which reference memory was measured, males and females 3 m.o APP/PS1 mice explored the quadrant of the platform in a similar way than their WT littermates, suggesting that there were not defects in the reference memory at young ages. However, in the 12 m.o and 18 m.o, male and female TG VEH mice presented a deteriorated performance in the test phase compared to their WT littermates (Figures 18 and 19), in agreement with that has been described by other authors (Webster, et al., 2014; Currais, et al., 2014; Daugherty , et al., 2017; Faivre & Hölscher, 2013; Fan, et al., 2018; Fragoulis, et al., 2017; Habib, et al., 2019; Hashimoto, et al., 2021; Heneka, et al., 2013; Savonenko, et al., 2005). Remarkably, the treatment with PBN significantly prevented such defects, increasing the time that 12 m.o and 18m.o male and female TG animals spent in the target quadrant, 24 hours after the acquisition phase (Figures 18 and 19). These results could mean that

PBN positively affects the mechanisms that mediate spatial learning in 12 m.o and 18 m.o APP/PS1 animals.

Finally, to assess whether there was a gender effect on the time that mice spent in the target quadrant, the performance of males and females by age was compared (Annexes Figure 40). Indeed, we found a significant difference between male and females at 18 m.o in WT PBN group.

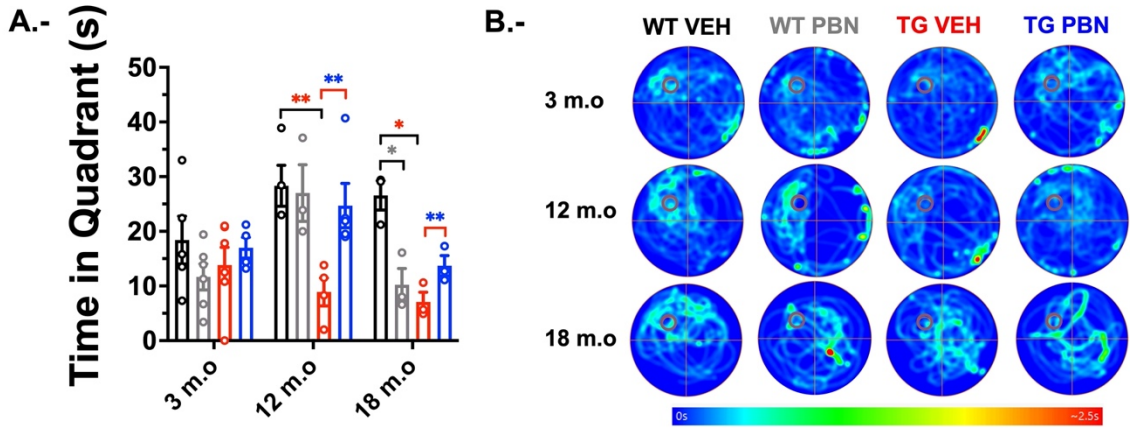

Figure 18 Probenecid treatment prevents reference memory impairments in 12m.o and 18 male APP/PS1 animals. A.- *Average time spent in the target quadrant in the probe phase of the Morris water maze task (3 m.o N=5 WT VEH (black); N = 6 WT PBN (gray); N=6 TG VEH (red) and N=4 TG PBN (blue); 12 m.o N=5 WT VEH (black); N = 3 WT PBN (gray); N=3 TG VEH (red) and N=7 TG PBN (blue); 18 m.o N=3 WT VEH (black); N = 3 WT PBN (gray); N=4 TG VEH (red) and N=3 TG PBN (blue)). Age (F(2,21)=4.287, * p=0.0275) and genotype (F(1,16)=13.73, ** p=0.0019) were the main sources of variation and there was a significant interaction between age x genotype (F(2,16)=4.347, * p=0.0311) and genotype x treatment (F(1,16)=26.16, *** p=0.0001).* ***B.-*** *Representative average heatmaps of probe phase of the Morris water maze task of 3 m.o, 12 m.o, and 18 m.o male APP/PS1 animals. Data are presented as mean ± SEM.*

Table 4. Average Time exploring the quadrants 24h after the acquisition phase of 3 m.o, 12 m.o and 18 m.o male APP/PS1 mice. *Data are presented as mean ± SEM.*

	WT VEH			
	NE (TQ)	**NW**	**SE**	**SW**
3 m.o	18.40 ± 4.37	13.92 ± 1.21	8.96 ± 1.65	16.84 ± 4.93
12 m.o	22.60 ± 5.30	11.28 ± 1.89	8.30 ± 1.77	16.42 ± 3.25

18 m.o	23.23 ± 6.02	18.83 ± 3.93	7.07 ± 0.75	9.07 ± 4.05
	WT PBN			
	NE (TQ)	**NW**	**SE**	**SW**
3 m.o	11.67 ± 2.39	13.12 ± 2.27	14.83 ± 3.77	18.78 ± 3.32
12 m.o	20.33 ± 10.86	21.13 ± 2.42	4.87 ± 2.09	11.70 ± 8.81
18 m.o	10.23 ± 2.96	13.80 ± 5.26	10.20 ± 6.23	24.43 ± 4.99
	TG VEH			
	NE (TQ)	**NW**	**SE**	**SW**
3 m.o	13.82 ± 3.26	14.70 ± 3.42	9.31 ± 2.38	20.92 ± 7.89
12 m.o	8.90 ± 2.56	20.73 ± 4.40	20.45 ± 8.41	9.20 ± 4.94
18 m.o	6.28 ± 1.49	17.38 ± 1.35	17.40 ± 2.99	17.78 ± 4.40
	TG PBN			
	NE (TQ)	**NW**	**SE**	**SW**
3 m.o	17.00 ± 1.91	16.83 ± 1.76	8.35 ± 2.57	16.65 ± 3.21
12 m.o	23.30 ± 3.59	13.08 ± 2.32	10.35 ± 3.56	12.25 ± 2.18
18 m.o	13.7 ± 1.86	16.27 ± 2.11	9.77 ± 3.66	19.03 ± 0.79

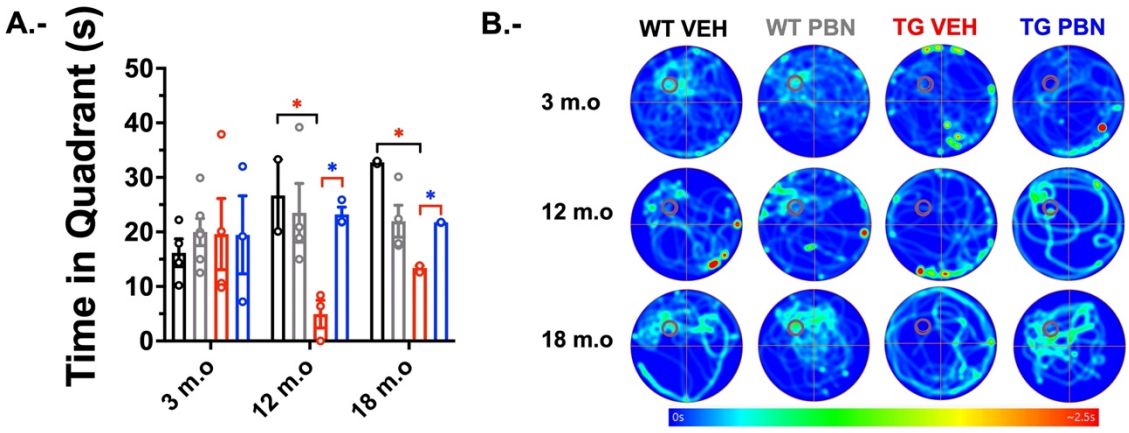

Figure 19 Probenecid treatment prevents reference memory impairments in 12m.o and 18 female APP/PS1 animals. A.- *Average time spent in the target quadrant in the probe phase of the Morris water maze task (3 m.o N=4 WT VEH (black); N = 6 WT PBN (gray); N=4 TG VEH (red) and N=3 TG PBN (blue); 12 m.o N=3 WT VEH (black); N = 4 WT PBN (gray); N=3 TG VEH (red) and N=3 TG PBN (blue); 18 m.o N=3 WT VEH (black); N = 4 WT PBN (gray); N=3 TG VEH (red) and N=2 TG PBN (blue)). Genotype (F(1,10)=10.74, ** p=0.0083) was the main source of variation and there was a significant interaction between age x genotype (F(2,10)=4.283, * p=0.0453), genotype x treatment (F(1,10)=8.140, * p=0.0172) and age x genotype x treatment (F(2,10)=4.569, * p=0.039) by Three-way ANOVA; and Tukey's multiple comparisons tests revealed a significant difference between 12 m.o WT VEH-TG VEH * p=0.0223 TG VEH – TG PBN * p=0.0347; 18 m.o WT VEH-TG VEH * p=0.0488 TG VEH – TG PBN * p=0.0483.* ***B.-*** *Representative average heatmaps of probe phase of the Morris water maze task of 3 m.o, 12 m.o, and 18 m.o female APP/PS1 animals. Data are presented as mean ± SEM.*

Table 5. ***Average Time exploring the quadrants 24h after the acquisition phase of 3 m.o, 12 m.o and 18 m.o female APP/PS1 mice.*** *Data are presented as mean ± SEM.*

	WT VEH			
	NE (TQ)	**NW**	**SE**	**SW**
3 m.o	15.80 ± 1.99	16.52 ± 1.81	11.82 ± 1.64	13.67 ± 2.64
12 m.o	26.70 ± 6.60	8.25 ± 1.25	10.00 ± 6.10	14.40 ± 2.30
18 m.o	32.75 ± 0.25	19.15 ± 1.65	2.95 ± 2.15	2.70 ± 1.60
	WT PBN			
	NE (TQ)	**NW**	**SE**	**SW**
3 m.o	20.08 ± 3.07	16.02 ± 1.15	11.5 ± 2.22	9.76 ± 1.49
12 m.o	23.50 ± 5.38	12.13 ± 2.67	9.93 ± 2.14	14.08 ± 5.25
18 m.o	21.98 ± 2.93	18.53 ± 1.34	7.35 ± 2.66	9.95 ± 2.51
	TG VEH			
	NE (TQ)	**NW**	**SE**	**SW**
3 m.o	22.6 ± 8.21	13.43 ± 3.09	5.90 ± 4.18	21.23 ± 9.44
12 m.o	4.93 ± 2.53	7.80 ± 7.80	25.93 ± 5.36	20.93 ± 4.57
18 m.o	13.4 ± 0.40	18.37 ± 6.53	9.57 ± 2.76	18.63 ± 4.85
	TG PBN			
	NE (TQ)	**NW**	**SE**	**SW**
3 m.o	17.90 ± 5.30	13.43 ± 1.38	12.13 ± 2.48	16.25 ± 4.83
12 m.o	22.27 ± 2.00	5.67 ± 2.72	14.93 ± 5.93	15.97 ± 4.45
18 m.o	21.75 ± 0.05	17.00 ± 1.40	12.55 ± 0.35	7.20 ± 1.90

5. Probenecid prevents Panx1 overactivity in hippocampal slices of 3 and 12 m.o APP/PS1 mice.

Once behavioral tests were finished, experimental groups were sacrificed to dissect brains and obtain acute slices for *ex vivo* experiments.

To demonstrate that the treatment with PBN inhibits the Panx1 activity, we evaluated the uptake of the fluorescent tracer ethidium bromide in hippocampal slices of 3 m.o (Figures 20 and 21) and 12 m.o (Figures 22 and 23) APP/PS1 mice. In the case of 3 m.o animals a slight increase in the EtBr uptake in hippocampal slices of both females and

males was observed in TG VEH compared to WT. These differences were significantly decreased in tissues from TG mice treated with PBN (Figures 20 and 21). Instead, in male and female 12m.o APP/PS1 mice we observed a significant increase in the levels of uptake of the EtBr tracer in the hippocampal slices of TG VEH animals, which significantly decreased in the tissues from TG mice treated with PBN (Figures 22 and 23).

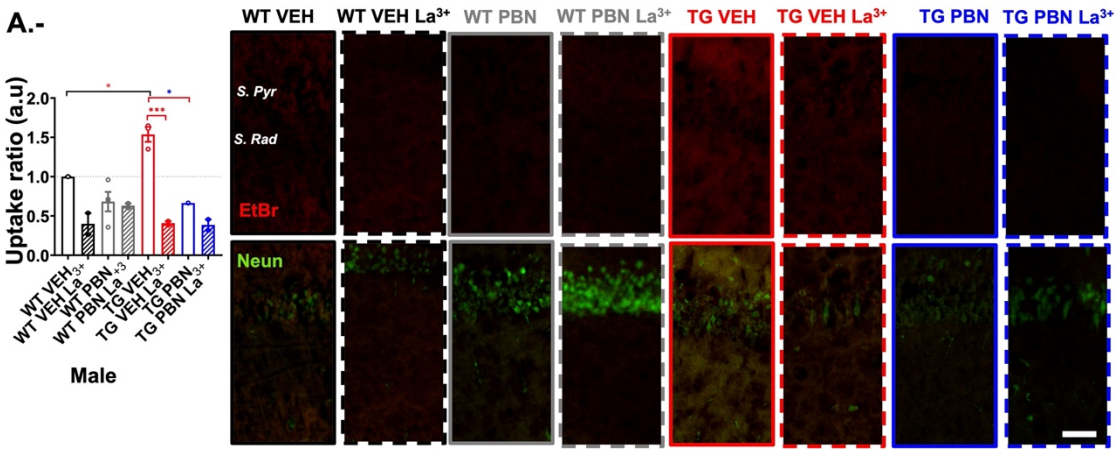

Figure 20 PBN treatment reduces the Panx1 activity in hippocampal slices of 3 m.o male APP/PS1 mice. A.- *EtBr uptake ratio normalized to WT VEH group and representative images of EtBr by pyramidal neurons from hippocampal CA1 area treated with 200 ∫M La^{+3} under resting conditions of 3 m.o male APP/PS1 mice (N=2 WT VEH (black); N = 2 WT PBN (gray); N=2 TG VEH (red) and N=1 TG PBN (blue)) Ordinary one-way ANOVA showed a significant difference between groups (F(7,10)=13.88, *** p = 0.0002) and Tukey's multiple comparisons test showed a significant difference between WT VEH-TG VEH * p=0.0212 TG VEH – TG VEH La^{3+} *** p=0.0004: TG VEH-TG PBN * p = 0.0175 Data are presented as mean per animal ± SEM.S pyr, stratum pyramidale; S rad. Stratum radiatum. Scale bar = 50μm.*

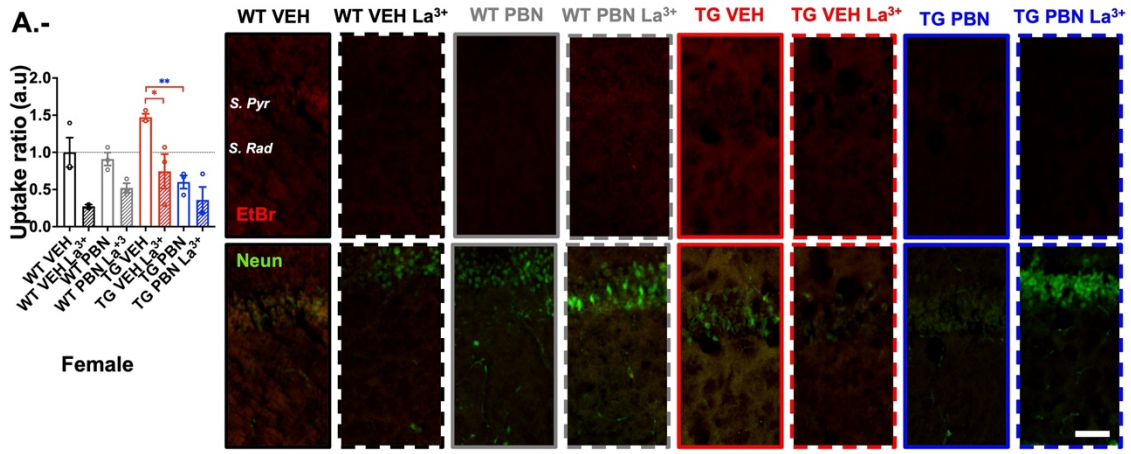

Figure 21 PBN treatment reduces the Panx1 activity in hippocampal slices of 3 m.o female APP/PS1 mice. A.- *EtBr uptake ratio normalized to WT VEH group and representative images of EtBr by pyramidal neurons from hippocampal CA1 area treated with 200 ⎍M La^{+3} under resting conditions of 3 m.o female APP/PS1 mice (N=3 WT VEH (black); N = 3 WT PBN (gray); N=3 TG VEH (red) and N=3 TG PBN (blue)). Ordinary one-way ANOVA showed significant difference between groups (F(7,15)=7.270, *** p = 0.0007) and Tukey's multiple comparisons test showed significant difference between: TG VEH – TG VEH La^{3+} * p=0.0348: TG VEH-TG PBN ** p = 0.0089. Data are presented as mean per animal ± SEM.S pyr, stratum pyramidale; S rad. Stratum radiatum. Scale bar = 50μm.*

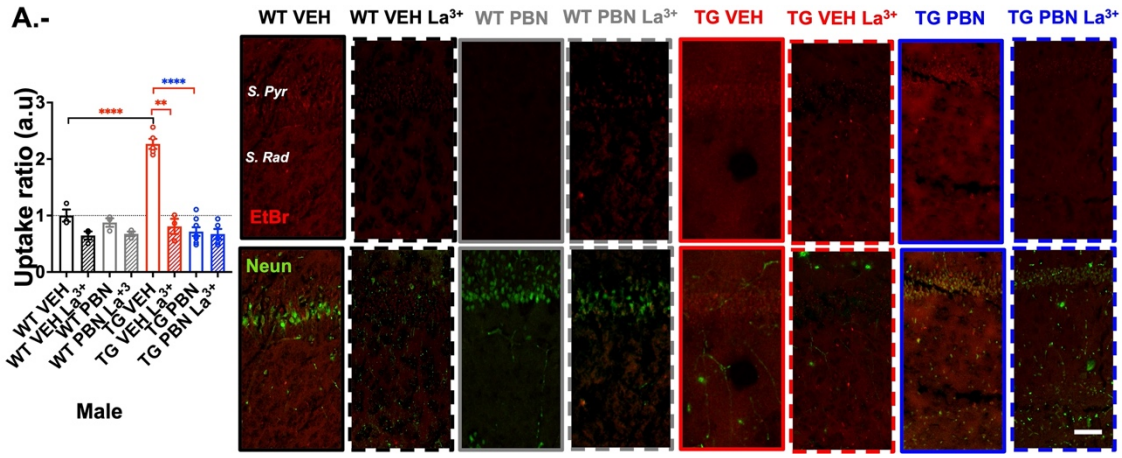

Figure 22 PBN treatment reduces the Panx1 activity in hippocampal slices of 12 m.o male APP/PS1 mice. A.- *EtBr uptake ratio normalized to WT VEH group and representative images of EtBr by pyramidal neurons from hippocampal CA1 area treated with 200 ⎍M La^{+3} under resting conditions of 12 m.o male APP/PS1 mice (N=3 WT VEH (black); N = 3 WT PBN (gray); N=3 TG VEH (red) and N=3 TG PBN (blue)) Ordinary one-way ANOVA showed a significant difference between groups (F(7,25)=39.52, ****

*p<0.0001) and Tukey's multiple comparisons test showed significant difference between: WT VEH-TG VEH **** p<0.0001; TG VEH – TG VEH La^{3+} **** p<0.0001: TG VEH-TG PBN **** p<0.0001. Data are presented as mean per animal ± SEM.S pyr, stratum pyramidale; S rad. Stratum radiatum. Scale bar = 50μm.*

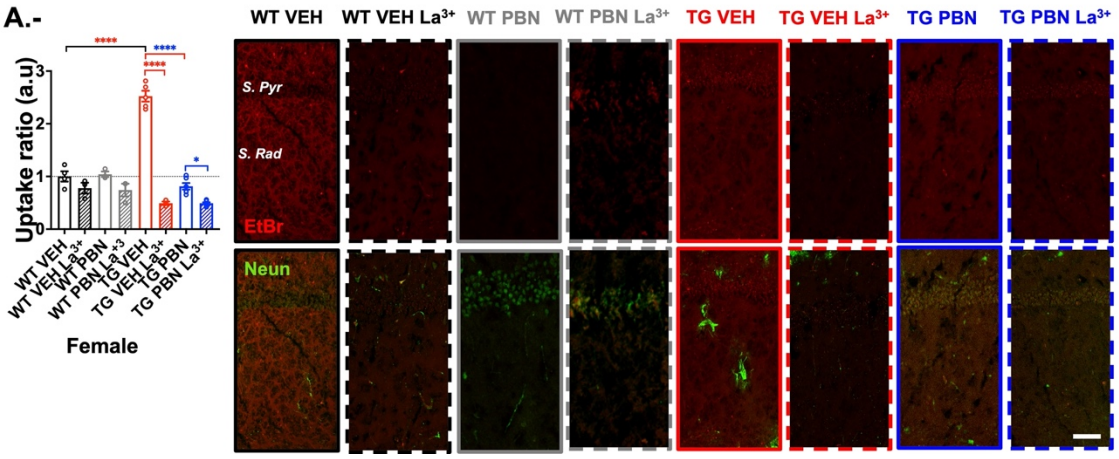

Figure 23 PBN treatment reduces the Panx1 activity in hippocampal slices of 12 m.o female APP/PS1 mice. A.- *EtBr uptake ratio normalized to WT VEH group and representative images of EtBr by pyramidal neurons from hippocampal CA1 area treated with 200 ΜM La^{+3} under resting conditions of 12 m.o female APP/PS1 mice (N=3 WT VEH (black); N = 3 WT PBN (gray); N=3 TG VEH (red) and N=3 TG PBN (blue)). Ordinary one-way ANOVA showed a significant difference between groups (F(7,27)=7.270, *** p = 0.0007) and Tukey's multiple comparisons tests showed a significant difference between WT VEH-TG VEH **** p<0.0001; TG VEH – TG VEH La^{3+} **** p<0.0001: TG VEH-TG PBN **** p<0.0001. Data are presented as mean per animal ± SEM.S pyr, stratum pyramidale; S rad. Stratum radiatum. Scale bar = 50μm.*

6. Probenecid Treatment improved the number of viable cells of 3 m.o, 12 m.o, and 18 m.o APP/PS1 animals.

To analyze the effects of the PBN treatment on neurodegeneration, we stained hippocampal slices with Cresyl Violet. In the CA1 region of the hippocampus and its adjacent cortex, 100x100 μm areas were selected, in which all the cell bodies of viable

and non-viable neurons (signs of neurodegeneration) were quantified. The criteria to differentiate neurodegeneration was the presence of cytoplasmic hyperchromatism and cell shrinkage (pyknosis). There was a positive effect of the PBN treatment on the number of viable cells, and consequently a reduction in the number of unviable cells in the hippocampus of 18 m.o male (Figure 24) and female TG PBN brains at all the studied ages (Figure 25). A similar positive effect of PBN was observed in the adjacent cortex of brains from 18 m.o TG PBN mice (Annexes Figure 41).

To assess whether there was a gender effect on the neuronal loss, the percentage of viable cells of males and females was compared at different ages (Annexes Figure 41).

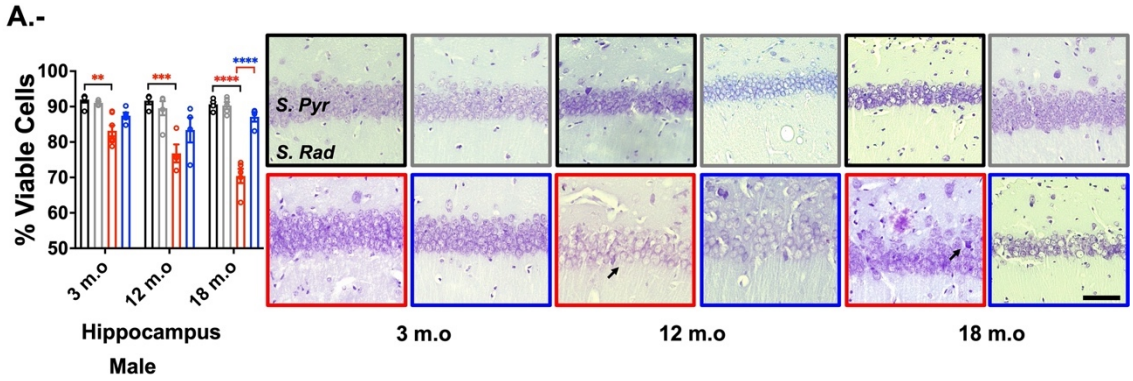

Figure 24. ***Probenecid prevents hippocampal neuronal loss in 18 m.o male APP/PS1 mice. A.-*** *Probenecid improved the number of viable cells in 18 m.o (N=2 WT VEH (black), N=2 WT PBN (gray), N= 2 TG VEH (red), and N= 2 TG PBN (blue)) but not in 3 m.o (N=2 WT VEH (black), N=2 WT PBN (gray), N= 2 TG VEH (red), and N= 2 TG PBN (blue)) and 12 m.o males TG animals (N=2 WT VEH (black), N=2 WT PBN (gray), N= 2 TG VEH (red), and N= 2 TG PBN (blue)) and representative images of Nissl staining in the CA1 region of the hippocampus all experimental groups. Scale bar = 20 μm S rad: Stratum radiatum. Age ($F(2,25)=5.445$, * $p=0.0109$), genotype ($F(1,20)=109.6$, **** $p<0.0001$) and treatment ($F(1,25)=15.66$, *** $p=0.0006$) were the main sources of variation and there was a significant interaction between age x genotype ($F(2,20)=3.567$, * $p=0.0473$), age x treatment ($F(2,25)=4.345$, * $p=0.0240$), genotype x treatment ($F(1,20)=33.74$, **** $p<0.0001$) and age x genotype x treatment ($F(2,20)=3.973$, * $p=0.0352$) by Three-way ANOVA; and Tukey's multiple comparisons tests revealed a*

*significant difference between 3 m.o WT VEH-TG VEH ** p=0.0089; 12 m.o WT VEH-TG VEH *** p=0.0002; 18 m.o WT VEH-TG VEH **** p<0.0001 TG VEH – TG PBN **** p<0.0001.*

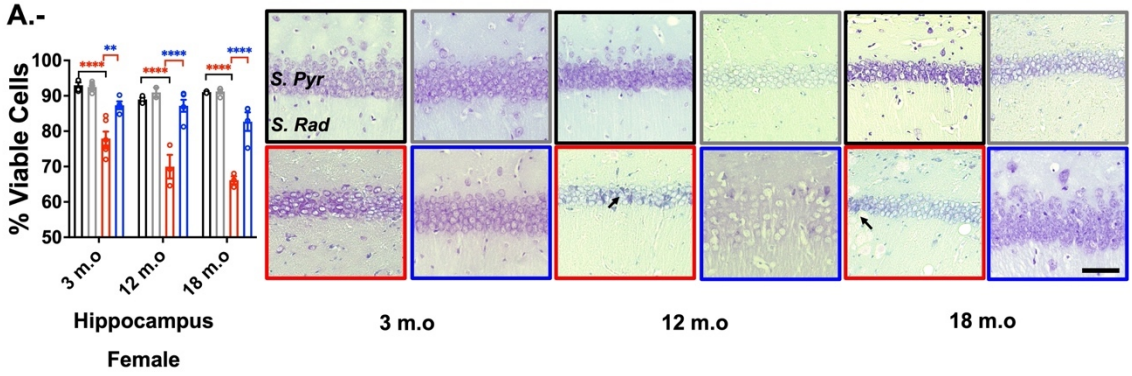

Figure 25. ***Probenecid prevents hippocampal neuronal loss in 3 m.o, 12 m.o and 18 m.o female APP/PS1 mice. A-*** *Probenecid improved the number of viable cells in 3 m.o (N=2 WT VEH (black), N=2 WT PBN (gray), N= 2 TG VEH (red), and N= 2 TG PBN (blue)), 12 m.o (N=2 WT VEH (black), N=2 WT PBN (gray), N= 2 TG VEH (red), and N= 2 TG PBN (blue)) and 18 m.o (N=2 WT VEH (black), N=2 WT PBN (gray), N= 2 TG VEH (red), and N= 2 TG PBN (blue)) female TG animals and representative images of Nissl staining in the CA1 region of the hippocampus all experimental groups. Scale bar = 20 μm S rad: Stratum radiatum. Age (F(2,36)=9.749, *** p=0.0004), genotype (F(1,36)=161.3, **** p<0.0001) and treatment (F(1,36)=55.63, **** p<0.0001) were the main sources of variation and there was a significant interaction between age x genotype (F(2,36)=3.567, * p=0.0473) and genotype x treatment (F(1,36)=47.56, **** p<0.0001) by Three-way ANOVA; and Tukey's multiple comparisons tests revealed a significant difference between 3 m.o WT VEH-TG VEH **** p<0.0001 TG VEH-TG PBN ** p=0.0032; 12 m.o WT VEH-TG VEH **** p<0.0001 TG VEH-TG PBN **** p<0.0001; 18 m.o WT VEH-TG VEH **** p<0.0001 TG VEH – TG PBN **** p<0.0001.*

7. Basal excitatory synaptic transmission and paired-pulse facilitation are unchanged by PBN treatment.

To analyze the effects of the PBN treatment on the synaptic deficit in APP/PS1 mice, we next performed electrophysiological field recordings in hippocampal slices obtained from young and old WT and TG mice, to evaluate excitatory synaptic transmission and plasticity.

First, we measured the input-output relationship (I/O) between the initial slope of the field excitatory postsynaptic potential and the stimulus intensity. As observed in Figure 26, the excitatory synaptic transmission was not different between WT and TG mice at any of the ages tested (Figure 26). The treatment with PBN had no effects on the I/O relationship in any of the experimental groups. However, it is noteworthy that the aged group treated with PBN exhibited greater values of fEPSP slopes at higher stimulations than the vehicle, in agreement with previous observations reported in WT animals and PANX1-KO animals (Prochnow, et al., 2012; Ardiles, et al., 2014).Accordingly, Paired-pulse facilitation, a parameter inversely related to the neurotransmitter release probability, was not different between experimental groups (Figure 27), suggesting that PBN does not affect basal presynaptic efficacy.

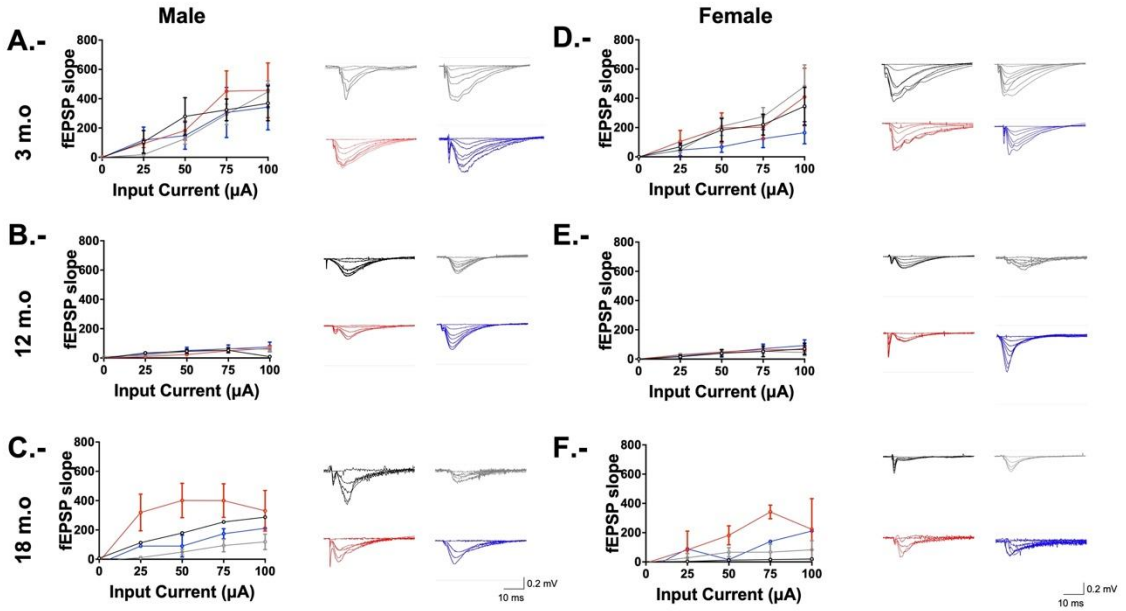

Figure 26. Basal excitatory synaptic transmission was unchanged by the PBN treatment*. Hippocampal slices from WT and APP/PS1 mice treated with PBN or the vehicle were subjected to electrophysiological field recordings. CA3- Schaffer collaterals were stimulated, and the post-synaptic responses were recorded in CA1 pyramidal neurons to estimate evoked basal transmission. On the left fEPSP slopes were plotted against growing stimulus amplitude ranging from 25-100 µA for all the experimental conditions. On the right, representative traces are shown for all the experimental*

conditions. ***A.-*** *3 m.o male APP/PS1 and WT mice. Input current (F(4,60)=5.877, *** p=0.0005) was the main source of variation by Three-way ANOVA* ***B.-*** *12 m.o male APP/PS1 and WT mice. Input current (F(4,30)=4.584, ** p=0.0052) was the main source of variation by Three-way ANOVA* ***C.-*** *18 m.o male APP/PS1 and WT mice. Input current (F(4,45)=3.019, * p=0.0274) was the main source of variation by Three-way ANOVA* ***D.-*** *3 m.o female APP/PS1 and WT mice. Input current (F(4,140)=9.905, **** p<0.0001) was the main source of variation by Three-way ANOVA* ***E.-*** *12 m.o female APP/PS1 and WT mice. Input current (F(4,29)=9.543, **** p<0.0001) was the main source of variation by Three-way ANOVA* ***F.-*** *18 m.o female APP/PS1 and WT mice. Groups are presented as male: 3m.o: WT VEH n= 6 slices from 3 animals (Black); WT PBN n= 2 slices from 1 animal (Gray); TG VEH n= 7 slices from 2 animals (Red); TG PBN n= 5 slices from 2 animals (Blue); 12 m.o: WT VEH n= 2 slices from 1 animal (Black); WT PBN n= 2 slices from 1 animal (Gray); TG VEH n= 2 slices from 1 animal (Red); TG PBN n= 4 slices from 1 animal (Blue); 18 m.o: WT VEH n= 1 slice from 1 animal (Black); WT PBN n= 4 slices from 1 animal (Gray); TG VEH n= 7 slices from 2 animals (Red); TG PBN n= 2 slices from 1 animal (Blue) and female: WT VEH n= 6 slices from 2 animals (Black); WT PBN n= 6 slices from 3 animal (Gray); TG VEH n= 4 slices from 1 animal (Red); TG PBN n= 4 slices from 1 animal (Blue); 12 m.o: WT VEH n= 2 slices from 1 animal (Black); WT PBN n= 4 slices from 1 animal (Gray); TG VEH n= 4 slices from 1 animal (Red); TG PBN n= 3 slices from 1 animal (Blue); 18 m.o: WT VEH n= 1 slice from 1 animal (Black); WT PBN n= 2 slices from 1 animal (Gray); TG VEH n= 2 slices from 2 animals (Red); TG PBN n= 2 slices from 1 animal (Blue). Results are presented as mean±SEM.*

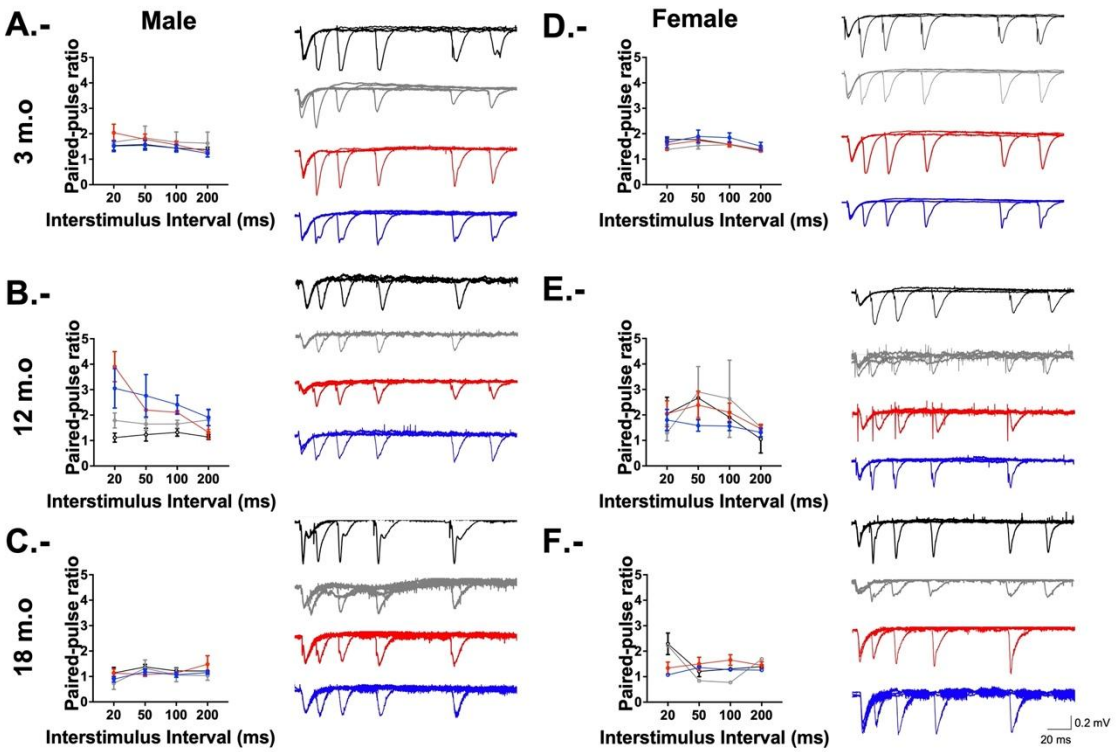

Figure 27 Paired-pulse facilitation was unchanged by the PBN treatment. Hippocampal slices from *WT and APP/PS1 mice treated with PBN or the vehicle were* stimulated with two stimuli of the same intensity separated by a time of 50 ms*, at growing inter-stimulus intervals ranging from 20 to 200 ms,* for *estimation of a paired-pulse-facilitation (PPF) ratio. On the left, paired pulse ratio by different stimulation intervals is plotted. On the right, representative traces are shown per each experimental condition.* ***A.-*** *PPF from 3m.o male APP/PS1 and WT slices. No significant difference by Three-way ANOVA.* ***B.-*** *PPF from 12m.o male APP/PS1 and WT slices. No significant difference by Three-way ANOVA.* ***C*** *PPF from 18m.o male APP/PS1 and WT slices. No significant difference by Three-way ANOVA.* ***D.-*** *PPF from 3m.o female APP/PS1 and WT slices. No significant difference by Three-way ANOVA.* ***E.-*** *PPF from 12m.o female APP/PS1 slices. No significant difference by Three-way ANOVA.* ***F.-*** *PPF from 18 m.o female APP/PS1 and WT slices. No significant difference by Three-way ANOVA. Groups are presented as male: 3m.o: WT VEH n= 6 slices from 3 animals (Black); WT PBN n= 2 slices from 1 animal (Gray); TG VEH n= 7 slices from 2 animals (Red); TG PBN n= 5 slices from 2 animals (Blue); 12 m.o: WT VEH n= 2 slices from 1 animal (Black); WT PBN n= 2 slices from 1 animal (Gray); TG VEH n= 2 slices from 1 animal (Red); TG PBN n= 4 slices from 1 animal (Blue); 18 m.o: WT VEH n= 1 slice from 1 animal (Black); WT PBN n= 4 slices from 1 animal (Gray); TG VEH n= 7 slices from 2 animals (Red); TG PBN n= 2 slices from 1 animal (Blue) and female: WT VEH n= 6 slices from 2 animals (Black); WT PBN n= 6 slices from 3 animal (Gray); TG VEH n= 4 slices from 1 animal (Red); TG PBN n= 4 slices from 1 animal (Blue); 12 m.o: WT VEH n= 2 slices from 1 animal (Black); WT PBN n= 4 slices from 1 animal (Gray); TG VEH n= 4 slices from 1 animal (Red); TG PBN n= 3 slices from 1 animal (Blue); 18 m.o: WT VEH n= 1 slice from 1 animal (Black);*

WT PBN n= 2 slices from 1 animal (Gray); TG VEH n= 2 slices from 2 animals (Red); TG PBN n= 2 slices from 1 animal (Blue). Results are presented as mean±SEM.

8. Synaptic plasticity defects in APP/PS1 brains are prevented by the PBN treatment.

To evaluate the effect of PBN on the induction of NMDA-dependent synaptic plasticity, we induced LTP in acute hippocampal slices from young and old APP/PS1 (TG) mice by applying a standard TBS protocol (Ardiles, et al., 2014). As shown in figure 28, hippocampal slices from 3 m.o female TG, 12m.o and 18 m.o male and female TG exhibited impaired LTP as compared to hippocampal slices from the respective WT mice. In 3m.o female APP/PS1 animals, the treatment with PBN increased the potentiation of the excitatory synaptic response in TG PBN slices, reaching values near to that observed in the WT slices (Figure 29B). Also, the PBN treatment prevented the LTP defects in 12 m.o and 18m.o TG mice (Figure 28 and 29), suggesting that the inhibition of Panx1 with PBN could be an efficient pharmacological tool to avoid the synaptic dysfunction at early and late stages of the AD.

To assess whether there was a gender effect on the synaptic plasticity, the LTP magnitude of the last 10 min of recordings was compared at different ages (Annexes Figure 43) and we did not find any differences between gender.

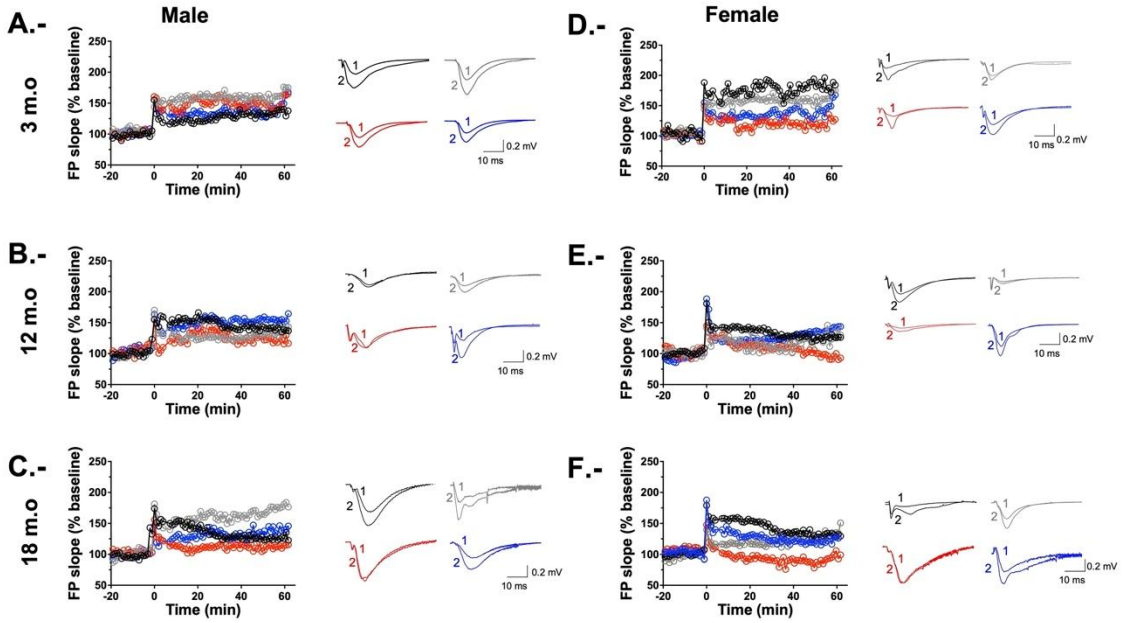

Figure 28. 30 days treatment with PBN prevented synaptic plasticity defects in the excitatory hippocampal synapses of 3 m.o female and in 12 and 18 m.o male and female APP/PS1 mice. *Long-term potentiation of the CA3-CA1 excitatory synapses was induced by a standard theta burst stimulation (TBS) protocol in hippocampal slices from WT and APP/PS1 mice treated with PBN or the vehicle. Excitatory postsynaptic field potentials (fEPSP) were recorded during 60 min after the application of the TBS protocol. On the left* ***are plotted*** *the percentage of potentiation in time respect to the baseline; on the right are shown representative traces for all the experimental conditions.* ***A****.- LTP in hippocampal slices from 3 m.o male APP/PS1 and WT mice Groups are presented as WT VEH n= 8 slices from 3 animals (Black); WT PBN n= 4 slices from 1 animal (Gray); TG VEH n= 8 slices from 2 animal (Red); TG PBN n= 6 slices from 2 animals (Blue).* ***B.-*** *LTP in hippocampal slices from 12 m.o male APP/PS1 and WT mice. Groups are presented as WT VEH n= 3 slices from 2 animals (Black); WT PBN n= 3 slices from 2 animals (Gray); TG VEH n= 4 slices from 1 animal (Red); TG PBN n= 2 slices from 1 animal (Blue).* ***C.-*** *LTP in hippocampal slices from 18 m.o male APP/PS1 and WT mice Groups are presented as WT VEH n= 8 slices from 1 animal (Black); WT PBN n= 7 slices from 1 animal (Gray); TG VEH n= 6 slices from 1 animal (Red); TG PBN n= 8 slices from 1 animal (Blue).* ***D.-*** *LTP in hippocampal slices from 3 m.o female APP/PS1 and WT mice Groups are presented as WT VEH n= 6 slices from 2 animals (Black); WT PBN n= 5 slices from 3 animals (Gray); TG VEH n= 4 slices from 1 animal (Red); TG PBN n= 8 slices from 1 animal (Blue).* ***E.-*** *LTP in hippocampal slices from 12 m.o female APP/PS1 and WT mice****.*** *Groups are presented as WT VEH n= 4 slices from 1 animal (Black); WT PBN n= 3 slices from 1 animal (Gray); TG VEH n= 2 slices from 1 animal (Red); TG PBN n= 4 slices from 1 animal (Blue).* ***F.-*** *LTP in hippocampal slices from 18 m.o female APP/PS1 and WT mice Groups are presented as WT VEH n= 3 slices from 1 animal (Black); WT PBN n= 4 slices from 1 animal (Gray); TG VEH n= 2 slices from 1 animal (Red); TG PBN n= 6 slices from 1 animal (Blue).*

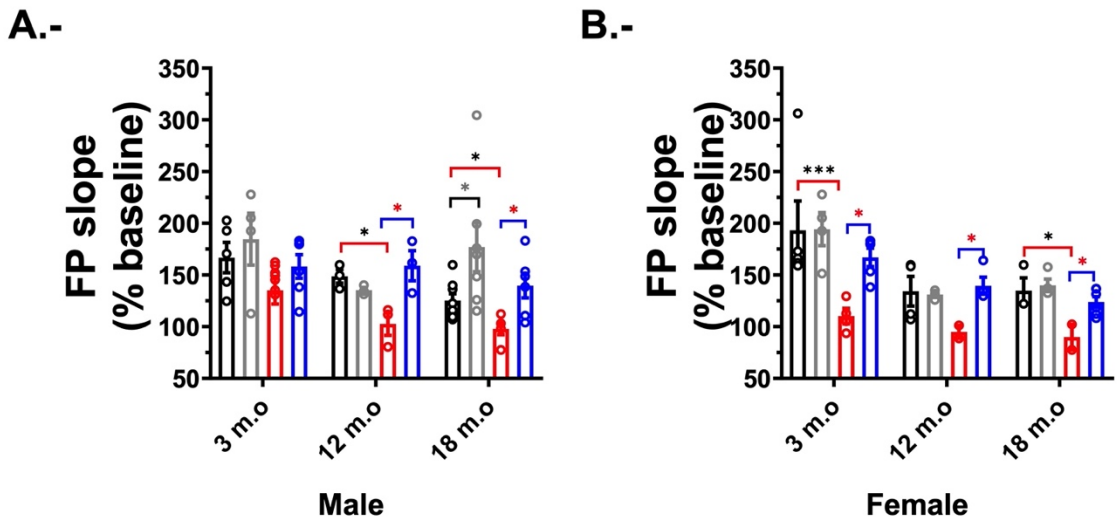

Figure 29 Probenecid treatment prevented synaptic plasticity defects in excitatory hippocampal synapses of 3 m.o female, 12 m.o and 18m.o male and female APP/PS1 mice. A.- *Average LTP magnitude during the last 10 min of recording of male 3 m.o, 12 m.o and 18 m.o APP/PS1 mice. Age (F(2,29)=3.667, *p=0.0377), genotype (F(1,20)=6.753, *0.0172) and treatment (F(1,29)=9.242, ** p=0.0050) were significant sources of variation by Three-way ANOVA.* ***B.-*** *Average LTP magnitude during the last 10 min of recording of male 3 m.o, 12 m.o and 18 m.o APP/PS1 mice. Age (F(2,34)=11.77, ***p=0.0001), genotype (F(1,34)=14.57, *** p=0.0005) and treatment (F(1,34)=9.242, * p=0.0132) were significant sources of variation and there was a significant interaction between genotype x treatment (F(1,34)=6.256, * p=0.0174) by Three-way ANOVA.*

9. Probenecid treatment increases spine density in 3 m.o, 12 m.o, and 18 m.o APP/PS1 TG animals.

To evaluate the effect of PBN on the spine loss that occurs in the context of AD (Zhang, et al., 2016; Dong, et al., 2019; Knafo, et al., 2009; Lonnemann, et al., 2022; Huang, et al., 2019) we performed Golgi staining in brains isolated from all the experimental groups. To measure spine density, we analyzed only spines that emerged

perpendicular to the dendritic shaft in CA1 hippocampal neurons, and we calculated the spine density as the number of spines per 1 μm of the dendritic shaft.

In 3m.o male APP/PS1 animals (Figure 30), there were no differences in the spine density between WT and TG VEH animals, as was previously reported by other authors (Tzeng, et al., 2018). Instead, in neurons from 3 m.o female APP/PS1 animals (Figure 31) we observed a significant decrease in the spine density compared to their WT littermates. Remarkably, the neurons from hippocampal slices isolated from 3 m.o TG female mice treated with PBN exhibited a significant increase in the spine density compared to the treatment with the vehicle (Figure 31).

As it has been reported that the Panx1 blockade promotes structural changes in neuronal and synaptic morphology (Sanchez-Arias, et al., 2019; Flores-Muñoz, et al., 2022), we also measured additional spine parameters such as the length of the spine, and the width of the head and neck to estimate a head/neck ratio in WT and TG under VEH and PBN conditions (Annexes Figure 46). We observed an increase in the spine length in neurons from male and female 18 m.o PBN-treated groups (Annexes Figure 46A and B), but no effect in the head/neck ratio (Annexes Figure 46 C and D).

In agreement with previous reports (Zhang, et al., 2016; Dong, et al., 2019; Knafo, et al., 2009; Lonnemann, et al., 2022; Huang, et al., 2019), the TG-aged male and female animals (12 and 18 m.o) exhibited a significantly decreased spine density compared to age-matched WT mice (Figure 30 and 31); this difference was prevented by the 30-days treatment with PBN.

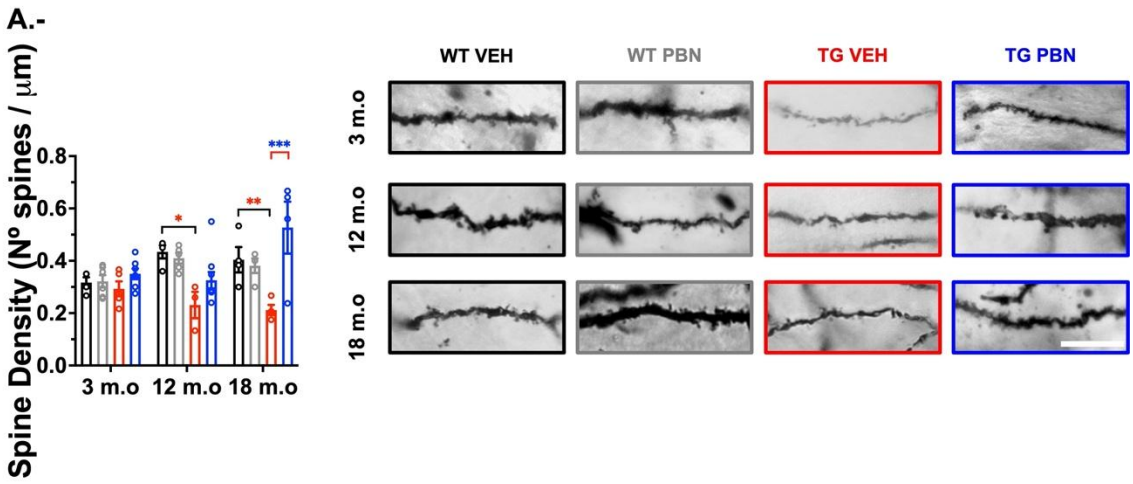

Figure 30 The treatment with Probenecid prevents dendritic spine loss in 18 m.o male TG APP/PS1 mice*. Hippocampal slices from WT and APP/PS1 male mice treated with PBN or its vehicle were stained with the Golgi-staining and visualized by bright field microscopy. Pyramidal neurons were analyzed to evaluate the number of dendritic spines per 1 um of dendritic shaft (dendritic spine density). On the left dendritic spine density is plotted per each experimental group. On the right representative images of the experimental conditions are shown. Scale bar = 10μm. Groups are presented as 3m.o: WT VEH n= 3 neurons (80 spines), (Black); WT PBN n= 3 neurons (300 spines) (Gray); TG VEH n= 3 neurons (63 spines) (Red); TG PBN n= 7 neurons (407 spines) (Blue); 12m.o: WT VEH n= 3 neurons (79 spines), (Black); WT PBN n= 4 neurons (84 spines) (Gray); TG VEH n= 3 neurons (116 spines) (Red); TG PBN n= 7 neurons (315 spines) (Blue) and 18m.o: WT VEH n= 3 neurons (67 spines), (Black); WT PBN n= 3 neurons (89 spines) (Gray); TG VEH n= 3 neurons (85 spines) (Red); TG PBN n= 3 neurons (184 spines) (Blue). Genotype (F(1,47)=6.074, * p=0.0174) and treatment (F(1,47)=10.10, ** p= 0.0026) were the main sources of variation and there was a significant interaction between age x genotype (F(2,47)=4.210, * p=0.0208), genotype x treatment (F(1,47)=14.52, *** p=0.0004) and age x genotype x treatment (F(2,47) =3.630, * p=0.0342) and Tukey's multiple comparisons test showed significant difference between 12 m.o: WT VEH-TG VEH * p= 0.0112; 18 m.o: WT VEH-TG VEH ** p=0.0092 TG VEH-TG PBN *** p=0.0001.*

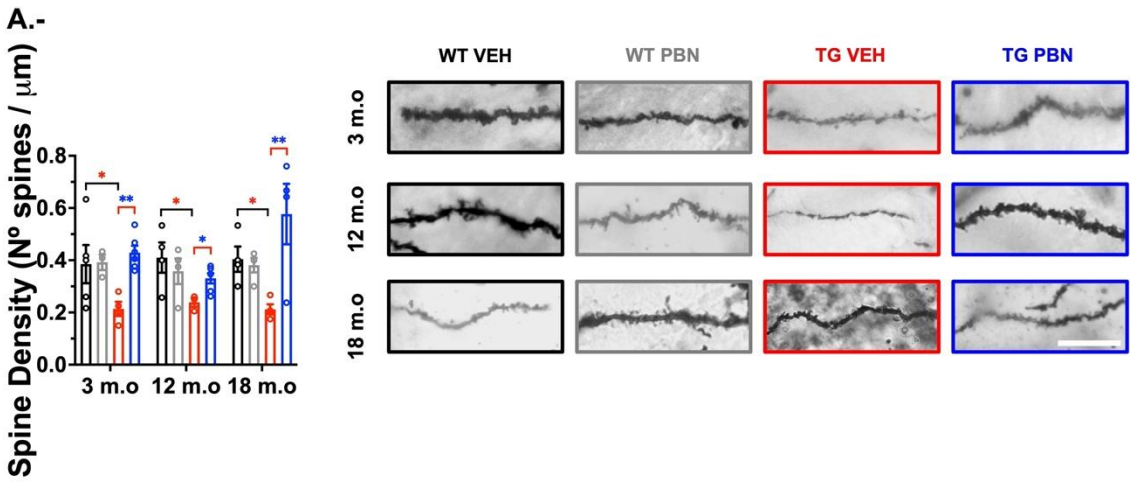

Figure 31 The treatment with Probenecid prevents dendritic spine loss in 3 m.o, 12 m.o and 18 m.o female TG APP/PS1 *mice. Hippocampal slices from WT and APP/PS1 female mice treated with PBN or its vehicle were stained with the Golgi-staining and visualized by bright field microscopy. Pyramidal neurons were analyzed to evaluate the number of dendritic spines per 1 um of dendritic shaft (dendritic spine density). On the left dendritic spine density is plotted per each experimental group. On the right representative images of the experimental conditions are shown. Scale bar = 10 ⁄m. Groups are presented as 3m.o: WT VEH n= 5 neurons (80 spines), (Black); WT PBN n= 3 neurons (301 spines) (Gray); TG VEH n= 4 neurons (63 spines) (Red); TG PBN n= 6 neurons (457 spines) (Blue); 12m.o: WT VEH n= 4 neurons (80 spines), (Black); WT PBN n= 4 neurons (85 spines) (Gray); TG VEH n= 3 neurons (116 spines) (Red); TG PBN n= 6 neurons (316 spines) (Blue) and 18m.o: WT VEH n= 4 neurons (67 spines), (Black); WT PBN n= 4 neurons (139 spines) (Gray); TG VEH n= 4 neurons (86 spines) (Red); TG PBN n= 4 neurons (184 spines) (Blue). Treatment (F(1,39)=11.30, ** p= 0.0017) was the main source of variation and there was a significant interaction between genotype x treatment (F(1,39)=19.98, *** p=0.0002) and Tukey's multiple comparisons tests showed significant difference between 3m.o: WT VEH-TG VEH * p=0.0474 TG VEH-TG PBN ** p =0.0038; 12 m.o: WT VEH-TG VEH * p=0.0353 TG VEH -TG PBN * p=0.019759.*

Discussion

Probenecid is an FDA-approved drug, formerly used in clinics as a urate-lowering agent for the treatment of the gout, due to its known blockade of organic anions transporter (Talbott et al., 1951). Currently evidence, identify new properties of PBN by the inhibition of P2X7 purinergic receptors (Bhaskaracharya, et al., 2014), and Panx1 channels (Silverman, et al., 2008). For some years it has been proposed as a new tool to treat pathologies associated with the central nervous system, due to its neuroprotective action (Colin-Gonzalez & Santamaria, 2013). In this regard, it has been suggested as a new therapeutic tool in neuropathologies such as epilepsy (Aquilino, et al., 2020; Dossi, et al., 2018), ischemia (Wei, et al., 2015; Xiong, et al., 2014; Jian, et al., 2016), multiple sclerosis (Hainz, et al., 2017), experimental autoimmune encephalomyelitis (Hainz, et al., 2016) and Alzheimer's disease (Flores-Muñoz, et al., 2020; Harcha, et al., 2015). Since all these pathologies associate with inflammatory processes (Voet, et al., 2019; Hashioka, et al., 2021) and considering that Panx1 channels are critical players for inflammation involved in these signaling pathways (Kameritsch & Pogoda, 2020; Seo et al., 2021), its blocking would be beneficial to prevent this pathophysiological process and consequently improve the cellular microenvironment (García-Rodríguez et al., 2023).

The aim of this work was to evaluate the impact of the treatment with PBN on the Panx1 channel activity as well as in the synaptic structure and cognitive function in a murine model of AD, with a view to understanding the *potential "neuroprotective" of PBN*. As our data show, a 30-days treatment with PBN managed to prevent recognition, spatial, and reference memory impairments in aged APP/PS1 mice, a murine model of AD

(Jankowski et al., 1993). The PBN treatment also prevented the neuronal loss, dendritic spine loss, and synaptic plasticity impairments observed in hippocampal slices from APP/PS1 mice. This PBN treatment also caused a significant reduction in the Panx1 activity in the hippocampus of APP/PS1 (TG) mice, strongly suggesting that the "neuroprotective effect of PBN is likely due to the inhibition of Panx1. It is noteworthy the AD deficiencies observed in APP/PS1 animals seem to manifest much earlier in females than in males since the prevention exerted by PBN was evident at earlier ages. But, h*ow the inhibition of Panx1 channels could have a "neuroprotective" effect in the context of AD?* A possibility is by interfering with the role of Panx1 in the inflammatory pathways that are enhanced in the AD context. In this regard Panx1 is involved in the NLRP3 inflammasome activation in neurons and astrocytes (Silverman, et al., 2009). It is an intracellular receptor for DAMPs, danger-associated molecular patterns, that trigger the innate immune response (Kelley, et al., 2019), which has been shown to be importantly activated in the AD context (Heneka, et al. 2013). Inflammasome complexes formation is a crucial part of the activation mechanism for the microglial inflammatory function (Hanslik & Ulland, 2020).

Interestingly, a profile of sexual dimorphism was identified in the APPPS1 model, with females exhibiting pathologically higher levels of proinflammatory cytokines, astrocytosis, and microgliosis, besides synaptic degeneration (Jiao, et al., 2016). They also exhibit greater amounts of Aβ40 and soluble Aβ42 (Wang, et al., 2003), amyloid plaque deposition in hippocampus and cortex (Janus, et al., 2015), and aberrant glucose metabolism (Xin, et al., 2016), that is proposed to be explained by differential profiles of microglia (Kadlecova, et al., 2023). In the mature brain, microglia regulate the

inflammatory response to brain parenchymal damage and directly influence synaptic function by regulate synaptic pruning, but also is critical for synaptic plasticity and learning and memory processes (Lenz & Nelson, 2018; Stogsdill & Eroglu, 2017. At the different stages of the development, microglia have different morphologies and express distinct sets of genes (Bennet et al., 2016). Moreover, ameboid morphology generally associated to “activated” state can differ between the different phases of the brain development and pathological conditions (Bennett, et al., 2016). In this regard, female APPPS1 microglia is glycolytic, less phagocytic, and associated with increased amyloidosis, whereas microglia from APPPS1 males are amoeboid and exhibits a reduced plaque load (Guillot-Sestier, et al., 2021). Taking into account these differences, we applied the experimental approaches in both genders of APPPS1 mice, considering the sex of the animals as an analysis variable. Even though a *“neuroprotective”* effect of PBN was observed in both females and males, some gender differences were evident between the experimental groups. It is important to highlight that APP/PS1 females seem to have a more severe phenotype from early ages compared to males. Already at 12 months, the difference observed between transgenic females and males was accentuated, in accordance with what other authors have observed (Miffilin, et al., 2021).

Regarding the dose of PBN tested in this study, we used 100mg/kg, which corresponds to 2.5 times the maintenance dose administered to people to block the renal excretion of penicillin and does not represent toxic or teratogenic risks in mice (Bucher, et al., 1986). Using this daily dose during 30 days, no changes were observed in the weight of the mice at the end of the treatment, according to what was informed in the toxicological manual of this drug (National Toxicology Program, 1991), nonetheless, there were differences in the average weight between females and males as previously

reported (Miffilin, et al., 2021; National Toxicology Program, 1991). To get mice voluntarily administered PBN, we used a sucralose gel medium that has been used previously for oral drug delivery in mice (Christy, et al., 2014).

Regarding the behavioral tests that we applied to evaluate cognitive functions, namely NOR and MWM, those are tasks whose performance depends on the hippocampus and cortex, brain structures primarily affected in AD (Scheff & Price, 2003; Buckner, 2004). Impairments in the NOR and MWM performance correlate with early cognitive alterations in AD, such as agnosia (the loss of the ability to recognize people and objects, Brooks 3rd, et al., 1993). In our hands, the loss of recognition memory in the AD model was age-dependent, observing that young TG animals kept intact their preference for novelty in accordance with that reported by other authors (Montgomery, et al., 2016; Hoejimakers, et al., 2018; Martin-Sanchez, et al., 2021). Whilst, a significant deficit in the recognition memory was evidenced in both male and female-aged TG mice, in agreement with that observed previously (Coles, et al., 2020; Ibrahim, et al., 2017; Lyra e Silva, et al., 2021). Remarkably, the treatment with PBN seemed to prevent these alterations in TG mice, reaching performances near to that observed in the WT controls (Figure 13 and 14). The latter strongly suggests PBN could exert an important neuroprotective effect in the brain areas critical for recognition memory.

Similarly to that observed in the NOR test, PBN also impacted positively in spatial memory in TG mice. At the earliest stages, in transgenic males, we observed a similar performance to the control, in accordance with previous reports (Li, et al., 2016), whilst in females there was a greater difference with their respective controls. It has been proposed that in young TG animals, there would be a poor navigation strategy that leads

to a greater number of errors during the acquisition of spatial memory (Karunakaran, 2020; Martin-Sanchez, et al., 2021). In the oldest mice (12 m.o and 18m.o) we observed alterations in both acquisition and reference memory, in agreement with previous reports (Faivre, et al., 2018; Xu, et al.; Jarvela, et al., 2018; Jia, et al., 2013; Jiao, et al., 2015; Lalonde, et al., 2005; Timmer, et al., 2010; Li, et al., 2021; Muller, et al., 2021). In both of them, the treatment with PBN prevented the defects observed in the oldest TG mice. As we didn't observe a significant difference in the locomotor activity between the oldest WT and APPS1 mice, it is unlikely that such differences are due to motility defects in the experimental groups. In agreement with this idea, other authors have reported the absence of differences in locomotion between APPPS1 and WT mice (Garcia, et al., 2014).

Given that the molecular basis of learning and memory relies on the mechanisms that lead to synaptic plasticity, we evaluated the impact of the PBN treatment on the induction and maintenance of long-term-potentiation(LTP) of the synaptic strength, which is proposed as a cellular model of learning and memories (Lynch, 2004) and has been demonstrated that is impaired at early stages in APPPS1 mice (Li, et al., 2017). Indeed, we observed that already at 3 m.o the female TG mice exhibit LTP deterioration (Figure 28B) and that the treatment with PBN prevented such defects; in the same way, PBN also prevented the LTP impairments observed in aged male and female TG mice (Figure 28).

The reasons why Panx1 inhibition with PBN could lead to increased LTP are not entirely clear. As we previously demonstrated, Panx1 is overexpressed in the brain of APPS1 mice (Flores Muñoz et al., 2020), and the acute treatment of hippocampal slices

with PBN increases LTP in this model (Flores Muñoz et al., 2020). It seems that the overexpression of Panx1 could contribute to modify the excitability in the APPPS1 brains affecting the threshold for the LTP induction. In that case, the blockade of Panx1 with PBN could prevent these defects. On the contrary, other authors have proposed that the cognitive defects are associated with an increased neuronal network excitability in TG mice, even promoting epileptic forms of discharges from 3 m.o to 10 m.o APP/PS1 mice (Kazim, et al., 2021). If that is the case, it could imply that the inhibitory synaptic transmission could be affected early in the AD context. In this regard, a recent work demonstrated that postmortem brains from human AD patients exhibited loss of inhibitory synapses (Kurcuru, et al., 2022) suggesting that an imbalance in the excitatory/inhibitory neurotransmission contributes to the cognitive decline in the AD context. In addition to that, an increase in glutamatergic transmission because of reduced glutamate uptake by astrocytic glutamate transporters (Mookherjee, et al., 2011; Scimemi, et al., 2013) and enhanced spillover explains the increased neuronal excitability and synaptic plasticity defects observed in AD context (Li, et al 2009; Li, et al., 2011).

As the efficiency of the synaptic transmission relies on the proper synaptic structure, we also analyzed the impact of the PBN treatment on the dendritic spine density in hippocampal and cortical neurons. A number of works suggest that the loss of dendritic spines, and consequently the loss of functional synapses is the major correlate with the onset of the cognitive decline in AD (Colom-Cadena, et al., 2020; Ribaric, 2023).

In APPPS1 mice, the loss of dendritic spines occurs early from 3 m.o (Ammassari-Teule, 2020; Smith, et al., 2009). We observed a significant reduction in the dendritic

spine density in TG compared to WT mice, starting from 3 m.o in females and becoming evident in males and females at 12 m.o and 18 m.o, in accordance with what other authors have observed (Knafo, et al., 2009). It has been shown that the spine loss is more evident in the vicinity of amyloidogenic plaques due to the disruption in the Ca^{2+} homeostasis that is associated with the activation of the phosphatase Calcineurin (CaN) (Kuchibhotla, et al., 2008) and the induction of morphological changes in synapses. Remarkably, it has been demonstrated in aged APP/PS1 mice that at advanced stages of the disease, the senescent synapses that exhibit deficient mitochondrial metabolism, are marked, by complement proteins to be subsequently phagocyted by microglia (Gyorffy, et al., 2020). After the treatment with PBN, the loss of spines was prevented in 18-month-old male TG mice and in all the age groups of TG females, showing a possible differential progression of AD pathology and the effect of PBN treatment between males and females. Likewise, we observed an increase in the size of the spines in the oldest animals (12 and 18 m.o) treated with PBN in both WT and TG (Annexes Figure 45). Considering that the number and size of dendritic spines are critically dependent on the neuronal actin cytoskeleton (Lamprecht, 2021; Konietzny, et al., 2017), it is feasible to assume that the PBN treatment could modulate actin cytoskeleton remodeling. In fact, we recently demonstrated that in the absence of Panx1, there is an increase in the neuronal actin polymerization, leading to enhanced dendritic arborization and spine density in hippocampal neurons from a knock-out mouse (Flores-Munoz et al., 2022). This effects of Panx1 deletion on actin cytoskeleton was mediated by a disbalance in Rho GTPases activity promoting actin polymerization (Flores-Munoz et al., 2022). Something similar could occur in APPPS1 neurons subjected to the treatment with PBN, which could explain an increase in the number and size of dendritic spines compared to the TG condition treated only with the vehicle.

Because AD is characterized by a progressive neurodegeneration, viable and non-viable somas were quantified in the CA1 area of the hippocampus and in the cortex adjacent to this structure, both areas involved in learning and memory processes (Buckner, 2004; Scheff & Price, 2003). By using cresyl violet staining, we observed a decrease in the number of viable cells in TG mice of the all age groups in both the hippocampus and cortex, especially in the cortical area of 18 m.o TG females. In response to the treatment with PBN, the number of viable cells of females TG APP/PS1 increased in all the age groups, as well as in males 12 m.o and 18 m.o TG mice in both, hippocampus and cortex (Figure 24 and Annexes Figure 41). These results strongly suggest that the treatment with PBN prevents the neuronal loss or related toxic pathways observed in the AD context. In agreement with this idea, it has been reported that rats injected with soluble Aß oligomers into the hippocampus exhibit a significant decrease in the number of viable neurons in the CA1 area, which was prevented in rats injected intraperitoneally with a dose of 50mg/Kg of PBN (Carrillo-Mora, et al., 2010).

Panx1 is a protein that forms channels in the cell membrane and is involved in various physiological processes, including cell communication, and signaling (Seo, et al., 2021; Michalski, et al., 2020; Qu, et al., 2020; Yeung, et al., 2020). Whereas the role of Panx1 in AD is not yet fully understood, emerging research suggests its potential involvement in the pathogenesis of AD. Studies have shown that Panx1 channels can facilitate the release of ATP and other signaling molecules from cells (Narahari, et al., 2021). ATP acts as an extracellular signaling molecule and plays a role in modulating neuronal activity and synaptic plasticity (Sebastiao & Ribeiro, 2015) as well as neuroinflammation (Idzko, et al., 2014). Dysregulated ATP signaling has been implicated

in the pathology of AD (Sanchez-Arias, et al., 2021). One hypothesis is that abnormal Panx1 channel activity may contribute to the neuroinflammatory response observed in AD (Seo, et al., 2021). Increased Panx1 channel opening could lead to an excessive release of ATP and subsequent activation of purinergic receptors, triggering neuroinflammation and promoting neuronal damage (Seo, et al., 2021; Lee, et al., 2011). Neuroinflammation is a hallmark of AD and is thought to play a significant role in the progression of the disease (Calsolaro & Edison, 2016).

To assess the activity of Panx1 channels, we measured the uptake of the fluorescent tracer ethidium bromide in hippocampal slices from APP/PS1 TG animals. We observed that there was an increase in the uptake of the fluorescent tracer in 3 m.o and 12 m.o TG animals, and that this enhanced uptake was prevented by the PBN-treatment in TG mice. These data strongly suggest that the neuroprotective effects attributable to PBN by our current data and by other authors (Aquilino, et al., 2020; Biju, et al., 2018; Carrillo-Mora, et al., 2010; Dossi, et al., 2018; Flores-Muñoz, et al., 2020; Hainz, et al., 2016; Hainz, et al., 2017; Jian, et al 2016; Karatas, et al., 2013; Wei, et al., 2015; Zhang, et al., 2019), seem to be due to the inhibition of Panx1 activity. Together, our results contribute to understanding the mechanisms through which PBN could exert a neuroprotective effect in the AD context, shedding light on its therapeutic potential.

General Conclusion

In APPPS1 mice, one of the most widely used AD animal models, the treatment with PBN had a positive impact on the cognitive function, synaptic plasticity and structure, and cell viability, likely, as a consequence of the decrease of the Panx1 activity.

Our results revealed a gender effect in the appearance of AD hallmarks, showing more severe and early deficits in female TG animals. Accordingly, PBN treatment efficiently prevented these deficits in young and aged females.

Considering that recently FDA-approved anti-Aß treatments (e.g., aducanumab and lecanemab) as the first disease-modifying therapies, lack of clinical benefit due to the appearance of side effects such as brain swelling and bleeding, the present data open a possibility to explore new contributors to the pathogenesis of AD and indicates that AD is a more complex process that requires multiple approaches more than that canonical pathogenic factors.

References

Goedert , M., & Spillantini, M. G. (2006). A Century of Alzheimer's Disease. *Science*, 777-781.

Patterson, C. (2018). World Alzheimer Report 2018: The state of the art of dementia research: New frontiers. *Alzheimer's Disease International*.

MINSAL. (2010). Encuesta Nacional de Salud ENS Chile.

MINSAL. (2015). Documento Preliminar para la elaboración del Plan Nacional para las demencias.

Bertram, L., Lill, C. M., & Tanzi, R. E. (2010, October 21). The Genetics of Alzheimer Disease: Back to the Future. *Neuron, 68*, 270-281.

Haas, C., & Selkoe, D. J. (February de 2007). Soluble protein oligomers in neurodegeneration: lessons from the Alzheimer's amyloid b-peptide. *Molecular Cell Biology, 8*, 101-112.

Hatanpää, K., Isaacs, K. R., Shirao , T., Brady, D. R., & Rapoport , S. I. (June de 1999). Loss of proteins regulating synaptic plasticity in normal aging of the human brain and in Alzheimer Disease. *Journal of Neuropathology and Experimental Neurology, 58*(6), 637-643.

Masliah, E., Mallory, M., Alford, M., DeTeresa, R., Hansen, L. A., MacKeel, D. W., & Morris, J. C. (2001). Altered expression of synaptic proteins occurs early during progression of Alzheimer's disease. *Neurology, 56*, 127-129.

Terry, R. D., Masliah, E., Salmon , D. P., Butters, N., DeTeresa, R., Hill, R., . . . Katzman, R. (1991, October). Physical basis of cognitive alteration in Alzheimer's Disease: Synapse Loss is the major correlate of cognitive impairment. *Annals of Neurology, 30*(4), 572-580.

Fukumoto, H., Tokuda, T., Kasai, T., Ishigami, N., Hidaka, H., Kondo, M., . . . Nakagawa, M. (2010, August). High-molecular-weight b-amyloid oligomers are elevated in cerebrospinal fluid of Alzheimer patients. *The FASEB Journal, 24*, 2716-2726.

Gong , Y., Chang, L., Viola, K. L., Lacor, P. N., Lambert, M. P., Finch , C. E., . . . Klein, W. L. (2003, September 2). Alzheimer's disease-affected brain: Presence of oligomeric AB ligands (ADDLs) suggests a molecular basis for reversible memory loss. *Proceedings of the National Academy of Science (PNAS), 100*(18), 10417-10422.

Price, K. A., Varghese, M., Sowa, A., Yuk, F., Brautigam, H., Ehrlich, M. E., & Dickstein, D. L. (2014). Altered synaptic structure in the hippocampus in a mouse model of Alzheimer's disease with soluble amyloid-b oligomers and no plaque pathology. *Molecular Neurodegeneration, 9*(41), 1-13.

Mucke, L., Masliah, E., Yu, G.-Q., Mallory, M., Rockenstein, E. M., Tatsuno, G., . . . McConlogue, L. (2000, June 1). High-Level Neuronal Expression of AB1-42 in Wild-Type human amyloid protein precursor transgenic mice: Synaptotoxicity without plaque formation. *The Journal of Neuroscience, 20*(11), 4050-4058.

Sheng, M., Sabatini, B. L., & Südhof, T. C. (2012). Synapses and Alzheimer's Disease. *Cold Spring Harbor Perspectives in Biology, 4*(a005777), 1-19.

Li, S., Hong, S., Shepardson, N. E., Walsh, D. M., Shankar, G. M., & Selkoe, D. (2009, June 25). Soluble Oligomers of Amyloid b protein facilitate hippocampal long term depression by disrupting neuronal glutamate uptake. *Neuron, 62*, 788-801.

Abramov, E., Dolev, I., Fogel, H., Ciccotosto, G. D., Ruff, E., & Slutsky, I. (2009, December). Amyloid-b as a positive endogenous regulator of release probability at hippocampal synapses. *Nature Neuroscience, 12*(12), 1567-1578.

Chow, V. W., Mattson, M. P., Wong , P. C., & Gleichmann, M. (2010, November 24). An Overview of APP Processing Enzymes and Products. *Neuromolecular Medicine, 12*, 1-12.

Brody, A. H., & Strittmatter, S. M. (2018). Synaptotoxic Signaling by Amyloid Beta Oligomers in Alzheimer's Disease Through Prion Protein and mGluR5. *Advances in Pharmacology, 82*, 293 - 323.

Venkitaramani, D. V., Chin, J., Netzer, W. J., Gouras, G. K., Lesne, S., Malinow, R., & Lombrosso, P. J. (2007, October 31). b-Amyloid Modulation of synaptic transmission and plasticity. *The Journal of Neuroscience, 27*(44), 11832-11837.

Decker, H., Jürgensen, S., Adrover, M. F., Brito-Moreira, J., Bomfin, T. R., Klein, W. L., . . . Ferreira, S. T. (2010). N-Methyl-D-aspartate receptors are required for synaptic targeting of Alzheimer's toxic amyloid-b peptide oligomers. *Journal of Neurochemistry, 115*, 1520-1529.

Renner, M., Lacor, P. N., Velasco, P. T., Xu, J., Contractor, A., Klein, W. L., & Triller, A. (2010, June 10). Deleterious effects of amyloid b oligomers Acting as an extracellular Scaffold for mGluR5. *Neuron, 66*, 739-754.

Laurén, J., Gimbel, D. A., Nygaard, H. B., Gilbert, J. W., & Strittmatter, S. M. (2009, February 26). Cellular prion protein mediates impairment of synaptic plasticity by amyloid-b oligomers. *Nature, 457*, 1128-1134.

Um, J. W., Kaufman, A. C., Kostyle, M., Heiss, J. K., Stagi, M., Takahashi, H., . . . Strittmatter, S. M. (2013, September 4). Metabotropic Glutamate Receptor 5 is a

Correceptor for Alzheimer Ab Oligomer Bound to Cellular Prion Protein. *Neuron, 79*, 887-902.

Alberdi , E., Sanchez-Gomez, M. V., Cavaliere, F., Perez-Sanmartin, A., Zugaza, J. L., Trullas, R., . . . Matute, C. (2010). Amyloid b oligomers induce Ca2+ dysregulation and neuronal death through activation of ionotropic glutamate receptors. *Cell Calcium, 47*, 264-272.

De Felice, F. G., Velasco, P. T., Lambert, M. P., Viola, K., Fernandez, S. J., Ferreira, S. T., & Klein, W. L. (2007, April 13). Ab Oligomers Induce Neuronal Oxidative Stress through an N-Methyl-D-aspartate Receptor-dependent Mechanism that is Blocked by the Alzheimer Drug Memantine. *The Journal of Biological Chemistry, 282*(15), 11590-11601.

Demuro, A., Mina, E., Kayed, R., Milton, S. C., Parker, I., & Glabe, C. C. (2005, April 29). Calcium Dysregulation and Membrane Disruption as a Ubiquitous Neurotoxic Mechanism of Soluble Amyloid Oligomers. *The Journal of Biological Chemistry, 280*(17), 17294-17300.

Kelly, B. L., & Ferreira, A. (2006, September 22). b-Amyloid-induced Dynamin 1 degradation is mediated by N-Methyl-D-Aspartate Receptors in Hippocampal Neurons. *The Journal of Biological Chemistry, 281*(38), 28079-28089.

Paula-Lima, A. C., Adasme, T., SanMartin, C., Sebolleta, A., Hetz, C., Carrasco, M. A., . . . Hidalgo, C. (2011). Amyloid b-Peptide Oligomers Stimulate RyR-Mediated Ca2+ Release Inducing Mitochondrial Fragmentation in Hippocampal Neurons and Prevent RyR-Mediated Dendritic Spine Remodeling Produced by BDNF. *Antioxidants & Redox Signaling, 14*(7), 1209.

Citri, A., & Malenka, R. C. (2008). Synaptic Plasticity: Multiple Forms, Functions, and Mechanisms. *Neuropsychopharmacology, 33*, 18-41.

Bear, M. F., & Malenka, R. C. (1994). Synaptic plasticity: LTP and LTD. *Current Opinion in Neurobiology, 4*(3), 389-399.

Lisman , J. E., & Harris, K. M. (1993). Quantal analysis and synaptic anatomy-integrating two views of hippocampal plasticity. *TINS, 16*(4), 141-147.

Okamoto, K., Bosch, M., & Hayashi, Y. (2009, December). The Roles of CaMKII and F-actin in the Structural Plasticity of Dendritic Spines: A potential Molecular Identity of a Synaptic Tag? *Physiology, 24*, 357-366.

Hsieh, H., Boehm, J., Sato, C., Iwatsubo, T., Tomita, T., Sisodia, S., & Malinow, R. (2006, December 7). AMPAR Removal Underlies Ab-Induced Synaptic Depression and Dendritic Spine Loss. *Neuron, 52*, 831-843.

Lacor, P. N., Buniel, M. C., Furlow, P. W., Clemente, A. S., Velasco, P. T., Wood, M., . . . Klein, W. L. (2007, January 24). Ab Oligomer-Induced Aberrations in Synapse Composition, Shape, and Density Provide a Molecular Basis for Loss of Connectivity in Alzheimer's Disease. *The Journal of Neuroscience, 27*(4), 796-807.

Walsh, D. M., Klyubin, I., Fadeeva, J. V., Cullen, W. K., Anwyl, R., Wolfe, M. S., . . . Selkoe, D. J. (2002, April 4). Naturally secreted oligomers of amyloid b protein potently inhibit hippocampal long-term potentiation in vivo. *Nature, 416*, 535-539.

Wang, H.-W., Pasternak, J. F., Kuo, H., Ristic, H., Lambert, M. P., Chromy, B., . . . Trommer, B. L. (2002). Soluble oligomers of b amyloid (1-42) inhibit long-term potentiation but not long-term depression in rat dentate gyrus. *Brain Research, 924*, 133-140.

Chen, X., Lin, R., Chang, L., Xu, S., Wei, X., Zhang, J., . . . Wang, Q. (2013). Enhancement of Long-Term Depression by soluble amyloid b protein in rat

hippocampus is mediated by metabotropic glutamate receptor and involves activation of P38 MAPK and Caspase-3. *Neuroscience, 253*, 435-443.

Hu, N.-W., Nicoll, A. J., Zhang, D., Mably, A. J., O'Malley, T., Purro , S. A., . . . Rowan, M. J. (2014). mGLu5 receptors and cellular prion protein mediate. amyloid-b-facilitated synaptic long-term depression in vivo. *Nature, 5*(3374), 1-13.

Kim, J.-J., Anwyl, R., Suh, Y.-H., Djamgoz, M. B., & Rowan, M. J. (2001, February 15). Use-Dependent Effects of Amyloidogenic Fragments of β-amyloid Precursor Protein on Synaptic Plasticity in Rat Hippocampus in vivo. *The Journal of Neuroscience, 21*(4), 1327-1333.

Cleary, J. P., Walsh, D. M., Hofmeister, J. J., Shankar, G. M., Kuskowski, M. A., & Selkoe, D. J. (2005, January 15). Natural oligomers of the amyloid-b protein specifically disrupt cognitive function. *Nature Neuroscience, 8*(1), 79-84.

Lesne, S., Koh, M. T., Kotilinek, L., Kayed, R., Glabe, C. G., Yang, A., . . . Ashe, K. H. (2006, March 16). A specific amyloid-b protein assembly in the brain impairs memory. *Nature, 440*, 352-357.

Reed, M. N., Hofmeister, J. J., Jungbauer, L., Welzel, A. T., Yu, C., Sherman, M. A., . . . Cleary, J. P. (2011). Cognitive effects of cell-derived and synthetically derived Ab oligomers. *Neurobiology of Aging, 32*, 1784-1794.

Bao, L., Locovei, S., & Dahl, G. (2004). Pannexin membrane channels are mechanosensitive conduits for ATP. *FEBS Letters, 572*, 65-68.

Prochnow, N., Abdulazim, A., Kurtenbach, S., Wildförster, V., Dvoriantchikova, G., Hanske, J., . . . Zoidl, G. (2012, December). Pannexin1 Stabilizes Synaptic plasticityand is Needed for learning. *Plos One, 7*(12), 1-10.

Ardiles, A. O., Flores-Muñoz, C., Toro-Ayala, G., Cárdenas, A. M., Palacios, A. G., Muñoz, P., . . . Martinez, A. D. (2014, October 14). Pannexin 1 regulates

bidirectional hippocampal synaptic plasticity in adult mice. *Frontiers in Cellular Neuroscience, 8*(326), 1-14.

Gajardo, I., Salazar, C. S., Lopez-Espindola, D., Estay, C., Flores-Muñoz , C., Elgueta, C., . . . Ardiles, A. O. (2018, April). Lack of Pannexin 1 Alters Synaptic GluN2 Subunit Composition and Spatial Reversal Learning in Mice. *Frontiers in Molecular Neuroscience, 11*(114), 1-14.

Sanchez-Arias, J. C., Liu, M., Choi, C. S., Ebert, S. N., Brown, C. E., & Swayne, L. A. (2019, May/June). Pannexin 1 Regulates Network Ensembles and Dendritic Spine Development in Cortical Neurons. *eNeuro, 6*(3), 1-19.

Flores-Muñoz, C., García-Rojas, F., Pérez, M. A., Santander, O., Mery, E., Ordenes, S., . . . Ardiles, A. O. (2022). The Long-Term Pannexin 1 Ablation Produces Structural and Functional Modifications in Hippocampal Neurons. *Cells, 11*(3646), 1-31.

Flores-Muñoz, C., Gómez, B., Mery, E., Mujica, P., Gajardo, I., Córdova, C., . . . Ardiles, A. O. (2020, March 19). Acute Pannexin 1 Blockade Mitigates Early Synaptic Plasticity Defects in a Mouse Model of Alzheimer's Disease. *Frontiers in Cellular Neuroscience, 14*(46), 1-16.

Qu, R., Dong, l., Zhang, j., Yu, X., Wang, L., & Zhu, S. (2020). Cryo-EM structure of human heptameric Pannexin 1 channel. *Cell Research, 30*, 446-448.

Michalski, K., Syrjanen, J. L., Henze, E., Kumpf, J., Furukawa, H., & Kawate, T. (2020). The Cryo-EM structure of pannexin 1 reveals unique motifs for ion selection and inhibition. *eLIFE, 9*(e54670), 1-14.

Mou, L., Ke, M., Song, M., Shan, Y., Xiao, Q., Liu, Q., . . . Deng, D. (2020). Structural basis for gating mechanisms of Pannexin 1 channel. *Cell Research, 30*, 452-454.

Deng, Z., He, Z., Maksaev, G., Bitter, R. M., Rau, M., Fitzpatrick, J. A., & Yuan, P. (2020, April). Cryo-EM structures of the ATP release channel pannexin 1. *Nature Structural & Molecular Biology, 27*, 373-381.

Iglesias, R. M., & Spray, D. C. (2012). Pannexin-Mediated ATP Release Provides Signal Transmission Between Neuro2A Cells. *Neurochemical Research, 37*, 1355-1363.

Brough, D., Pelegrin, P., & Rothwell, N. J. (2009). Pannexin-1-dependent caspase-1 activation and secretion of IL-1b is regulated by zinc. *European Journal of Immunology, 39*, 352-358.

Pelegrint, P., & Supernant, A. (2006). Pannexin-1 mediates large pore formation and interleukin-1b release by the ATP-gated P2X7 receptor. *The EMBO Journal, 25*(21), 5071-5082.

Wei, L., Sheng, H., Chen, L., Hao, B., Shi, X., & Chen, Y. (2016). Effect of pannexin-1 on the release of glutamate and cytokines in astrocytes. *Journal of Clinical Neuroscience, 23*, 135-141.

Abeele, F. V., Bidaux, G., Gordienko, D., Beck, B., Panchin, Y. V., Baranova, A. V., . . . Prevarskaya, N. (2006, August 14). Functional implications of calcium permeability of the channel formed by pannexin 1. *The Journal of Cell Biology, 174*(4), 535-546.

Thompson, R. J., Jackson, M. F., Olah, M. E., Rungta, R. L., Hines, D. J., Beazely, M. A., . . . MacVicar, B. (2008, December 5). Activation of Pannexin-1 Hemichannels Augments Aberrant Bursting in the Hippocampus. *Science, 322*, 1555-1559.

Weilinger, N. L., Lohman, A. W., Rakai, B. D., Ma, E. M., Bialecki, J., Maslieieva, V., . . . Thompson, R. (2016). Metabotropic NMDA receptor signaling couples Src family kinases to pannexin-1 during excitotoxicity. *Nature Neuroscience*, 1-14.

Vogt, A., Hormuzdi, S. G., & Monyer, H. (2005). Pannexin1 and Pannexin2 expression in the developing and mature rat brain. *Molecular Brain research, 141*, 113-120.

Bruzzone, R., Hormuzudi, S. G., Barbe, M. T., Herb, A., & Monyer, H. (2003, November 11). Pannexins, a family of gap junctions proteins expressed in brain. *Proceedings of the National Academy of Science, 100*(23), 13644-13649.

Ray, A., Zoidl, G., Weickert, S., Wahle, P., & Dermietzel, R. (2005). Site-specific and developmental expression of pannexin1 in the mouse nervous system. *European Journal of Neuroscience, 21*, 3277-3290.

Zoidl, G., Petrasch-Parwez, E., Ray, A., Meier, C., Bunse, S., Habbes, H. W., . . . Dermietzel, R. (2007). Localization of the Pannexin 1 Protein at Postsynaptic Sites in the Cerebral Cortex and Hippocampus. *Neuroscience, 146*, 9-16.

Thompson, R. J., Zhou, N., & MacVicar, B. A. (2006, May 12). Ischemia Opens Neuronal Gap Junction Hemichannels. *Science, 312*, 924-927.

Weilinger, N. L., Tang , P. L., & Thompson, R. J. (2012, September 5). Anoxia-Induced NMDA Receptor Activation Opens Pannexin Channels via Src Family Kinases. *The Journal of Neuroscience, 32*(36), 12579-12588.

Navis, K. E., Fan, C. Y., Trang, T., Thompson, R. J., & Derksen, D. J. (2020, August 5). Pannexin 1 Channels as a Therapeutic Target: Structure, Inhibition, and Outlook. *ACS Chemical Neuroscience, 11*(15), 2163-2172.

Dossi, E., Blauwblomme, T., Moulard, J., Chever, O., Vasile, F., Guinard, E., . . . Rouach, N. (2018, May 30). Pannexin-1 channels contribute to seizure generation in human epileptic brain tissue and in a mouse model of epilepsy. *Science Translational Medicine, 10*(eaar3796), 1-13.

Lopatar, J., Dale, N., & Frenguelli, B. G. (2015). Pannexin-1-mediated ATP release from area CA3 drives mGlu5-dependent neuronal oscillation. *Neuropharmacology, 93*, 219-228.

Orellana , J. A., Froger, N., Ezan, P., Jiang, J. X., Bennett, M. V., Naus, C. C., . . . Sáez, J. C. (2011). ATP and glutamate released via astroglial connexin 43 hemichannels mediate neuronal death through activation of pannexin 1 hemichannels. *Journal of Neurochemistry, 118*, 826-840.

Harcha, P. A., Vargas, A., Yi, C., Koulakoff, A. A., Giaume, C., & Sáez, J. C. (2015, June 24). Hemichannels are required for amyloid b-peptide-induced degranulation and are activated in brain mast cells of APPswe/PS1dE9 Mice. *The Journal of Neuroscience, 35*(25), 9526-9538.

Yi, C., Mei, X., Ezan, P., Mato, S., Matias, I., Giaume, C., & Koulakoff, A. (2016). Astroglial connexin43 contributes to neuronal suffering in mouse model of Alzheimer's disease. *Cell Death and Differentiation, 23*, 1691-1701.

Abudara, V., Roux, L., Dallerac, G., Matias, I., Dulong, J., Mothet, J. P., . . . Giaume, C. (2015, January 30). Activated Microglia Impairs Neuroglial Interaction by Opening Cx43 Hemichannels in Hippocampal Astrocytes. *Glia, 63*(5), 1-17.

Backhouse , N., Delporte, C., Givernau, M., Cassels, B., Valenzuela, A., & Speisky, H. (1994). Anti-inflammatory and antipyretic effects of boldine. *Agents Actions, 42*, 114-117.

Yi, C., Ezan, P., Fernandez, P., Schmitt, J., Sáez, J. C., Giaume, C., & Koulakoff, A. (2017, July 13). Inhibition of glial hemichannels by boldine treatment reduces neuronal suffering in a murine model of Alzheimer's disease. *Glia, 65*(10), 1-19.

Engel, B., Gomn, W., Broich, K., Maier, W., Weckbecker, K., & Haenisch, B. (2018). Hyperuricemia and dementia - a case-control study. *BMC Neurology, 18*(131), 1-7.

Khan, A. A., Quinn, T. J., Hewitt, J., Fan, Y., & Dawson, J. (2016). Serum uric acid level and dementia: systematic review and meta-analysis. *Age, 38*(16), 1-11.

Lu, N., Dubreuil, M., Zhang, Y., Neogi, T., Rai, S. K., Ascherio, A., . . . Choi, H. K. (2016). Gout and the risk of Alzheimer's disease: a population-based, BMI-matched cohort study. *Annals of Rheumatic Diseases, 75*(3), 547-551.

Colin-Gonzalez, A. L., & Santamaria, A. (2013, November). Probenecid: An Emerging Tool for Neuroprotection. *CNS & neurological disorders drug targets, 12*(7), 1050-1065.

Chen, G.-F., Xu, T.-h., Yan, Y., Zhou, Y.-r., Jiang, Y., Melcher, K., & Xu, H. E. (2017, September). Amyloid beta: Structure, biology and structure-based therapeutic development. *Acta Pharmacologica Sinica, 38*(9), 1205-1235.

Ardiles, A. O., Grabrucker, A. M., Scholl, F. G., Rudenko, G., & Borsello, T. (2017). Molecular and Cellular Mechanisms of Synaptopathies. *Neural Plasticity, 11*(1), 5731.

Webster, S. J., Bachstetter, A. D., Nelson, P. T., Schmitt, F. A., & Van Eldik, L. J. (2014, April 23). Using mice to model Alzheimer's dementia: an overview of the clinical disease and the preclinical behavioral changes in 10 mouse models. *Frontiers in Genetics, 5*(88), 1-23.

Tzeng, C.-T., Hasegawa, Y., Iguchi, R., Cheung, A., Caffrey, D. R., Thatcher, E. J., . . . Golenbock, D. T. (2018, September 4). Inflammasome-derived cytokine IL18 suppresses amyloid-induced seizures in Alzheimer-prone mice. *Proceedings of the National Academy of Sciences, 115*(36), 9002-9007.

Silverman, W., Locovei, S., & Dahl, G. (2008, September). Probenecid, a gout remedy, inhibits pannexin 1 channels. *American Journal of Physiology Cell Physiology, 295*(3), C761-C767.

Bhaskaracharya, A., Dao-Ung, P., Jalilian, I., Spildrejorde, M., Skarratt, K. K., Fuller, S. J., . . . Stokes, L. (2014, Mach 26). Probenecid blocks human P2X7 receptor-induced dye uptake via a pannexin-1 independent mechanism. *PLoS One, 9*(3), e93058.

Aquilino, M. S., Whyte-Fagundas, P., Lukewich, M. K., Zhang, L., Bardakjian, B. L., Zoidl, G. R., & Carlen, P. L. (2020, October 12). Pannexin-1 Deficiency Decreases Epileptic Activity in Mice. *Int J Mol Sci, 21*(20), 7510.

Wei, R., Wang, J., Xu, Y., Yin, B., He, F., Du, Y., . . . Luo, B. (2015, August 30). Probenecid protects against cerebral ischemia/reperfusion injury by inhibiting lysosomal and inflammatory damage in rats. *Neuroscience, 301*, 168-77.

Xiong, X. X., Gu, L. J., Shen, J., Kang, X. H., Zheng, Y. Z., Yue, S. B., & Zhu, S. M. (2014, January). Probenecid protects against transient focal cerebral ischemic injury by inhibiting HMGB1 release and attenuating AQP4 expression in mice. *Neurochemical Research, 39*(1), 216-24.

Jian, Z., Ding, S., Deng, H., Wang, J., Yu, W., Wang, L., . . . Xiong, X. (2016, July 15). Probenecid protects against oxygen-glucose deprivation injury in primary astrocytes by regulating inflammasome activity. *Brain Research, 1643*, 123-9.

Hainz, N., Wolf, S., Beck, A., Wagenpfeil, S., Tschernig, T., & Meier, C. (2017, December 8). Probenecid arrests the progression of pronounced clinical symptoms in a mouse model of multiple sclerosis. *Science Reports, 7*(1), 17214.

Hainz, N., Wolf, S., Tschernig, S., & Meier, C. (2016, FEB). Probenecid Application Prevents Clinical Symptoms and Inflammation in Experimental Autoimmune Encephalomyelitis. *Inflammation, 39*(1), 123-128.

Kameritsch, P., & Pogoda, K. (2020, October 29). The Role of Connexin 43 and Pannexin 1 During Acute Inflammation. *Frontiers Physiology, 11*, 594097.

Silverman, W. R., de Rivero Vaccari, J. P., Locovei, S., Qiu, F., Carlsson, S. K., Scemes , E., . . . Dahl, G. (2009, July 3). The pannexin 1 channel activates the inflammasome in neurons and astrocytes. *Journal of Biological Chemistry, 248*(27), 18143-51.

Jardanhazi-Kurutz , D., Kummer, M. P., Terwel, D., Vogel, K., Dyrks, T., Thiele, A., & Heneka, M. T. (2010, November). Induced LC degeneration in APP/PS1 transgenic mice accelerates early cerebral amyloidosis and cognitive deficits. *Neurochemistry International, 57*(4), 375-382.

Chaney, A., Bauer, M., Bochicchio, D., Smigova, A., Kassiou, M., Davies, K. E., . . . Boutin, H. (2018, February). Longitudinal investigation of neuroinflammation and metabolite profiles in the APPswexPS1de9 transgenic mouse model of Alzheimer's disease. *Journal of Neurochemistry, 144*(3), 318-335.

Ferguson , S. A., Sarkar, S., & Schmued, L. C. (2013, April 1). Longitudinal behavioral changes in the APP/PS1 transgenic Alzheimer's Disease model. *Behavioural Brain Research, 242*, 125-134.

Cheng, C.-H., Lin, K.-J., Hong, C.-T., Wu, D., Chang, H.-M., Liu, C.-H., . . . Hu, C.-J. (2019, September 13). Plasmon-Activated Water Reduces Amyloid Burden and Improves Memory in Animals With Alzheimer's Disease. *Scientific Reports, 9*(1), 13252.

Coles, M., Watt, G., Kreilaus, F., & Karl, T. (2020, December 4). Medium-Dose Chronic Cannabidiol Treatment Reverses Object Recognition Memory Deficits of APPswe/PS1dE9 Transgenic Female Mice. *Frontiers in Pharmacology, 11*(587604), 1-15.

Faivre, E., & Hölscher, C. (2013). Neuroprotective effects of D-Ala2GIP on Alzheimer's disease biomarkers in an APP/PS1 mouse model. *Alzheimer's Research & Therapy, 35*(2), 267-83.

Currais, A., Prior, M., Dargush, R., Armando, A., Ehren, J., Schubert, D., . . . Maher, P. (2014, April). Modulation of p25 and inflammatory pathways by fisetin maintains cognitive function in Alzheimer's disease transgenic mice. *Aging cell, 13*(2), 379-390.

Daugherty , D., Goldberg, J., Fischer, W., Dargusch, R., Maher, P., & Schubert, D. (2017, July 14). A novel alzheimer's disease drug candidate targeting inflammation and fatty acid metabolism. *Alzheimer's Research & Therapy, 9*(1), 2782.

Fan, S., Zheng, Y., Liu, X., Fang, W., Chen, X., Liao, W., . . . Liu, J. (2018). Curcumin-loaded PLGA-PEG nanoparticles conjugated with B6 peptide for potential use in Alzheimer's disease. *Drug Delivery, 25*(1), 1044-1055.

Fragoulis, A., Siegl, S., Fendt, M., Jansen, S., Soppa, U., Brandenburg, L.-O., . . . Christoph, J. W. (2017, August). Oral administration of methysticin improves cognitive deficits in a mouse model of Alzheimer's disease. *Redox Biology, 12*, 843-853.

Habib, A., Shytle, D. R., Sawmiller, D., Koilraj, S., Munna, S. A., Rongo, D., . . . Tan, J. (2019, September). Comparing the effect of the novel ionic cocrystal of lithium salicylate proline (LISPRO) with lithium carbonate and lithium salicylate on

memory and behavior in female APPswe/PS1dE9 Alzheimer's mice. *Journal of Neuroscience Research, 97*(9), 1066-1080.

Hashimoto, Y., Kusakari, S., Nawa, M., Okamoto, K., Toyama, Y., & Matsuoka, M. (2021, January 13). Restoration of the reduced CLSP activity alleviates memory impairment in Alzheimer disease. *Translational Psychiatry, 11*(1), 44.

Heneka, M. K., Kummer, M. P., Stutz, A., Delakate, A., Schwartz, S., Vieira-Saecker, A., . . . Golenbock, D. T. (2013, January 31). NLRP3 is activated in Alzheimer's disease and contributes to pathology in APP/PS1 mice. *Nature, 493*(7434), 674-8.

Savonenko, A., Xu, G. M., Melnikova, T., Morton, J. L., Gonzales, V., Wong, M. P., . . . Borchelt, D. R. (2005, April). Episodic-like memory deficits in the APP/Swe/PS1dE9 mouse model of Alzheimer's disease: Relationships to b-amyloid deposition and neurotransmitter abnormalities. *Neurobiology of Disease, 18*(3), 602-617.

Talbott , J. H. (1951, September). Clinical and metabolic effects of benmid in gout. *Bulletin on the Rheumatic Diseases, 2*(1), 1-2.

Talbott, J. H., Bishop, C., Norcross, B. M., & Lockie, L. M. (1951). The clinical and metabolic effects of benmid in patients with gout. *Transactions of the Association of American Physicians, 64*, 372-7.

Donovan, M. D., O'Brien, F. E., Boylan, G. B., Cryan, J. F., & Griffin, B. T. (2015, April). The effect of organic anion transporter 3 inhibitor probenecid on bumetanide levels in the brain: an integrated in vivo micro dialysis study in the rat. *The Journal of Pharmacy and Pharmacology, 67*(4), 501-10.

Hagos, F. T., Daood, M. J., Ocque, J. A., Nolin, T. D., Bayir, H., Poloyac, S. M., . . . Empey, P. E. (2017, April). Probenecid, an organic anion transporter 1 and 3

inhibitor, increases plasma and brain exposure of N-acetylcysteine. *Xenobiotica, 47*(4), 346-353.

Bang , S., Kim, K. Y., Yoo, S., Lee, S.-H., & Hwang, S. W. (2007, September 25). Transient receptor potential V2 expressed in sensory neurons is activated by probenecid. *Neuroscience Letters, 425*(2), 120-5.

Gisclon , L. G., Boyd, R. A., Williams, L. R., & Giacomini, K. M. (1989, April). The. effect of probenecid on the renal elimination of cimetidine. *Clinical Pharmacology Therapy, 45*(4), 444-52.

Inotsume, N., Nishimura, M., Nakano, M., Fujiyama, S., & Sato, T. (1990, January). The inhibitory effect of probenecid on renal excretion of famotidine in young, healthy volunteers. *Journal of Clinical Pharmacology, 30*(1), 50-56.

McKinney, T. D., Myers, P., & Speeg Jr, K. V. (1981, July). Cimetidine secretion by rabbit renal tubules in vitro. *The American Journal of Physiology, 241*(1), F69-76.

Ma, W., Hui, H., Pelegrin , P., & Supernant, A. (2009, February). Pharmacological characterization of pannexin-1 currents expressed in mammalian cells. *The Journal of Pharmacology and Experimental Therapeutics, 328*(2), 409-18.

Cunningham, R. F., Israili, Z. H., & Dayton, P. G. (1981, March April). Clinical pharmacokinetics of probenecid. *Clinical Pharmacokinetics, 6*(2), 135-51.

Garcia-Rodriguez , C., Mujica, P., Illanes-Gonzales, P., Lopez, A., Vargas, C., Sáez, J. C., . . . Ardiles, A. O. (2023). Probenecid, an Old Drug with Potential New Uses for Central Nervous System Disorders and Neuroinflammation. *Biomedicines, 11*(6), 1516.

Seo, J. H., Dalal, M. S., & Contreras, J. E. (2021, May 14). Pannexin-1 Channels as Mediators of Neuroinflammation. *International Journal of Molecular Science, 22*(10), 5189.

Zheng, Y., Tang, W., Zeng, H., Peng, Y., Yu, X., Yan, F., & Cao, S. (2022, March 23). Probenecid-Blocked Pannexin-1 Channels Protects Against Early Brain Injury via inhibiting Neuronal AIM2 Inflammasome Activation After Subarachnoid Hemorrhage. *Frontiers in Neurology, 13*, 854671.

Urenjak, J., Obrenovitch, T. P., & Zilkha, E. (1997, January). Effect of probenecid on depolarizations evoked by N-methyl-D-aspartate (NMDA) in the rat striatum. *Naunyn Schmiedebergs Archives of Pharmacology, 355*(1), 36-42.

Taylor, D. L., Urenjak, J., Zilkha, E., & Obrenovitch, T. P. (1997, August). Effects of probenecid on the elicitation of spreading depression in the rat striatum. *Brain Research, 764*(2), 117-125.

Orellana, J. A., Moraga-Amaro, R., Diaz-Galarce, R., Rojas, S., Maturana, C. J., Stehberg, J., & Sáez, J. C. (2015, April 15). Restraint stress increases hemichannel activity in hippocampal glial cells and neurons. *Frontiers in Cellular Neuroscience, 9*(102), 1-12.

Lewerenz, J., & Maher, P. (2015, December). Chronic Glutamate Toxicity in Neurodegenerative Diseases - What is the Evidence? *Frontiers in Neuroscience, 9*(469), 1-20.

Kim, G. H., Kim, J. E., Rhie, S. J., & Yoon, S. (2015, December). The Role of Oxidative Stress in Neurodegenerative Diseases. *Experimental Neurobiology, 24*(4), 325-340.

Du, L., Empey, P. E., Ji, J., Chao, H., Kochanek, P. M., Bayir, H., & Clark, R. S. (2016, October 15). Probenecid and N-Acetylcysteine Prevent Loss of Intracellular Glutathione and Inhibit Neuronal Death after Mechanical Stretch Injury In Vitro. *Journal of Neurotrauma, 33*(20), 1913-1917.

Jiao, S.-S., Bu, X.-L., Liu, Y.-H., Zhu, C., Wang, Q.-H., Shen, L.-L., . . . Wang, Y.-J. (2016, February). Sex Dimorphism Profile of Alzheimer's Disease-Type Pathologies in an APP/PS1 Mouse Model. *Neurotoxicity Research, 29*(2), 256-66.

Wang, J., Tanila, H., Puolivali, J., Kadish, I., & van Groen, T. (2003, December). Gender differences in the amount and deposition of amyloid β in APPswe and PS1 double. *Neurobiology of Disease, 14*(3), 318-327.

Bucher, J. R., Huff, J., & Kluwe, W. M. (1986, May). Toxicology and carcinogenesis studies of isophorone in F3444 rats and B6C3F1 mice. *Toxicology, 39*(2), 207-19.

National Toxicology Program. (1991, September). NTP Toxicology and Carcinogenesis Studies of Probenecid (CAS No. 57-66-9 in F344/N Rats and B6C3F1 (Gavage Studies). *National Toxicology Program Technical Report Series, 395*, 1-215.

Christy , A. C., Byrnes, K. R., & Settle, T. L. (2014, March). Evaluation of medicated gel as a supplement to providing acetaminophen in the drinking water of C57BL/6 mice after surgery. *Journal of American Association for Laboratory Animal Science, 53*(2), 180-4.

Scheff, S. W., & Price, D. A. (2003, December). Synaptic pathology in Alzheimer's disease: a review of ultrastructural studies. *Neurobiology of Aging, 24*(8), 1029-46.

Buckner, R. L. (2004, September 30). Memory and executive function in aging and AD: multiple factors that cause decline and reserve factors that cause decline and reserve factors that compensate. *Neuron, 44*(1), 195-208.

Brooks 3rd, J. O., Yesavaga, J. A., Taylor, J., Friedman, L., Tanke , E. D., Luby, V., & Tinkenberg, J. (1993, Fall). Cognitive decline in Alzheimer's disease: elaborating

on the nature of the longitudinal factor structure of the Mini-Mental State Examination. *International Psychogeriatrics, 5*(2), 135-46.

Faivre, E., Coelho, J. E., Zornbach, K., Malik, E., Baqi, Y., Schneider, M., . . . Sergeant, N. (2018, July 12). Beneficial Effect of a selective Adenosine A2A receptor antagonist in the APPswe/PS1dE9 Mouse model of Alzheimer's Disease. *Frontiers in Molecular Neuroscience, 11*(235), 1-13.

Kazim, S. F., Seo, J. H., Bianchi, R., Larson, C. S., Sharma, A., Wong, R. K., . . . Pereira, A. C. (2021, April). Neuronal Network Excitability in Alzheimer's Disease: The Puzzle of similar versus Divergent Roles of Amyloid B and Tau. *eNeuro, 8*(2), 1-35.

Garcia, K. O., Ornellas, F. L., Matsumoto Martin, P. K., Patti, C. L., Mello, L. E., Frussa-Filho, R., . . . Longo, B. M. (2014, March). Therapeutic effects of the transplantation of VEGF overexpressing bone marrow mesenchymal stem cells in the hippocampus of murine model of Alzheimer's disease. *Frontiers in Aging Neuroscience, 6*(30), 1-15.

Guillot-Sestier, M. V., Araiz, A. R., Mela, V., Gaban, A. S., O'Neill, E., Joshi, L., . . . Lynch, M. A. (2021, June 10). Microglia metabolism is a pivotal factor in sexual dimorphism in Alzheimer's disease. *Communications Biology, 4*(1), 1-13.

Gyorffy, B. A., Toth, V., Torok, G., Gulyassy, P., Kovacs, R. A., Vadaszi, H., . . . Kardos, J. (2020, December). Synaptic mitochondrial dysfunction and septin accumulation are linked to complement mediated synapse loss in Alzheimer's disease animal model. *Cellular and Molecular Life Sciences, 77*(24), 5243-5258.

Montgomery, K. S., Edwards III, G., Levites, Y., Kumar, A., Myers, C. E., Gluck, M. A., . . . Bizon, J. L. (2016, April). Deficits in Hippocampal-Dependent Transfer

Generalization Learning Accompany Synaptic Dysfunction in a Mouse Model of Amyloidosis. *Hippocampus, 26*(4), 455-471.

Hoejimakers , L., Amelianchik, A., Verhaag, F., Kotah, J., Lucassen, P. J., & Korosi, A. (2018, March 7). Early-Life Stress Does not Aggravate Spatial Memory of the Process of Hippocampal Neurogenesis in Adult and Middle-Aged APP/PS1 Mice. *Frontiers in Aging Neuroscience, 10*(61), 1-14.

Knafo, S., Venero, C., Merino-Serrais, P., Fernaud-Espinosa, I., González-Soriano, J., Ferrer, I., . . . DeFelipe, J. (2009, September). Morphological alterations to neurons of the amygdala and impaired fear conditioning in a transgenic mouse model of Alzheimer's disease. *Journal of Pathology, 219*(1), 41-51.

Xu, Z., Xiao, N., Chen, Y., Huang, H., Marshall, C., Gao, J., . . . Xiao, M. (n.d.). Deletion of aquaporin-4 in APP/PS1 mice exacerbates brain AB accumulation and memory deficits.

Ibrahim, N. F., Yanagisawa, D., Durani, L. W., Hamezah, H. S., Damanhuri, H. A., Wan Ngah, W. Z., . . . Kiuchi, Y. (2017). Tocotrienol-Rich Fraction Modulates Amyloid Pathology and Improves Cognitive Function in ABPP/PS1 Mice. *Journal of Alzheimer's Disease, 55*(2), 597-612.

Janus, C., Flores, A. Y., Xu, G., & Borchelt, D. R. (2015, September). Behavioral abnormalities in APPswe/PS1dE9 mouse model of AD-like pathology: comparative analysis across multiple behavioral domains. *Neurobiology of Aging, 36*(9), 2519-2532.

Jarvela, T. S., Womack, T., Georgiou, P., Gould, T. D., Eriksen, J. L., & Lindberg, I. (2018, June 28). 7B2 chaperone knockout in APP model mice results in reduced plaque burden. *Scientific Reports, 8*(1), 9813.

Jia, N., Han, K., Kong, J. J., Zhang, X. M., Sha, S., Ren, G.-R., & Cao, Y.-P. (2013, August). (-)-Epigallotechin-3-gallate alleviates spatial memory impairment in APP/PS1 mice by restoring IRS-1 signaling defects in the hippocampus. *Molecular and Cellular Biochemistry, 380*(1-2), 211-8.

Jiao, S.-S., Yao, X.-Q., Liu, Y.-H., Wang, Q.-H., Zeng, F., Lu, J.-J., . . . Li, J. (2015, April 21). Edaravone alleviates Alzheimer's disease-type pathologies and cognitive deficits. *Proceedings of National Academy of Science, 112*(16), 5225-30.

Karunakaran, S. (2020, December 15). unraveling Early Signs of Navigational Impairment in APPswe/PS1dE9 Mice Using Morris Water Maze. *Frontiers in Neuroscience, 14*(568200), 1-12.

Kuchibhotla, K. V., Goldman, S. T., Lattarulo, C. R., Wu, H.-Y., Hyman, B. T., & Bacskai, B. J. (2008, July 31). AB Plaques Lead to Aberrant Regulation of Calcium Homeostasis In Vitro Resulting in Structural and Functional Disruption of Neuronal Networks. *Neuron, 59*(2), 214-25.

Lalonde , R., Kim, H., Maxwell, J., & Fukuchi, K. (2005, December 23). Exploratory activity and spatial learning in 12-month-old APP695SWE/co+PS1/DE9 mice with amyloid plaques. *Neuroscience Letters, 390*(2), 87-92.

Timmer, N. M., van Dijik, L., van der Zee, C. E., Kiliaan, A., de Waal, R. M., & Verbeek, M. M. (2010, October). Enoxaparin treatment administered at both early and late stages of amyloid b deposition improves cognition of APPswe/PS1dE9 mice with differential effects on AB levels. *Neurobiology of Disease, 40*(1), 340-347.

Li, L., Luo, J., Chen, D., Tong, J.-b., Zeng, L.-p., Cao, Y.-q., . . . Huang, J.-f. (2016, March). BACE1 in the retina: a sensitive biomarker for monitoring early pathological changes in Alzheimer’s disease. *Neural Regeneration Research, 11*(3), 447-453.

Li, Q., Navakkode, S., Rothkegel, M., Soong, T. W., Sajikumar, S., & Korte , M. (2017, May 23). Metaplasticity mechanisms restore plasticity and associativity in an animal model of Alzheimer's disease. *Proceedings of the National Academy of Science, 114*(21), 5527-5532.

Li, Q., Wang, Q., Guan, H., Zou, Y., & Li, L. (2021, January 29). Schisandrin Inhibits NLRPI Inflammasome-Mediated Neuronal Pyroptosis in Mouse Models of Alzheimer's Disease. *Neuropsychiatric Disease and Treatment, 17*, 261-268.

Xin, L., Feng, Y., Wu, W., Zhao, J., Fu, C., Li, Y., . . . Zhou, X. (2016, August). Sex differences between APPswePS1dE9 mice in A-beta accumulation and pancreatic islet function during the development of Alzheimer's disease. *Laboratory Animals, 50*(4), 275-285.

Lyra e Silva, N. M., Gonzalves, R. A., Pascoal, T. A., Lima-Filho, R. A., França Resende, E. d., Vieira, E. L., . . . Hashigushi. (2021, April 28). Pro-inflammatory interleukin-6 signaling links cognitive impairments and peripheral metabolic alterations in Alzheimer's disease. *Translational Psychiatry, 11*(1), 1-15.

Martin-Sanchez, A., Piñero, J., Nonell, L., Arnal, M., Ribe, E. M., Nevado-Holgado, A., . . . Valverde, O. (2021, April 2). Comorbidity between Alzheimer's disease and major depression: a behavioural and transcriptomic characterization study in mice. *Alzheimer's Research & Therapy, 13*(1), 1-19.

Miffilin, M. A., Winslow, W., Surendra, L., Tallino, S., Vural, A., & Velazquez, R. (2021, May). Sex difference in the IntelliCage and the Morris water maze in the APP/PS1 mouse model of amyloidosis. *Neurobiology of Aging, 101*, 130-140.

Muller, L., Guerra, N. P., Sentzel, J., Ruhlmann, C., Lindner, T., Krause, B. J., . . . Kuhla, A. (2021, March 18). Long-Term Caloric Restriction Attenuates B-Amyloid

Neuropathology and is accompanied by Autophagy in APPswe/PS1delta9 Mice. *Nutrients, 13*(3), 985.

Carrillo-Mora, P., Méndez-Cuesta, L. A., Pérez-Dela Cruz, V., Fortoul-van Der Goes, T. I., & Santamaria, A. (2010, July 11). Protective effect of systemic L-Kynurenine and probenecid administration on behavioral and morphological alterations induced by toxic soluble amyloid beta (25-35) in rat hippocampus. *Behavioral Brain Research, 210*(2), 240-250.

Yeung, A. K., Patil, C. S., & Jackson, M. F. (2020, September). Pannexin-1 in the CNS: Emerging concepts in health and disease. *Journal of Neurochemistry, 154*(5), 468-485.

Narahari, A. K., Kreutzberger, A. J., Gaete, P. S., Chiu, Y.-H., Leonhardt, S. A., Medina, C. B., . . . Tamm. (2021, January 7). ATP and large signaling metabolites flux through caspase-activated Pannexin 1 channels. *eLife, 10*(e64787), 1-21.

Sebastiao, A. M., & Ribeiro, J. A. (2015, September 24). Neuromodulation and metamodulation by adenosine: Impact and subtleties upon synaptic plasticity regulation. *Brain Research, 1621*, 102-13.

Sanchez-Arias, J. C., van der Slagt, E., Vecciarelli, H. A., Candlish, R. C., York, N., Young, P. A., . . . Swayne, L. A. (2021, September). Purinergic signaling in nervous system health and disease: Focus on pannexin 1. *Pharmacology & Therapeutics, 225*(107840), 1-17.

Calsolaro, V., & Edison, P. (2016, June). Neuroinflammation in Alzheimer's disease: Current evidence and future directions. *Alzheimer's and Dementia: The journal of the Alzheimer's Association, 12*(6), 719-32.

Lee, H. G., Won, S. M., Gwag, B. J., & Lee, Y. B. (2011, January). Microglial P2X7 receptor expression is accompanied by neuronal damage in the cerebral cortex

of the APPswe/PS1dE9 mouse model of AAlzheimer's disease. *Experimental and Molecular Medicine, 43*(1), 7-14.

Kurcuru, H., Colom-Cadena, M., Davies, C., Wilkins, L., King, D., Rose, J., . . . Spires-Jones, T. L. (2022, May). Inhibitory synapse loss and accumulation of amyloid beta in inhibitory presynaptic terminals in Alzhaimer's disease. *European Journal of Neurology, 29*(5), 1311-1323.

Lamprecht, R. (2021, July 15). Actin Cytoskeleton Role in the Maintenance of Neuronal Morphology and Long-Term Memory. *Cells, 10*(7), 1975.

Konietzny, A., Bar, J., & Mikhaylova, M. (2017, May 18). Dendritic Actin Cytoskeleton: Structure, Functions and Regulations. *Frontiers in cellular neuroscience, 11*(147), 1-10.

Zhang, Y., Huang, L.-J., Shi, S., Xu, S.-F., Wang, X.-L., & Peng, Y. (2016, December). L-3-butylphthalide Rescues Hippocampal Synaptic Failure and Attenuates Neuropathology in Aged APP/PS1 Mouse Model of Alzheimer's Disease. *CNS Neuroscience & Therapeutics, 22*(12), 979-987.

Dong, Q., Teng, S.-W., Wang, Y., Qin, F., Li, Y., Ai, L.-L., & Yu, H. (2019, March 23). Sitagliptin protects the cognition function of the Alzheimer's disease mice through activating glucagon-like peptide-1 and BDNF-TrkB signalings. *Neuroscience Letters, 696*, 184-190.

Lonnemann, N., Hosseini, S., Ohm, M., Geffers, R., Hiller, K., Dinarello, C. A., & Korte, M. (2022, August 30). IL-37 expression reduces acute and chronic neuroinflammation and rescues cognitice impairment in an Alzheimer's disease mouse model. *Elife, 11*(e75889), 1-41.

Huang , L., Zhang, Y., Peng, Y., Zhao, Z., Zhou, Y., Wang, X., & Peng, Y. (2019, September). Protective effect of potassium 2-(l-hydroxypentyl)-benzoate on

hippocampal neurons, synapses and dystrophic axons in APP/PS1 mice. *Psychopharmacology, 236*(9), 2761-2771.

Voet, S., Prinz, M., & van Loo, G. (2019, February). Microglia in Central Nervous System Inflammation and Multiple Sclerosis Patholigy. *Trends in Molecular Medicine, 25*(2), 112-123.

Hashioka, S., Wu, Z., & Klegeris, A. (2021). Glia-Driven Neuroinflammation and Systemis Inflammation in Alzheimer's Disease. *Current Neuropharmacology, 19*(7), 908-924.

Kelley, N., Jeltema, D., Duan, Y., & He, Y. (2019, July 6). The NLRP3 Inflammasome: An Overview of Mechanisms of Activation and Regulation. *International Journal of Molecular Science, 20*(13), 3328.

Colom-Cadena, M., Spires-Jones, T., Zetteberg, H., Blennow, K., Caggiano, A., DeKosky, S. T., . . . Izzo, N. (2020). The clinical promise of biomarkers of synapse damage or loss in Alzheimer's disease. *Alzheimer's Research & Therapy, 12*(21), 1-12.

Ribaric, S. (2023). Detecting Early Cognitive Decline in Alzheimer's Disease with Brain Synaptic Structural and Functional Evaluation. *Biomedicines, 11*(2), 355.

Ammassari-Teule, M. (2020). Early-Occurring Dendritic Spine Alterations in Mouse Models of Alzheimer's Disease Inform on Primary Causes of Neurodegeneration. *Frontiers in Synaptic Neuroscience, 12*(566615), 1-7.

Smith, D. L., Pozueta, J., Gong, B., Arancio, O., & Shelanski, M. (2009, September 29). Reversal of long-term dendritic spine alterations in Alzheimer disease models. *Proceedings of the National Academy of Sciences, 106*(39), 16877-82.

Biju, K. C., Evans, R. C., Shrestha, K., Carlisle, D. C., Gelfond, J., & Clark, R. A. (2018, June 1). Methylene Blue Ameliorates Olfactory Dysfunction and Motor Deficits in

a Chronic MPTP/Probenecid Mouse Model of Parkinson's Disease. *Neuroscience, 380*, 111-122.

Karatas, H., Erdener, S. E., Gursoy-Ozdemir, Y., Lule, S., Eren-Koçak, E., Sen, Z. D., & Dalkara, T. (2013, March 1). Spreading depression triggers headache by activating neuronal Panx1 channels. *Science, 339*(6123), 1092-5.

Zhang, Z., Lei, Y., Yan, C., Mei, X., Jiang, T., Ma, Z., & Wang, Q. (2019, June). Probenecid Relieves Cerebral Dysfunction of Sepsis by Inhibiting Pannexin 1-Dependent ATP Release. *Inflammation, 42*(3), 1082-1092.

Garcia-Rojas, F., Flores-Muñoz, C., Santander, O., Solis, P., Martinez, A. D., Ardiles, A. O., & Fuenzalida, M. (2023). Pannexin-1 Modulates Inhibitory Transmission and Hippocampal Synaptic Plasticity. *Biomolecules, 13*(887), 1-17.

Bialechi, J., Werner, A., Weilinger, N. L., Tucker, C. M., Vecchiarelli, H. A., Egaña, J., . . . Thompson, R. J. (2020, January 22). Suppression of Presynaptic Glutamate Release by Postsynaptic Metabotropic NMDA Receptor Signalling to Pannexin-1. *The Journal of Neuroscience, 40*(4), 729-742.

Patil, S. C., Li, H., Lavine, N. E., Shi, R., Bodalia, A., Siddiqui, T. J., & Jackson, M. F. (2022, September 6). ER-resident STIM1/2 couples Ca+2 entry by NMDA receptors to pannexin-1 activation. *Proceedings of the natural academy of science, 119*(36), e2112870119.

Selen, A., Amidon, G. L., & Welling, P. G. (1982, November). Pharmacokinetics of probenecid following oral doses to human volunteers. *Clinical Trial, 71*(11), 1238-42.

Mookherjee, P., Green, P. S., Watson, G. S., Marques, M. A., Tanaka, K., Meeker, K. D., . . . Cook, D. G. (2011). GLT-1 loss accelerates cognitive deficit onset in an

Alzheimer's disease animal model. *Journal of Alzheimer's Disease, 26*(3), 447-55.

Scimemi, A., Meabon, J. S., Woltjer, R. L., Sullivan, J. M., Diamond, J. S., & Cook, D. G. (2013, March 20). Amyloid-b1-42 slows clearence of synaptically released glutamate by mislocalizing astrocytic GLT-1. *The Journal of Neuroscience, 33*(12), 5312-8.

Kadlecova, M., Freude, K., & Haudekal, H. (2023, April 24). Complexity of Sex Differences and Their Impact on Alzheimer's Disease. *Biomedicines, 11*(5), 1261.

Lenz, K. M., & Nelson, L. H. (2018, April 13). Microglia and Beyond: Innate Immune Cells As Regulators of Brain Development and Behavioral Function. *Fontiers in Immunologu, 9*(698), 1-13.

Stogsdill, J. A., & Eroglu, C. (2017, February). The interplay between neurons and glia in synapse development and plasticity. *Current Opinion in Neurobiology, 42*(1), 1-8.

Bennett, M. L., Bennet, F. C., Liddelow, S. A., Ajami, B., Zamanian, J. L., Fernhoff, N. B., . . . Grant, G. A. (2016, March 22). New tools for studying microglia in the mouse and human CNS. *Proceedings of the National Academy of Sciences, 113*(12), E1738-46.

Idzko, M., Ferrari, D., & Eltzschig, H. K. (2014, May 15). Nucleotide signalling during inflammation. *Nature, 509*(7500), 310-7.

Li, S., Jin, M., Koeglsperger, T., Shepardson, N. E., Shankar, G. M., & Selkoe, D. J. (2011, May 4). Soluble AB oligomers inhibit long-term potentiation through a mechanism involving excessive activation of extrasynaptic NR2B-containing NMDA receptors. *The Journal of Neuroscience, 31*(18), 6627-38.

Hanslik, K. L., & Ulland, T. K. (2020, September 18). The Role of Microglia and the Nlrp3 Inflammasome in Alzheimer's Disease. *Frontiers in Neurology, 11*(570711), 1-9.

Annexes

Table 6 *Days of treatment of the animals used in this thesis.*

Age	Sex	Animal Code	Days of treatment
Young 3 months old	Female	12.7.1	46
	Female	12.7.2	46
	Female	12.7.3	46
	Female	12.7.4	48
	Male	12.8.1	48
	Male	12.8.2	46
	Male	12.9.1	46
	Male	12.9.2	47
	Male	12.9.3	47
	Female	12.10.1	46
	Female	12.10.2	46
	Female	12.10.3	48
	Female	12.10.4	48
	Male	12.11.1	47
	Male	12.11.2	47
	Male	12.11.3	48
	Male	12.11.4	45
	Female	15.4B.1	46
	Female	15.4B.4	46
	Male	15.5A.1	46
	Male	15.5A.3	46
	Male	15.5A.4	46
	Male	15.5A.5	46
	Male	15.5B.1	46
	Male	15.5B.2	46
	Male	15.5B.3	46
	Male	15.5B.4	46
	Male	15.5B.5	45
	Female	15.14.1	45
	Female	15.14.2	45
	Female	15.14.3	45
	Male	15.15.1	45
	Male	15.15.2	45
	Male	15.15.3	45
	Female	20.1.1	40
	Female	20.1.2	40

	Female	20.1.3	40
Aged 12 months old	Female	10.1.1	44
	Female	10.1.2	43
	Male	10.2.1	45
	Male	10.2.2	43
	Male	10.2.4	45
	Male	10.2.6	43
	Male	10.4.2	43
	Male	10.4.3	44
	Female	11.1.1	45
	Male	10.4.1	45
	Male	10.4.4	45
	Male	10.4.5	45
	Female	11.1.2	42
	Female	11.1.6	42
	Male	10.11A.1	43
	Male	10.11A.2	43
	Male	10.11A.3	44
	Male	12.13.5	46
	Male	12.16.1	46
	Male	12.16.2	46
	Male	14.5.3	43
	Male	15.9.1	43
	Male	15.9.2	43
	Male	15.9.3	43
	Female	14.5B.4	40
	Female	15.20.4	40
	Female	14.5B.3	40
	Female	14.5B.2	40
	Female	14.5B.1	40
Aged 18 months old	Female	6.3.3.1	44
	Female	6.3.3.2	45
	Male	12.6.2	46
	Male	12.4.2	46
	Male	12.4.3	46
	Female	12.12.1	46
	Female	12.12.3	46
	Male	12.13.2	46
	Male	12.13.3	46
	Male	12.13.4	46
	Male	D42-5	34
	Male	D42-4	34
	Female	D35-3	34
	Male	D42-3	34
	Male	D42-1	34
	Male	D42-2	34
	Female	D39-4	34

	Female	D39-5	34
	Male	D42-6	34
	Female	D35-2	34
	Male	D42-7	34
	Female	D35-5	34
	Female	14.3.2	40
	Female	14.3.3	40
	Female	15.10.1	40

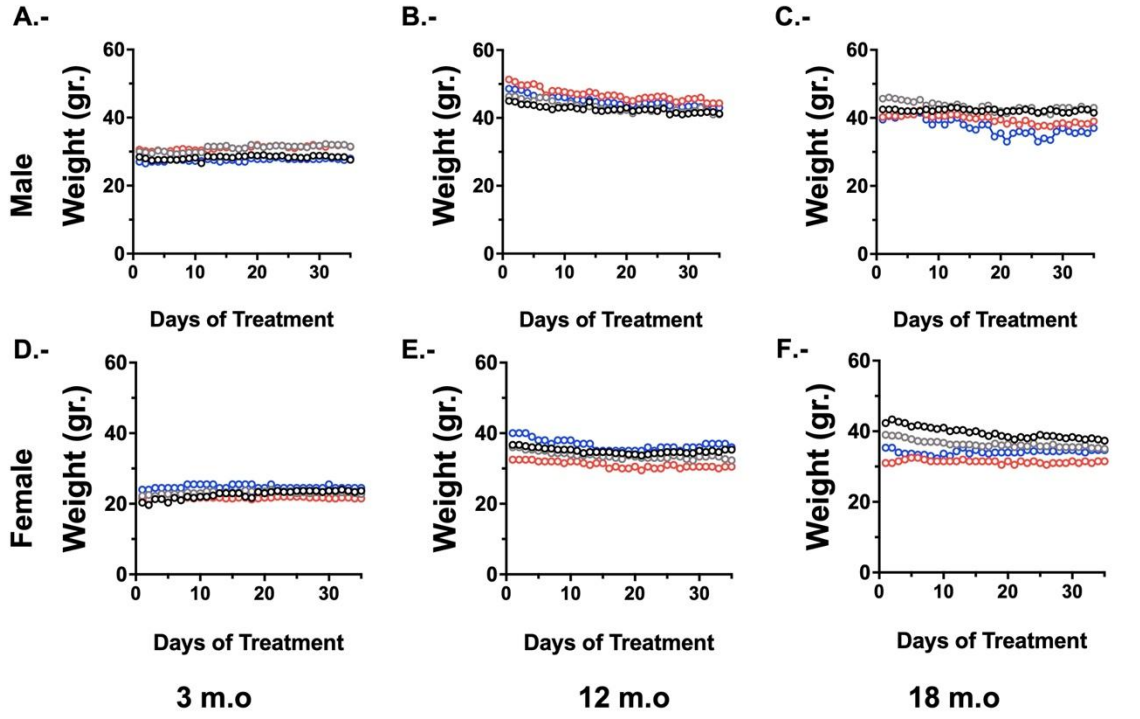

Figure 32 Weight gain during the treatment from day 1 until the day of euthanasia. ***A.-*** *Average body weight of male 3 m.o APP/PS1 animals from day 1 until the day of euthanasia in WT VEH (black), WT PBN (gray), TG VEH (red), and TG PBN (blue). Time (F(4.828,67.07)=4.145, ** p=0.0027) was the main source of variation by Three-way ANOVA. B.- All data are represented as mean ± SEM.* ***B.-*** *Average body weight of female 3 m.o APP/PS1 animals from day 1 until the day of euthanasia in WT VEH (black), WT PBN (gray), TG VEH (red), and TG PBN (blue). Time (F(3.077,27.23)=5.489, ** p=0.0042) was the main source of variation and there were significant interactions between time x genotype (F(46,407)=3.698, **** p<0.0001), time x treatment (F(46,407)=3.969, **** p<0.0001), time x genotype x treatment (F(46,407)=1.786, ** p=0.0019) by Three-way ANOVA.* ***C.-*** *Average body weight of male 12 m.o APP/PS1 animals from day 1 until the day of euthanasia in WT VEH (black), WT PBN (gray), TG VEH (red), and TG PBN (blue). Time (F(46,480)=2.478, **** p<0.0001), genotype (F(1,480)=96.19, **** p<0.0001), and treatment (F(1,480)=8.874, ** p=0.0030) were the main sources of variation and there was a significant interaction between genotype x treatment (F(1,480)=20.03, **** p<0.0001)by Three-way ANOVA.* ***D.-*** *Average body weight of female 12 m.o APP/PS1 animals from day 1 until the day of euthanasia in WT*

VEH (black), WT PBN (gray), TG VEH (red), and TG PBN (blue). There was no significant difference by Three-way ANOVA. ***E.-*** *Average body weight of male 18 m.o APP/PS1 animals from day 1 until the day of euthanasia in WT VEH (black), WT PBN (gray), TG VEH (red), and TG PBN (blue). Time (F(2.130,14.91)=8.774, ** p=0.0027) was the main source of variation and there was a significant interaction between time x genotype (F(46,322)=2.043, *** p=0.0002) and time x treatment (F(46,322)=2.463, **** p<0.0001) by Three-way ANOVA.* ***F.-*** *Average body weight of female 18 m.o APP/PS1 animals from day 1 until the day of euthanasia in WT VEH (black), WT PBN (gray), TG VEH (red), and TG PBN (blue). There was a significant interaction between time x genotype (F(46,368)=2.062, *** p=0.0001) by Three-way ANOVA. All data are represented as mean ± SEM.*

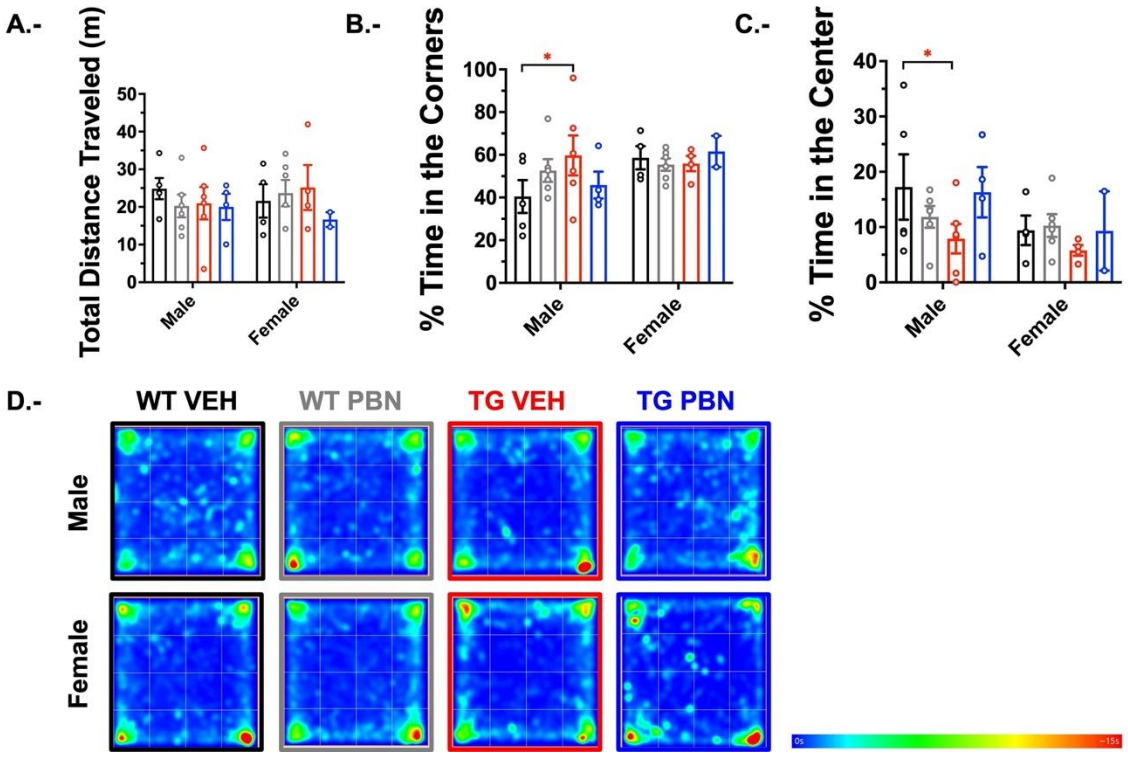

Figure 33: Locomotor activity assessed by the open field test was not affected in 3 m.o APP/PS1 mice. A.- *Total distance traveled by male and female 3 m.o APP/PS1 mice. There was no significant difference between groups by 3-way ANOVA.* ***B.-*** *Percentage of time spent in the corners by male and female 3 m.o APP/PS1 mice. There was a significant interaction by gender, genotype, and treatment (F(1,11) = 12.39 ** p = 0.0048) and the Tukey's multiple comparisons tests showed a significant difference between male WT VEH and male TG VEH * p = 0.026.* ***C.-*** *Percentage of time spent in the center by male and female 3 m.o APP/PS1 mice. There was a significant interaction by genotype and treatment (F(1,11) = 7.113 * p = 0.022) and the Tukey's multiple comparisons tests showed a significant difference between male WT VEH and male TG VEH * p = 0.047.* ***D.-*** *Representative average heatmaps of the open field test. Scale bar*

15 s. Data was presented as mean ± SEM (Male: WT VEH (5) WT PBN (6) TG VEH (6) TG PBN (4). Female: WT VEH (4) WT PBN (6) TG VEH (4) TG PBN (2))

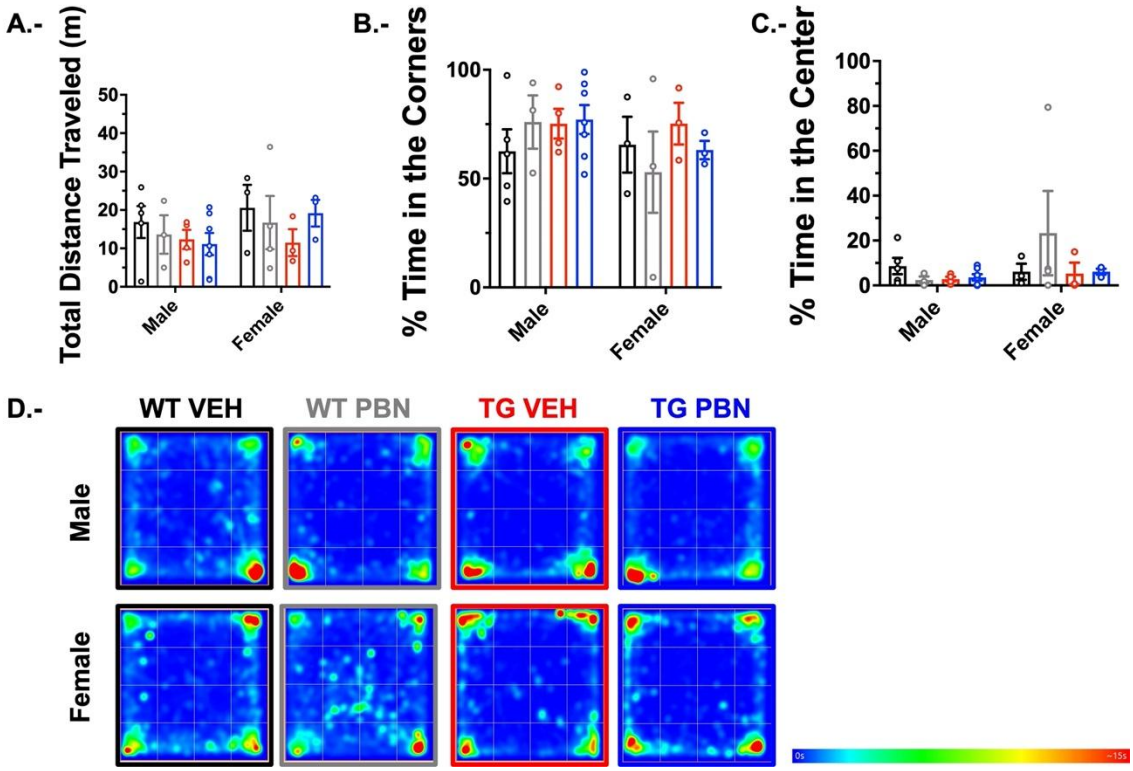

Figure 34 Locomotor activity assessed by the open field test was not affected in 12 m.o APP/PS1 mice. A.- *Total distance traveled by male and female 12 m.o APP/PS1 mice. There was no significant difference between groups by 3-way ANOVA.* ***B.-*** *Percentage of time spent in the corners by male and female 12 m.o APP/PS1 mice. There was no significant difference between groups by 3-way ANOVA.* ***C.-*** *Percentage of time spent in the center by male and female 12 m.o APP/PS1 mice. There was no significant difference between groups by 3-way ANOVA.* ***D.-*** *Representative average heatmaps of the open field test. Scale bar 15 s. Data was presented as mean ± SEM (Male: WT VEH (5) WT PBN (3) TG VEH (4) TG PBN (7). Female: WT VEH (3) WT PBN (4) TG VEH (3) TG PBN (3))*

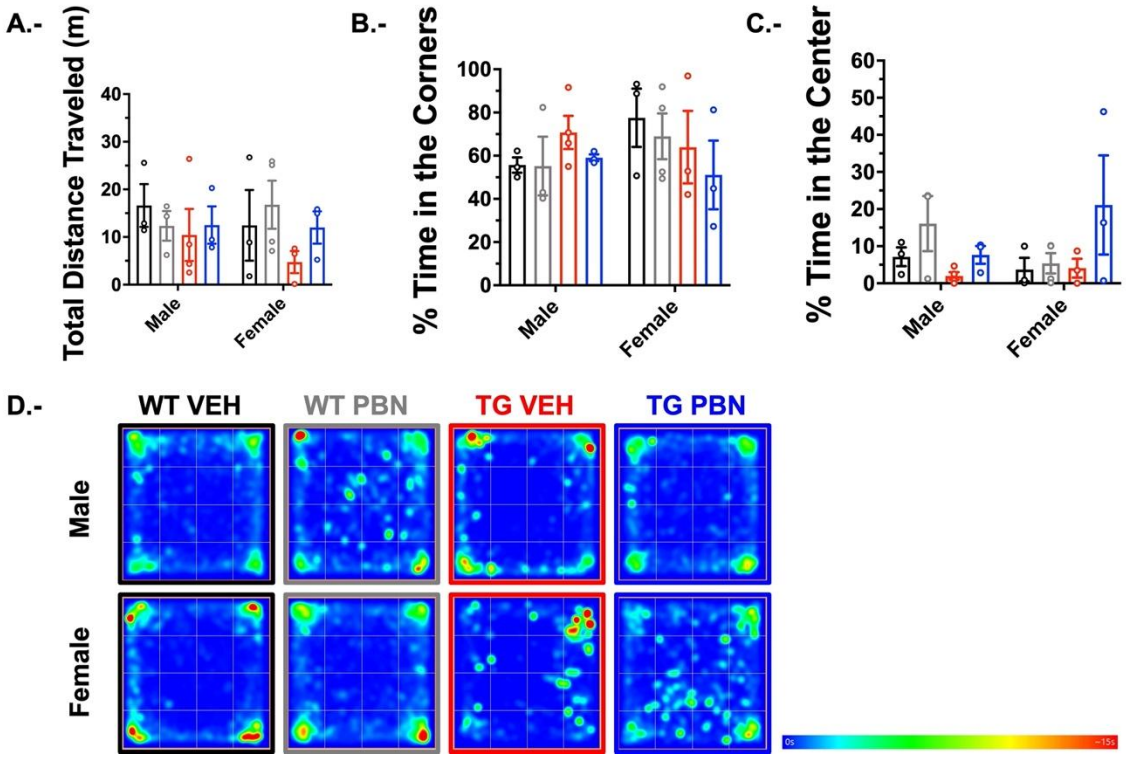

Figure 35 Locomotor activity assessed by the open field test was not affected in 18 m.o APP/PS1 mice. A.- *Total distance traveled by male and female 18 m.o APP/PS1 mice. There was no significant difference between groups by 3-way ANOVA.* ***B.-*** *Percentage of time spent in the corners by male and female 18 m.o APP/PS1 mice. There was no significant difference between groups by 3-way ANOVA.* ***C.-*** *Percentage of time spent in the center by male and female 12 m.o APP/PS1 mice. Treatment was a significant source of variation by 3-way ANOVA (F (1,18) = 4.788) * p = 0.042).* ***D.-*** *Representative average heatmaps of the open field test. Scale bar 15 s. Data was presented as mean ± SEM (Male: WT VEH (3) WT PBN (3) TG VEH (4) TG PBN (3). Female: WT VEH (3) WT PBN (4) TG VEH (3) TG PBN (3)).*

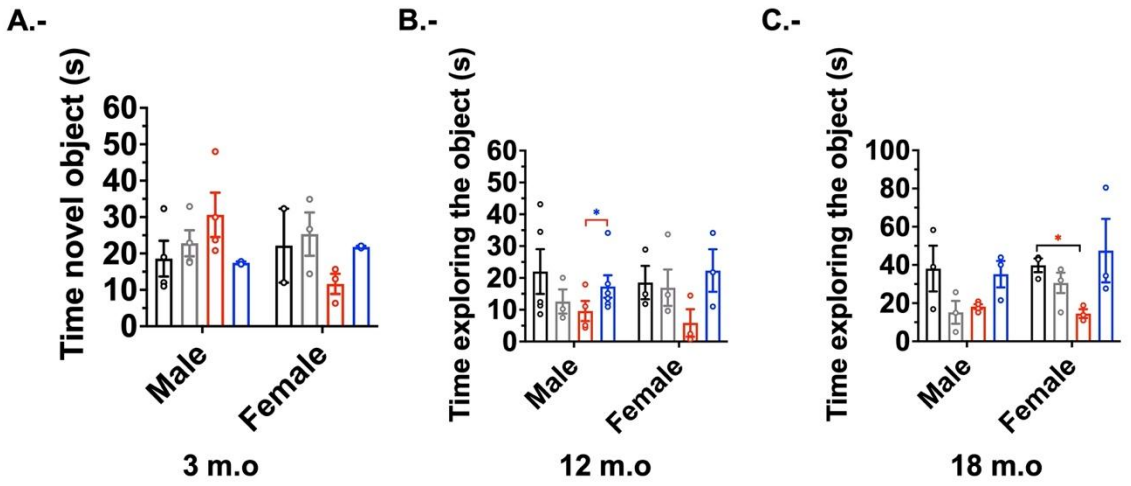

Figure 36 Gender did not affect the time exploring the novel object in the test phase in the novel object recognition task of 3 m.o, 12 m.o, and 18 m.o APP/PS1 animals. ***A.-*** Average time exploring the novel object in the NOR task of 3 m.o APP/PS1 animals. Gender was not a significant source of variation by Three-way ANOVA (Male: WT VEH N=4; WT PBN N=3; TG VEH N=4; TG PBN N=2. Female: WT VEH N=2; WT PBN N=3; TG VEH N=3; TG PBN N=2). ***B.-*** Average time exploring the novel object in the NOR task of 12 m.o APP/PS1 animals. Gender was not a significant source of variation, but there was a significant interaction between genotype x treatment ($F(1,23)=5.163$ * $p=0.0327$) by Three-way ANOVA, *p=0.04 (Male: WT VEH N=5; WT PBN N=3; TG VEH N=4; TG PBN N=6. Female: WT VEH N=3; WT PBN N=4; TG VEH N=3; TG PBN N=3). ***C.-*** Average time exploring the novel object in the NOR task of 18 m.o APP/PS1 animals. Gender was not a significant source of variation, but there was a significant interaction between genotype x treatment ($F(1,18)=13.90$ ** $p=0.0015$) by Three-way ANOVA, *p=0.0214 (Male: WT VEH N=3; WT PBN N=3; TG VEH N=4; TG PBN N=3. Female: WT VEH N=3; WT PBN N=4; TG VEH N=3; TG PBN N=3).

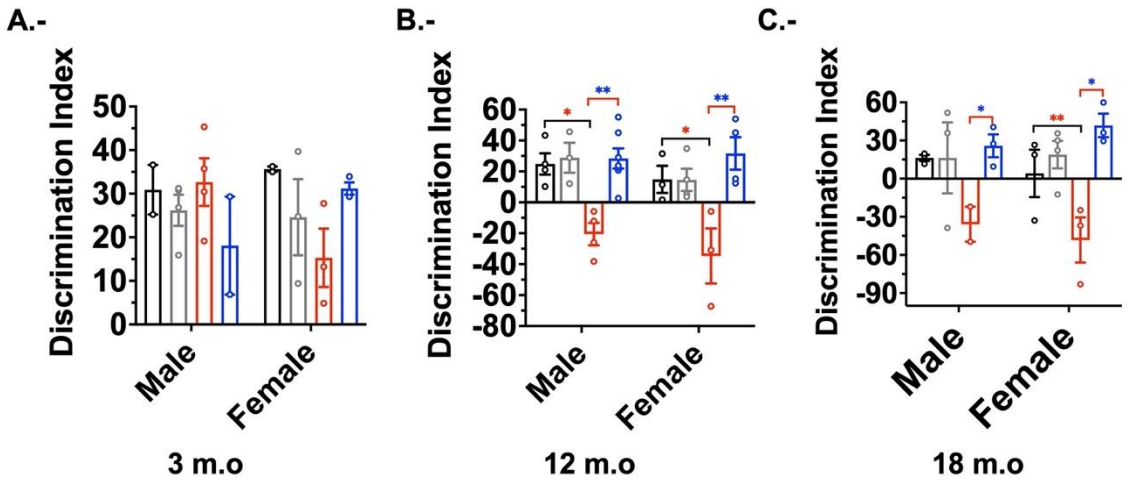

Figure 37 Gender did not affect the Discrimination Index in the novel object recognition task of 3 m.o, 12 m.o, and 18 m.o APP/PS1 animals. A.- Average discrimination index of 3 m.o APP/PS1 animals. Gender was not a significant source of variation but there was a significant interaction between gender x genotype x treatment ($F(1,5)= 9.820$ * $p=0.0258$ by Three-way ANOVA (Male: WT VEH N=4; WT PBN N=3; TG VEH N=4; TG PBN N=2. Female: WT VEH N=2; WT PBN N=3; TG VEH N=3; TG PBN N=2). ***B.-*** Average discrimination index of 12 m.o APP/PS1 animals. Genotype ($F(1,24)=8.745$ ** $p= 0.0069$) and treatment ($F(1,24)= 17.77$ *** $p=0.0003$ only were significant sources of variation, and there was a significant interaction between genotype x treatment ($F(1,24)=17.77$ *** $p=0.0003$) by Three-way ANOVA, and Tukey's multiple comparison tests revealed a significant difference between male: WT VEH-TG VEH * $p=0.0296$ TG VEH-TG PBN ** $p=0.0049$ and female: WT VEH-TG VEH * $p= 0.0455$ TG VEH-TG PBN ** $p=0.0015$ (Male: WT VEH N=5; WT PBN N=3; TG VEH N=4; TG PBN N=6. Female: WT VEH N=3; WT PBN N=4; TG VEH N=3; TG PBN N=3). ***C.-*** Average discrimination index of 18 m.o APP/PS1 animals. Gender was not a significant source of variation, but there was a significant interaction between genotype x treatment ($F(1,18)=13.90$ ** $p=0.0015$) by Three-way ANOVA, *$p=0.0214$ (Male: WT VEH N=3; WT PBN N=3; TG VEH N=4; TG PBN N=3. Female: WT VEH N=3; WT PBN N=4; TG VEH N=3; TG PBN N=3).

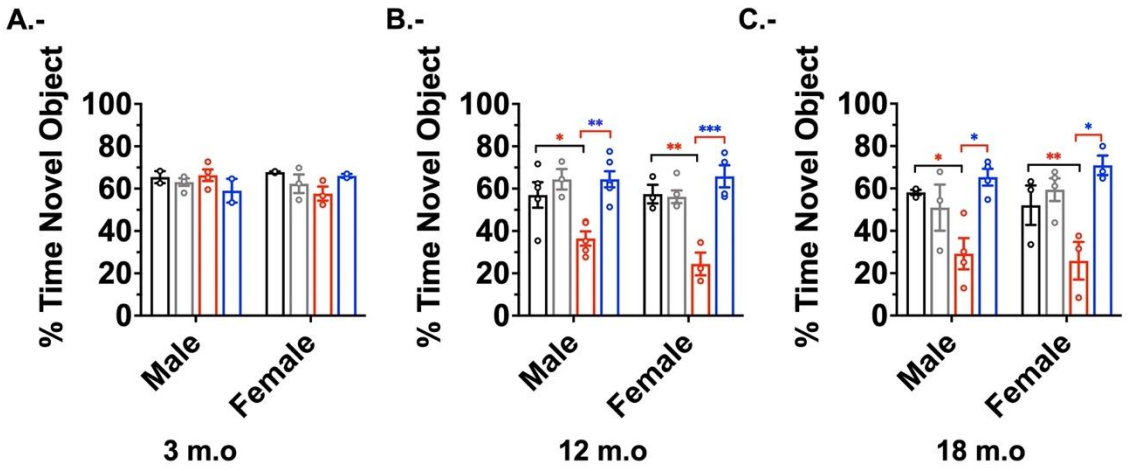

Figure 38 Gender did not affect the percentage time exploring the novel object in the test phase in the novel object recognition task of 3 m.o, 12 m.o, and 18 m.o APP/PS1 animals. A.- Average Percentage time exploring the novel object in the NOR task of 3 m.o APP/PS1 animals. Gender was not a significant source of variation but there was a significant interaction between gender x genotype x treatment ($F(1,4)= 19.42$ * $p=0.0116$) by Three-way ANOVA (Male: WT VEH N=4; WT PBN N=3; TG VEH N=4; TG PBN N=2. Female: WT VEH N=2; WT PBN N=3; TG VEH N=3; TG PBN N=2). ***B.-*** Average Percentage of time exploring the novel object in the NOR task of 12 m.o APP/PS1 animals. Genotype ($F(1,26)=10.67$ ** $p=0.0031$) and treatment ($F(1,26)=31.62$ **** $p<0.0001$) only were significant sources of variation, and there was a significant interaction between genotype x treatment ($F(1,26)=22.14$ **** $p<0.0001$) by Three-way ANOVA, and Tukey's multiple comparison tests revealed a substantial difference between male: WT VEH-TG VEH * $p=0.0361$ TG VEH-TG PBN ** $p=0.0010$; female: WT VEH-TG VEH ** $p=0.0049$ TG VEH-TG PBN *** $p=0.0001$ (Male: WT VEH N=5; WT PBN N=3; TG VEH N=4; TG PBN N=6. Female: WT VEH N=3; WT PBN N=4; TG VEH N=3; TG PBN N=3). ***C.-*** Average percentage of time exploring the novel object in the NOR task of 18 m.o APP/PS1 animals. Treatment ($F(1,11)=14.71$ ** $p=0.0028$) only was a significant source of variation, but there was a significant interaction between genotype x treatment ($F(1,8)=20.84$ ** $p=0.0018$) by Three-way ANOVA, and multiple t-tests revealed a substantial difference between male: WT VEH-TG VEH * $p=0.0263$ TG VEH-TG PBN * $p=0.0130$; female: WT VEH-TG VEH ** $p=0.0010$ TG VEH-TG PBN ** $p=0.0058$ (Male: WT VEH N=3; WT PBN N=3; TG VEH N=4; TG PBN N=3. Female: WT VEH N=3; WT PBN N=4; TG VEH N=3; TG PBN N=3).

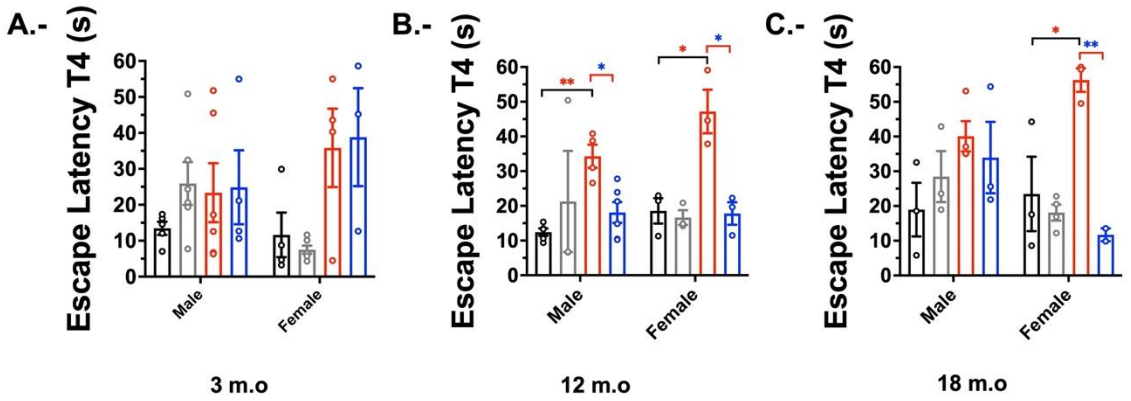

Figure 39 Gender did not affect the escape latency on the last day of training in the acquisition phase of the Morris water maze task, but there was a significant effect on treatment at 18 m.o female APP/PS1 mice. A.- *Average escape latency of 3 m.o male and female APP/PS1 animals (3 m.o male: N=5 WT VEH (black); N = 6 WT PBN (gray); N=6 TG VEH (red) and N=4 TG PBN (blue); female: N=4 WT VEH (black); N = 6 WT PBN (gray); N=4 TG VEH (red) and N=3 TG PBN (blue)). Genotype (F(1,12)=13.04, ** p=0.0036) was the only source of variation and there was a significant interaction between gender x genotype (F(1,12)=6.959, * p=0.0217) by Three-way ANOVA.* ***B.-*** *Average escape latency of 12 m.o male and female APP/PS1 animals (12 m.o male: N=5 WT VEH (black); N = 3 WT PBN (gray); N=3 TG VEH (red) and N=7 TG PBN (blue); female: N=3 WT VEH (black); N = 3 WT PBN (gray); N=3 TG VEH (red) and N=3 TG PBN (blue)). Genotype (F(1,9)=13.60, ** p=0.0050) and treatment (F(1,13)=5.852, * p=0.0310)were the only sources of variation and there was a significant interaction between genotype x treatment (F(1,9)=15.82, ** p=0.0032) by Three-way ANOVA.* ***C.-*** *Average escape latency of 18 m.o male and female APP/PS1 animals (18 m.o male: N=3 WT VEH (black); N = 3 WT PBN (gray); N=4 TG VEH (red) and N=3 TG PBN (blue); female: N=3 WT VEH (black); N = 4 WT PBN (gray); N=3 TG VEH (red) and N=2 TG PBN (blue)))). Genotype (F(1,7)=9.149, * p=0.0193) and treatment (F(1,10)=5.086, * p=0.0478) were the only sources of variation and there was a significant interaction between gender x treatment (F(1,10)=6.814, * p=0.0260) and genotype x treatment (F(1,7)=10.32, * p=0.0148) by Three-way ANOVA.*

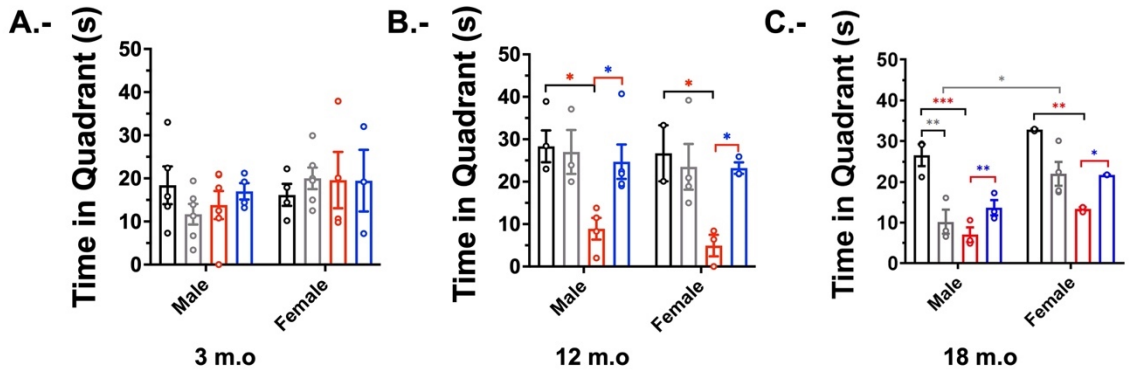

Figure 40 Gender affected the time spent in the target quadrant in the probe phase of the Morris water maze task in 18 m.o APP/PS1 mice. A.- *Average time spent in the*

target quadrant of 3 m.o APP/PS1 animals (3 m.o male: N=5 WT VEH (black); N = 6 WT PBN (gray); N=6 TG VEH (red) and N=4 TG PBN (blue); female: N=4 WT VEH (black); N = 6 WT PBN (gray); N=4 TG VEH (red) and N=3 TG PBN (blue)). There was not a significant difference between the groups by Three-way ANOVA. ***B.-*** *Average time spent in the target quadrant of 12 m.o APP/PS1 animals (12 m.o male: N=5 WT VEH (black); N = 3 WT PBN (gray); N=3 TG VEH (red) and N=7 TG PBN (blue); female: N=3 WT VEH (black); N = 3 WT PBN (gray); N=3 TG VEH (red) and N=3 TG PBN (blue)). Genotype (F(1,8)=17.93, ** p=0.0029) was the main source of variation and there was a significant interaction between genotype x treatment (F(1,8)=14.74, ** p=0.0050) by Three-way ANOVA, and the Tukey's multiple comparisons tests revealed a significant difference between male: WT VEH-TG VEH * p=0.0196, TG VEH-TG PBN * p=0.0469; female WT VEH-TG VEH * p= 0.0346 TG VEH-TG PBN * p=0.0108.* ***C.-*** *Average time spent in the target quadrant of 18 m.o APP/PS1 animals (18 m.o male: N=3 WT VEH (black); N = 3 WT PBN (gray); N=4 TG VEH (red) and N=3 TG PBN (blue); female: N=3 WT VEH (black); N = 4 WT PBN (gray); N=3 TG VEH (red) and N=2 TG PBN (blue)))). Gender (F(1,15)=22.41, *** p=0.0003 and Genotype (F(1,15)=27.22, *** p=0.0001) were the main sources of variation and there was a significant interaction between genotype x treatment (F(1,15)=38.04, **** p<0.0001 by Three-way ANOVA.*

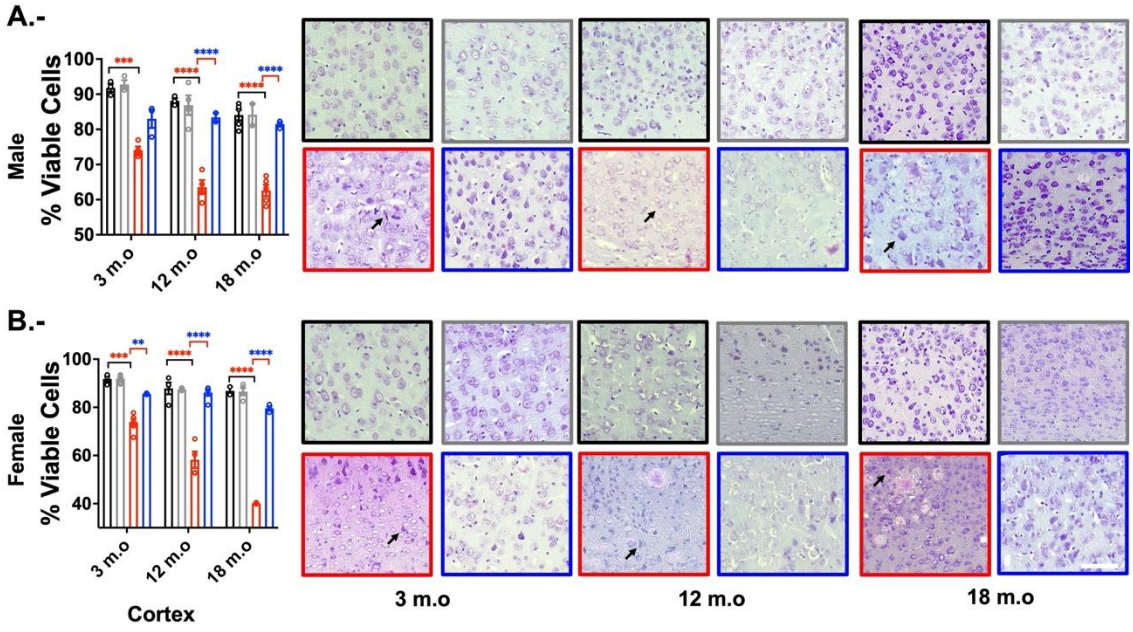

Figure 41 Probenecid prevents cortical neuronal loss in 3 m.o female, 12 m.o, and 18 m.o male and female APP/PS1 mice. A.- *Probenecid improved the number of viable cells in 12 m.o (N=2 WT VEH (black), N=2 WT PBN (gray), N= 2 TG VEH (red), and N= 2 TG PBN (blue)) and 18 m.o (N=2 WT VEH (black), N=2 WT PBN (gray), N= 2 TG VEH (red), and N= 2 TG PBN (blue)) but not in 3 m.o (N=2 WT VEH (black), N=2 WT PBN (gray), N= 2 TG VEH (red), and N= 2 TG PBN (blue)) males TG animals and representative images of Nissl staining in the cortical region adjacent to hippocampus of all experimental groups. Scale bar = 20 μm. Age (F(2,18)=16.14, **** p<0.0001),*

*genotype (F(1,12)=152.4, **** p<0.0001) and treatment (F(1,18)=53.05, **** p<0.0001) were the main source of variation and there was a significant interaction between genotype x treatment (F(1,12)=55.09, **** p<0.0001) by Three-way ANOVA; and Tukey's multiple comparisons tests revealed a significant difference between 3 m.o WT VEH-TG VEH *** p=0.0006; 12 m.o WT VEH-TG VEH **** p<0.0001 TG VEH-TG PBN **** p<0.0001; 18 m.o WT VEH-TG VEH **** p<0.0001 TG VEH – TG PBN **** p<0.0001.* ***B-*** *Probenecid improved the number of viable cells in 3 m.o (N=2 WT VEH (black), N=2 WT PBN (gray), N= 2 TG VEH (red), and N= 2 TG PBN (blue)) 12 m.o (N=2 WT VEH (black), N=2 WT PBN (gray), N= 2 TG VEH (red), and N= 2 TG PBN (blue)) and 18 m.o (N=2 WT VEH (black), N=2 WT PBN (gray), N= 2 TG VEH (red), and N= 2 TG PBN (blue)) females TG animals and representative images of Nissl staining in the cortical region adjacent to hippocampus of all experimental groups. Scale bar = 20 μm S rad: Stratum radiatum. Age (F(2,32)=39.49, **** p<0.0001), genotype (F(1,32)=259, **** p<0.0001) and treatment (F(1,32)=134.3, **** p<0.0001) were the main source of variation and there was a significant interaction between age x genotype (F(2,32)=14.32, **** p<0.0001), age x treatment (F(2,32)=12.06 *** p=0.001), genotype x treatment (F(1,32)=138.3, **** p<0.0001) and age x genotype x treatment (F(2,32)=12.98 **** p<0.0001) by Three-way ANOVA; and Tukey's multiple comparisons tests revealed a significant difference between 3 m.o WT VEH-TG VEH **** p<0.0001 TG VEH-TG PBN ** p=0.0090; 12 m.o WT VEH-TG VEH **** p<0.0001 TG VEH-TG PBN **** p<0.0001; 18 m.o WT VEH-TG VEH **** p<0.0001 TG VEH – TG PBN **** p<0.0001.*

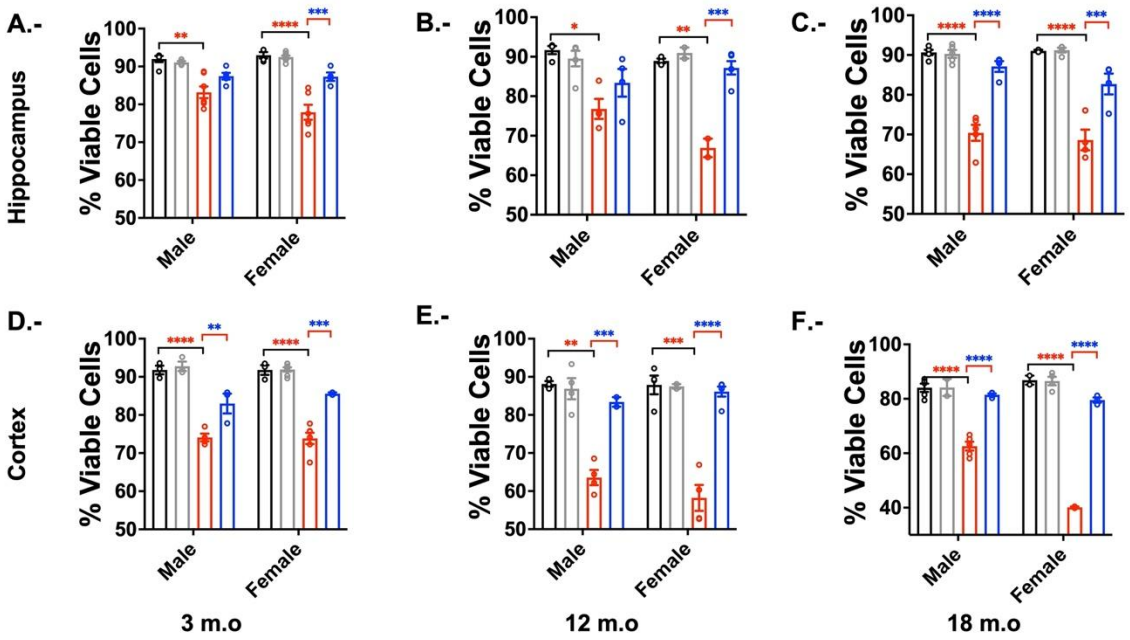

Figure 42 Gender affected the cortical neuronal loss in 18 m.o APP/PS1 mice A.- *Probenecid improved the number of viable cells in CA1 area 3m.o female APP/PS1 TG mice. Genotype (F(1,13)=94.93, **** p<0.0001) and treatment (F(1,22)=10.74, ** p=0.0034) were the main sources of variation and there was a significant interaction between gender x genotype (F(1,13)=5.162, *p=0.0407) and genotype x treatment*

*(F(1,13)=20.36, *** p=0.0006) by Three-way ANOVA and Tukey's multiple comparison tests revealed a significant difference between male: WT VEH-TH VEH ** p=0.0012 and female: WT VEH-TG VEH **** p<0.0001 TGVEH-TG PBN *** p=0.0002.* ***B.-*** *Probenecid improved the number of viable cells in CA1 area 12 m.o female APP/PS1 TG mice. Genotype (F(1,8)=49.20, *** p=0.0001) and treatment (F(1,13)=14.95, ** p=0.0019) were the main sources of variation and there was a significant interaction between gender x treatment (F(1,13)=6.609, *p=0.0233) and genotype x treatment (F(1,8)=16.56, ** p=0.0036) by Three-way ANOVA and Tukey's multiple comparison tests revealed a significant difference between male: WT VEH-TH VEH * p=0.0139 and female: WT VEH-TG VEH ** p=0.0062 TGVEH-TG PBN *** p=0.0003.* ***C.-*** *Probenecid improved the number of viable cells in CA1 area of 18 male and female APP/PS1 TG mice. Genotype (F(1,24)=158.1, **** p<0.0001) and treatment (F(1,24)=53.55, **** p<0.0001) were the main sources of variation and there was a significant interaction between gender x genotype (F(1,24)=4.922, *p=0.0362) and genotype x treatment (F(1,24)=54.81, **** p<0.0001) by Three-way ANOVA and Tukey's multiple comparison tests revealed a significant difference between male: WT VEH-TH VEH **** p<0.0001 TG VEH-TG PBN **** p<0.0001 and female: WT VEH-TG VEH **** p<0.0001 TGVEH-TG PBN **** p<0.0001.* ***D.-*** *Probenecid improved the number of viable cells in the cortical area of 3m.o male and female APP/PS1 TG mice. Genotype (F(1,23)=162.6, **** p<0.0001) and treatment (F(1,23)=28.68, **** p<0.0001) were the main sources of variation and there was a significant interaction between genotype x treatment (F(1,23)=23.18, **** p<0.0001) by Three-way ANOVA and Tukey's multiple comparison tests revealed a significant difference between male: WT VEH-TH VEH **** p<0.0001 TG VEH-TG PBN ** p=0.0039 and female: WT VEH-TG VEH **** p<0.0001 TG VEH-TG PBN *** p=0.0003.* ***E.-*** *Probenecid improved the number of viable cells in the cortical area of 12m.o male and female APP/PS1 TG mice. Genotype (F(1,20)=70.08, **** p<0.0001) and treatment (F(1,20)=42.75, **** p<0.0001) were the main sources of variation and there was a significant interaction between genotype x treatment (F(1,20)=49.02, **** p<0.0001) by Three-way ANOVA and Tukey's multiple comparison tests revealed a significant difference between male: WT VEH-TH VEH **** p<0.0001 TG VEH-TG PBN ** p=0.0010 and female: WT VEH-TG VEH **** p<0.0001 TG VEH-TG PBN *** p=0.0003.* ***F.-*** *Probenecid improved the number of viable cells in the cortical area of 18 m.o male and female APP/PS1 TG mice. Gender (F(1,19)=16.02, *** p=0.0008), genotype (F(1,19)=262.3, **** p<0.0001) and treatment (F(1,19)=145.9, **** p<0.0001) were the main sources of variation and there was a significant interaction between gender x genotype (F(1,19)=37.84, **** p<0.0001, gender x treatment (F(1,19)=17.55, *** p=0.0005), genotype x treatment (F(1,19)=148.3, **** p<0.0001) and gender x genotype x treatment (F(1,19)=19.04, *** p=0.0003) by Three-way ANOVA and Tukey's multiple comparison tests revealed a significant difference between male: WT VEH-TH VEH **** p<0.0001 TG VEH-TG PBN **** p<0.0001 and female: WT VEH-TG VEH **** p<0.0001 TG VEH-TG PBN *** p=0.0003.*

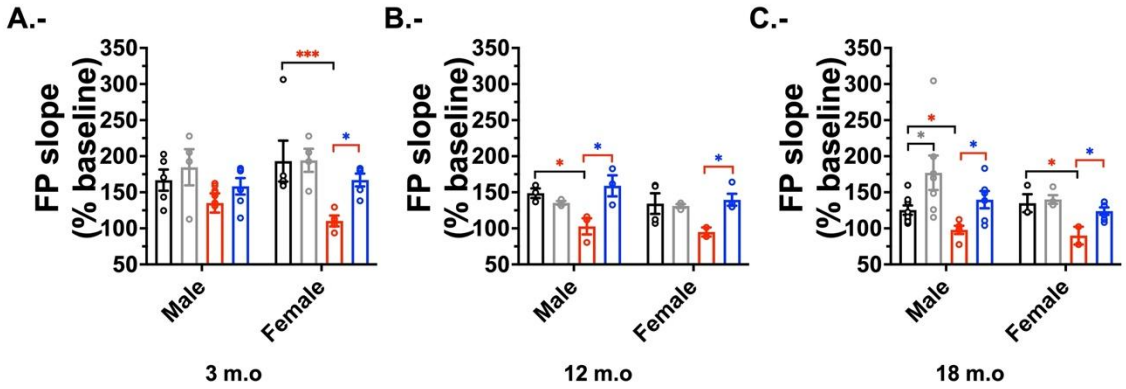

Figure 43 Gender did not affect the LTP magnitude of the last 10 min of recordings in hippocampal slices of 3 m.o, 12 m.o, and 18 m.o APP/PS1 mice. A.- *Average LTP magnitude during the last 10 min of recording of 3 m.o APP/PS1 mice. Genotype (F(1,13)=15.32, ** p=0.0018) was the main source of variation by Three-way ANOVA and Tukey's multiples comparisons test showed a significant difference between female: WT VEH-TG VEH *** p=0.0006 TG VEH TG PBN * p=0.0256.* ***B.-*** *Average LTP magnitude during the last 10 min of recording of 12 m.o APP/PS1 mice. Treatment (F(1,10)=5.470, * p=0.0414) was the main source of variation and there was a significant interaction between genotype x treatment (F(1,7)=28.38, ** p=0.0011) by Three-way ANOVA and Tukey's multiples comparisons test showed a significant difference between male: WT VEH-TG VEH * p=0.0412 TG VEH-TG PBN * p=0.0273; female: TG VEH-TG PBN * p=0.0263.* ***C.-*** *Average LTP magnitude during the last 10 min of recording of 18 m.o APP/PS1 mice. Genotype (F(1,33)=8.201, ** p=0.0072), and treatment (F(1,33)=9.125, ** p=0.0048) were the main sources of variation by Three-way ANOVA and Tukey's multiples comparisons test showed a significant difference between male: WT VEH-TG VEH * p=0.0141 WT PBN – WT VEH * p=0.0298 TG VEH-TG PBN * p=0.0160; female: WT VEH-TG VEH * 0.0315 TG VEH-TG PBN * p=0.0221.*

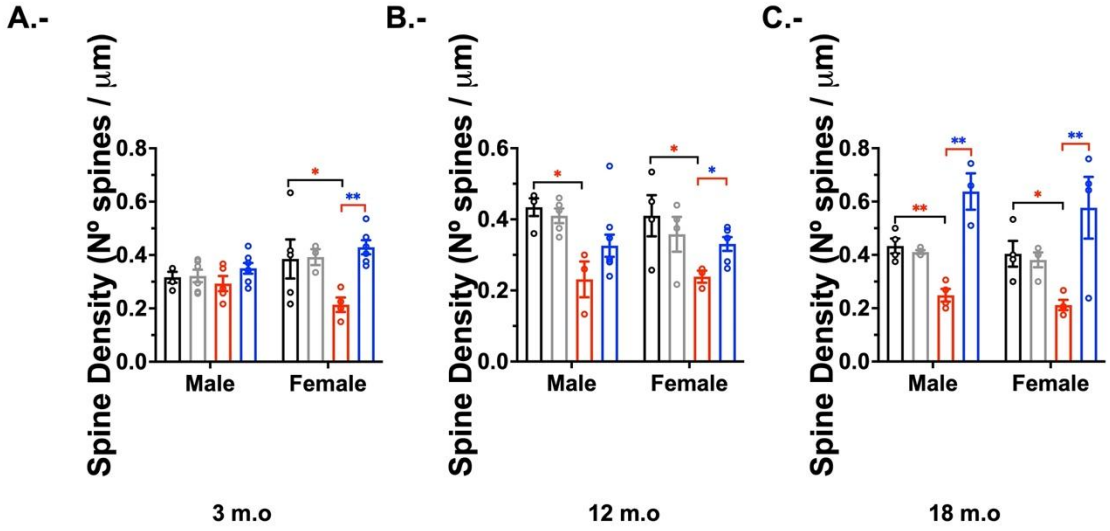

Figure 44 Gender did not affect the spine density in hippocampal slices of 3 m.o, 12 m.o, and 18 m.o APP/PS1 mice. A.- *Average dendritic spine density in male and female 3 m.o APP/PS1 mice. Treatment (F(1,32)=7.690, ** p=0.0092) was the main source of variation and there was a significant interaction between genotype x treatment (F(1,32)=6.468, * p=0.0160) by Three-Way ANOVA and Tukey's multiple comparisons tests showed a significant difference between female: WT VEH-TG VEH * p=0.0474 TG VEH-TG PBN ** p=0.0038.* ***B.-*** *Average dendritic spine density in male and female 12 m.o APP/PS1 mice. Genotype (F(1,30)=20.42, **** p<0.0001) was the main source of variation and there was a significant interaction between genotype x treatment (F(1,30)=5.984, * p=0.0205) by Three-Way ANOVA and Tukey's multiple comparisons tests showed a significant difference between male: WT VEH-TG VEH * p=0.0354 female: WT VEH-TG VEH * p=0.0353 TG VEH-TG PBN * p=0.0197.* ***C.-*** *Average dendritic spine density in males and females 18 m.o APP/PS1 mice. Treatment (F(1,23)=22.35, **** p<0.0001) was the main source of variation and there was a significant interaction between genotype x treatment (F(1,23)=28.47, **** p<0.0001) by Three-Way ANOVA and Tukey's multiple comparisons tests showed a significant difference between male: WT VEH-TG VEH ** p=0.0024 TG VEH-TG PBN ** p=0.0013; female: WT VEH-TG VEH * p=0.0102 TG VEH-TG PBN ** p=0.0011.*

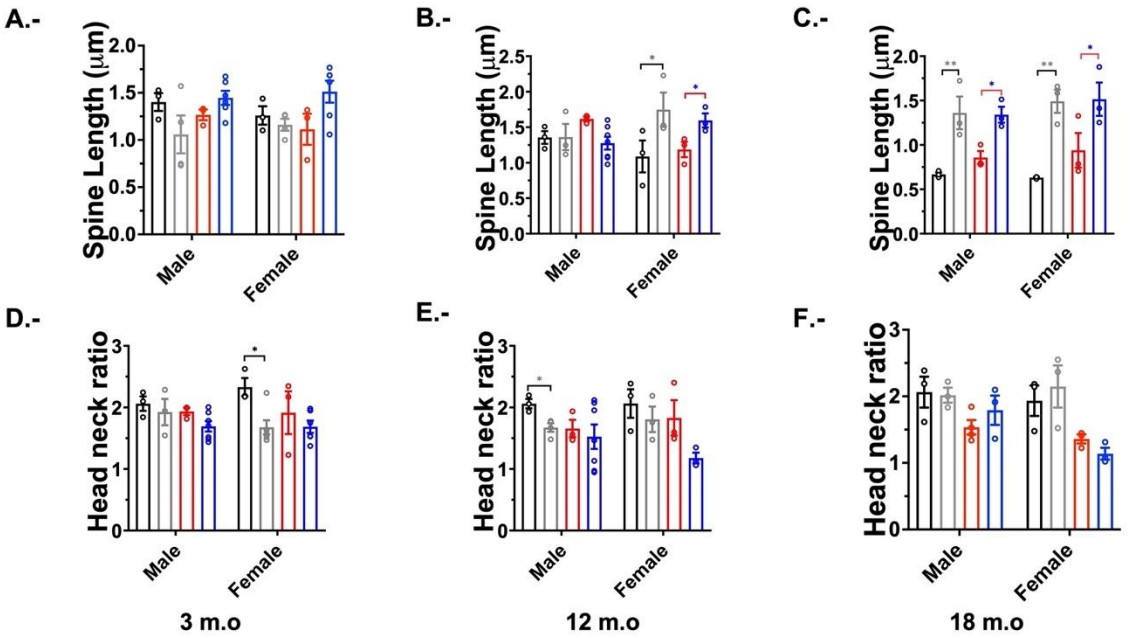

Figure 45 Gender did not affect the spine length and head-neck ratio in hippocampal slices of 3 m.o, 12 m.o, and 18 m.o APP/PS1 mice. A.- *Average spine length of dendritic spines in hippocampal CA1 neurons of 3 m.o male and female APP/PS1 mice. Genotype (F(1,8)=31.01, *** p=0.0005) was the main source of variation by Three-way ANOVA.* ***B.-*** *Average spine length of dendritic spines in hippocampal CA1 neurons of 12 m.o male and female APP/PS1 mice. There was a significant interaction between gender x treatment (F(1,20)=11.57, ** p=0.0028) by Three-way ANOVA and Tukey's multiple comparisons test showed a significant difference between females: WT VEH-WT PBN * p=0.0278 TG VEH-TG PBN * p=0.0489.* ***C.-*** *Average spine length of dendritic spines in hippocampal CA1 neurons of 18 m.o male and female APP/PS1 mice. Treatment (F(1,8)=35.92, *** p=0.0003) was the main source of variation by Three-way ANOVA and Tukey's multiple comparisons test showed a significant difference between males: WT VEH-WT PBN ** p=0.0089 TG VEH-TG PBN * p=0.0139 females: WT VEH-WT PBN ** p=0.0014 TG VEH-TG PBN * p=0.0317.* ***D.-*** *Average head-neck ratio of dendritic spines in hippocampal CA1 neurons of 3 m.o male and female APP/PS1 mice. Genotype (F(1,11)=5.106, * p=0.0451) and treatment (F(1,15)=6.503, * p=0.0222) were the main sources of variation by Three-way ANOVA and Tukey's multiple comparisons test showed a significant difference between female: WT VEH-WT PBN * p=0.0199.* ***E.-*** *Average head-neck ratio of dendritic spines in hippocampal CA1 neurons of 12 m.o male and female APP/PS1 mice. Genotype (F(1,21)=5.926, * p=0.0239) and treatment (F(1,21)=6.043, * p=0.0227) were the main sources of variation by Three-way ANOVA and Tukey's multiple comparisons test showed a significant difference between male: WT VEH-WT PBN * p=0.0133.* ***F.-*** *Average head-neck ratio of dendritic spines in hippocampal CA1 neurons of 18 m.o male and female APP/PS1 mice. Genotype (F(1,8)=31.01, *** p=0.0005) was the main source of variation by Three-way ANOVA.*

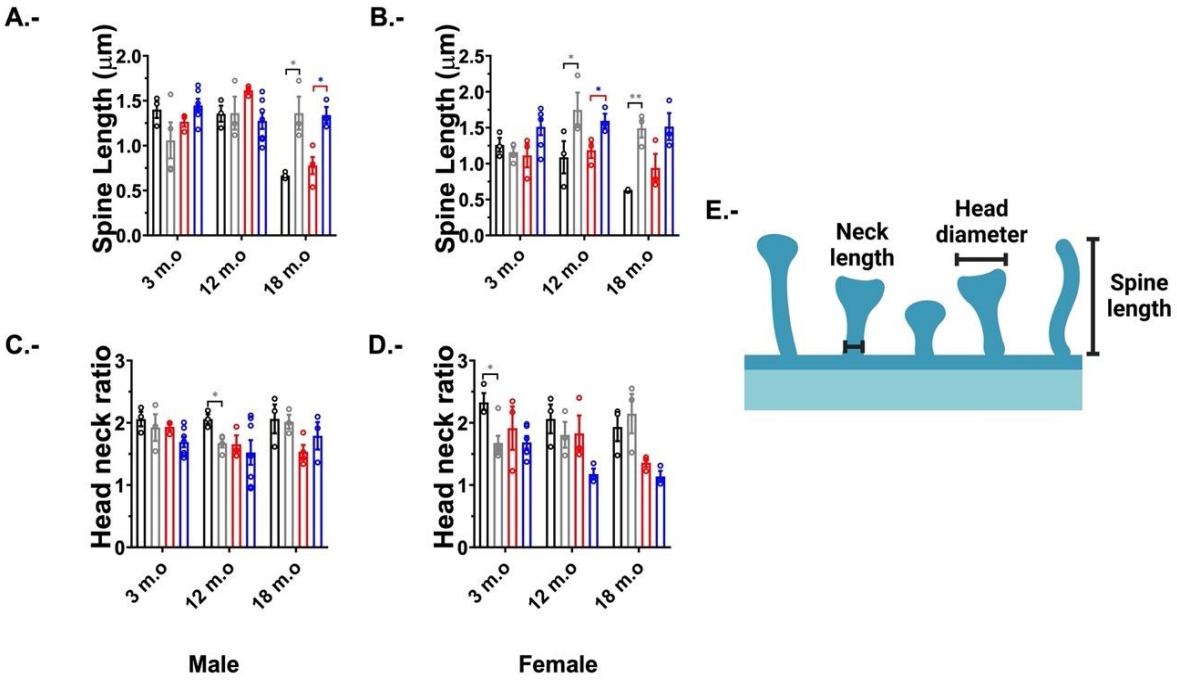

Figure 46 Probenecid treatment increased spine length in 12 m.o and 18 m.o APP/PS1 animals. A.- *Average spine length of dendritic spines in hippocampal CA1 neurons of 3 m.o, 12 m.o, and 18 m.o male APP/PS1 mice. Groups are presented as 3m.o: WT VEH n= 3 neurons (80 spines), (Black); WT PBN n= 3 neurons (300 spines) (Gray); TG VEH n= 3 neurons (63 spines) (Red); TG PBN n= 7 neurons (407 spines) (Blue); 12m.o: WT VEH n= 3 neurons (79 spines), (Black); WT PBN n= 4 neurons (84 spines) (Gray); TG VEH n= 3 neurons (116 spines) (Red); TG PBN n= 7 neurons (315 spines) (Blue) and 18m.o: WT VEH n= 3 neurons (67 spines), (Black); WT PBN n= 3 neurons (89 spines) (Gray); TG VEH n= 3 neurons (85 spines) (Red); TG PBN n= 3 neurons (184 spines) (Blue). Age (F(2,20)=8.350, ** p=0.0023) was a significant source of variation and there was a significant interaction between Age x Treatment (F(2,20)=11.43, *** p=0.0005) and Age x Genotype x Treatment (F(2,13)=4,062, * p=0.0426) by Three-way ANOVA, and Tukey's multiple comparisons tests showed a significant difference between 18 m.o WT VEH-WT PBN * p=0.0240 TG VEH-TG PBN * p=0.0131.* ***B.-*** *Average spine length of dendritic spines in hippocampal CA1 neurons of 3 m.o, 12 m.o, and 18 m.o female APP/PS1 mice. Groups are presented as 3m.o: WT VEH n= 5 neurons (80 spines), (Black); WT PBN n= 3 neurons (301 spines) (Gray); TG VEH n= 4 neurons (63 spines) (Red); TG PBN n= 6 neurons (457 spines) (Blue); 12m.o: WT VEH n= 4 neurons (80 spines), (Black); WT PBN n= 4 neurons (85 spines) (Gray); TG VEH n= 3 neurons (116 spines) (Red); TG PBN n= 6 neurons (316 spines) (Blue) and 18m.o: WT VEH n= 4 neurons (67 spines), (Black); WT PBN n= 4 neurons (139 spines) (Gray); TG VEH n= 4 neurons (86 spines) (Red); TG PBN n= 4 neurons (184 spines) (Blue). Treatment (F(1,15)=29.15, **** p<0.0001) was the main source of variation and there was a significant interaction between age x treatment (F(2,15)=3.966, * p=0.0414) by Three-way ANOVA and Tukey's multiple comparisons tests showed a significant difference between 12 m.o: WT VEH-WT PBN * p=0.0254 TG VEH-TG PBN * p=0.0489;*

*18 m.o: WT VEH-WT PBN ** p=0.0026.* ***C.-*** *Average Head Neck ratio of dendritic spines in hippocampal CA1 neurons of 3 m.o, 12 m.o, and 18 m.o male APP/PS1 mice. Genotype (F(1,13)=8.750, * p=0.0111) was the main source of variation by Three-way ANOVA and Tukey's multiple comparisons test showed a significant difference between 12 m.o: WT VEH-WT PBN * p=0.0133* ***D.-*** *Average Head Neck ratio of dendritic spines in hippocampal CA1 neurons of 3 m.o, 12 m.o, and 18 m.o female APP/PS1 mice. Genotype (F(1,15)=18.69, *** p=0.0006) and treatment (F(1,15)=7.005, * p=0.0283) were the main sources of variation by Three-way ANOVA and Tukey's multiple comparisons tests showed a significant difference between WT VEH-WT PBN * p=0.0120.* ***E.-*** *Representative diagram of the size parameters of the dendritic spines considered for this thesis.*